A NEW APPROACH TO SIMULATE THE AMELAND INLET'S RESPONSE TO SEA-LEVEL RISE AND SUBSIDENCE

Master of Science Thesis

Xinyu Chen

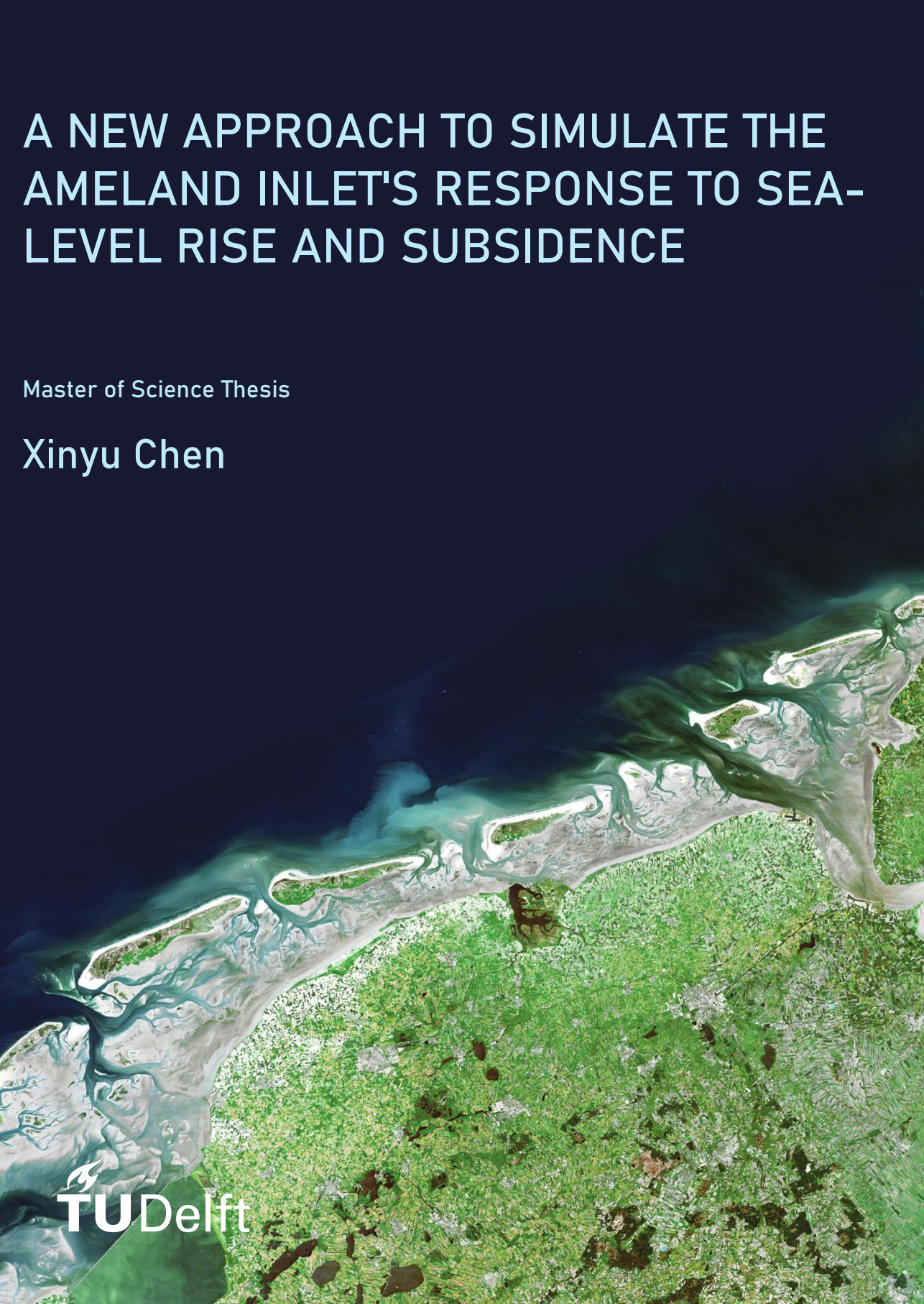

TU Delft

Cover image: Satellite image of the Wadden Sea
Source:
https://www.waddensea-worldheritage.org/resources/satellite-image-wadden-sea

A NEW APPROACH TO SIMULATE THE AMELAND INLET'S RESPONSE TO SEA-LEVEL RISE AND SUBSIDENCE

by

Xinyu CHEN

to obtain the degree of Master of Science
at the Delft University of Technology

Student number: 5035422

Thesis committee:		
	Prof. dr. ir. Z.B. Wang,	TU Delft, Deltares
	Dr. ir. M. van der Wegen,	IHE, Deltares
	Dr. Q.H. Ye,	Deltares
	Dr. ir. B.C. van Prooijen	TU Delft
	Dr. ir. E. Elias	Deltares
	Dr. Y. Huismans	Deltares
	Drs. Q.J. Lodder	TU Delft, Rijkswaterstaat

An electronic version of this thesis is available at
http://repository.tudelft.nl/.

TU Delft Deltares

All models are wrong but some are useful

George E. P. Box

ABSTRACT

The Wadden Sea is the largest system of tidal flats and barrier islands in the world extending from the northern Dutch coast to the coast of Denmark. Such a large natural area is of great importance to both human beings and ecosystems. Over 10,000 species of flora and fauna are found in the Wadden Sea being a perfect habitat due to the relatively calm environment and high food availability. However, accelerating sea-level rise and human interventions, such as gas extraction, may induce an unwanted morphological change in the Wadden Sea posing a threat to the natural habitats. This study investigates the morphological response of the Wadden Sea to SLR and subsidence induced by gas mining.

A new hybrid model whose aggregation level is between a process-based model (Delft3D) and a aggregated model (ASMITA) is applied in this thesis. The two-dimensional hybrid model applies depth integrated shallow water formulations and the advection diffusion equation for the transport of sediments like Delft3D, but calculates the exchange of sediment between bed and water column by means of an equilibrium bathymetry concept under scenarios disturbing these equilibrium conditions.

The Ameland inlet is chosen as the research area because it is a relatively autonomous and undisturbed basin. The high robustness of the hybrid model makes it possible to apply a high morphological scale factor and a coarser grid compared to the process-based model, which shortens the computation time by orders of magnitude. However, the equilibrium concept also fixes the shoal-channel structure and suppresses channel migrations. Three different scenarios of sea-level rise rate (4, 6, 8 mm/year) are applied over a simulation period of 100 years. The general morphological response simulated by the hybrid model shows that the channels and the ebb-tidal delta erode acting as the main source of sediment for accretion of the intertidal flats. The erosion/sedimentation is more pronounced with a higher sea-level rise rate.

Sensitivity analysis shows a significant influence of the sediment diameter on the channel erosion and sediment supply to the intertidal flats. Diffusivity plays an important role in the horizontal sediment exchange between the channel and the flat but only slightly influences the sediment import. Global equilibrium concentration and power n are similar to diffusivity in affecting morphological activity. The adaptation time scale is inversely proportional to both of these two parameters. The possibility of using more than one sediment fraction is proved and it can reproduce a more realistic sediment distribution as the observation.

The hybrid model is also applied to simulate the morphological response to local subsidence and the restoration after subsidence stops. The center of the subsidence circle dosen't lower as much as the subsidence rate, which indicates that sediment is transported to the center. Sediment is supplied to the area of subsidence by the adjacent main channel. The result proves the sediment transport principle underlying the hybrid model that sediment is always transported along the gradient of the sediment demand.

ACKNOWLEDGEMENTS

This is the final report of my master's degree thesis at the Delft University of Technology. My graduation project started in March, 2021 and with 8-month effort, I can finally accomplish it in November, 2021.

First of all, I would like to thank all the members in my committee. Even though due to COVID, we cannot even meet and discuss the problems I met face to face, I still can communicate with them efficiently by online meeting or email and always received their answers quickly. I really appreciate Prof. Zhengbing Wang for proposing this topic to me as my graduation thesis and his rigorous attitude to details taught me what is scientific spirit. And I also would like to thank Dr. Mick van der Wegen for every time helping me check the results and cheering me up when I got stuck. Thank Dr. Edwin Elias for always giving me crucial suggestions to help me solve the problems in the model and in interpreting the results. Thank Dr. Qinghua Ye for helping me solve tons of problems regarding Delft3D. Thank Dr. Ymkje Huismans for always being really kind and patient and giving me a lot of useful suggestions in every important meeting. Thank Dr. Bram van Prooijen and Drs. Quirijn Lodder for helping me revise my thesis and giving a lot of suggestions on my presentation.

And it's so fortunate that I can join Deltares as an intern student to finalize my thesis. Deltares' computation cluster helped me save so much time and I don't need to have the model running on my own laptop and use my t-shirt to cover the screen overnight. I would like to thank Denzel Harlequin for guiding me to get familiar with the model and the cluster. Thank Bert Jagers for every time explaining the source code of the model to me very specifically.

Of course, support from my friends and family is quite important for me. Thank my friend Philipp Bangen for all the drinks, Le Zhang, Chen Fa and Ni Ye for hosting me with delicious foods, and all my friends from Beemo, Delft Chinese football club for the necessary entertainment. And most importantly, thank my family for giving me support both financially and mentally all the time.

Xinyu Chen
Novemeber, 2021

CONTENTS

List of Figures

ABBREVIATIONS

SLR	Sea-level rise
ASMITA	Aggregated Scale Morphological Interaction between Tidal basin and Adjacent coast
LHS	Left hand side
RHS	Right hand side

1

INTRODUCTION

1.1. BACKGROUND

The Wadden Sea is the largest tidal flat system in the world which extends from the northern Dutch coast to Denmark along a coastline of about 500 kilometers, whose area is nearly 11,000 square kilometers. Due to Holocene SLR, the tidal system containing barrier islands, channels, and intertidal areas was formed as what we see today. Meanwhile, the dynamic balance between sediment supply and SLR took the shape of the back-barrier area (Wang et al., 2018). From 8000BC, the lower parts of Pleistocene river valleys were submerged due to the accelerated SLR and became tidal basins. After 2000BC, SLR slowed down and sediment supply balanced with SLR. At the landward edge of the basin, salt marshes developed which enhanced the formation of the intertidal area. At some areas with limited sediment supply from offshore and alongshore sediment transport, the barrier islands were the main source of sediment. Some barrier islands have been retreating for tens of kilometers until now at a speed of 1 to 2 meters per year (Oost et al., 2017).

Within and close to the Wadden Sea, human activities are quite frequent. The Wadden Sea covers some of the busiest shipping routes in the world (Bahlke, 2017). Therefore, lots of ports are built near the Wadden Sea coast. The Hamburg port and Wilhelmshaven port are the two most important ports of Germany, which are the biggest dry bulk port with 30 million tons and liquid bulk port with 17 million tons, respectively (ESPO, 2019). To maintain the shipping channels and the port basins, human intervention is inevitable. Dredging should be applied periodically to ensure there is enough water depth for shipping.

The tidal inlets in the Wadden Sea also protect the mainland area from flooding. The barrier islands, the intertidal flats and the plants such as salt marsh have a significant effect on damping waves which provides the mainland a relatively calmer hydrodynamic environment. Once the tidal inlets are inundated, the mainland will be exposed to extreme waves and storms and the flood risk will rise dramatically, posing a threat to human life and property.

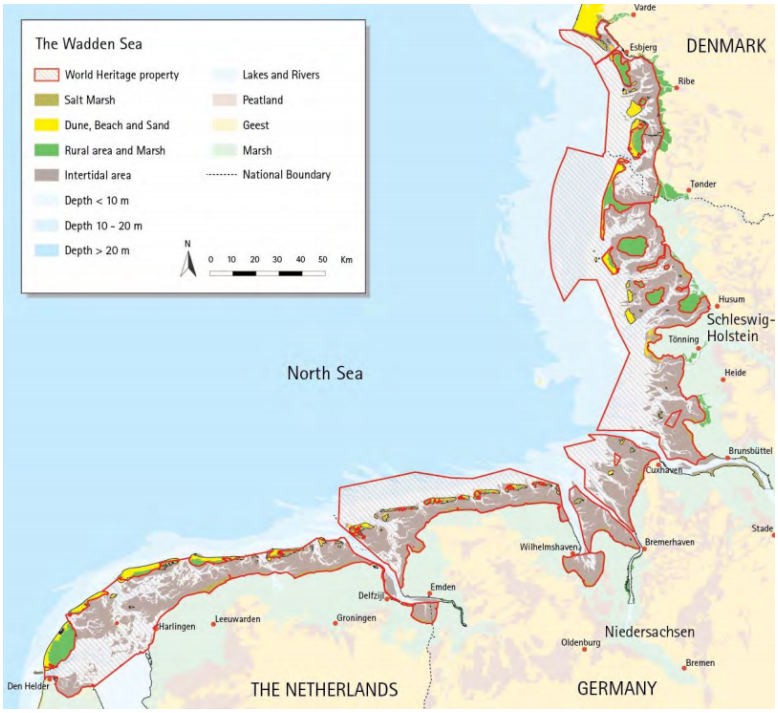

Figure 1.1: The Wadden Sea map (Oost et al., 2017)

Such a large area of natural tidal flat is of great importance to many species. The Wadden Sea basin provides a perfect habitat for flora and fauna. According to the Wadden Sea's website[1], the complex and dynamic system of the Wadden Sea is the habitat of around 10,000 species of flora and fauna. The Wadden Sea is a transition area between estuaries and the North Sea which provides fishes with high food availability and a relatively safe shelter place to avoid predators. Therefore, most fish will spend at least one stage of their lifespans in the Wadden Sea and some of them spend entire life here. However, since the 1980's, the nursery function of the Wadden Sea for fishes has decreased especially for flatfish species due to human interventions and climate change (Tulp et al., 2017).

The Wadden Sea is also of great importance to migratory and breeding birds. For the migratory birds, the Wadden Sea acts as a stop-over and wintering site. And they prefer to choose the high tide place as their roosting site where they are away from humans visiting and have easy access to food (Blew et al., 2017). With respect to breeding birds, they also rely on non-intertidal areas, for instance, the adjacent coastal wetland and grassland, for laying and breeding (Koffijberg et al., 2017). However, for both two kinds of birds, they have experienced a constant drop in populations in the Wadden Sea. Once the birds' habitats become smaller and their quality gets worse as past, there will

[1] https://www.waddensea-worldheritage.org/richly-diverse

be fewer and fewer birds choosing the Wadden Sea as a roosting or breeding site. And some of them may even be faced with extinction.

However, due to accelerating sea-level rise and human interventions, the morphological evolution of the Wadden sea becomes harder to be predicted. To protect the biodiversity in the Wadden Sea and maintain the habitats of birds and fishes, research on the morphodynamic change of the Wadden Sea with respect to the sea level rise is necessary.

1.2. PROBLEM STATEMENT

The accelerating sea-level rise poses a threat to the Wadden sea's future sustainability. In this project, we will mainly focus on the Wadden Sea within the Dutch border boundary. In the past few decades, the sea level in the Wadden Sea has been increasing roughly at the speed of 1.77 ± 0.49mm/year according to satellite records (Vermeersen et al., 2018). According to the field observation, some systems remain stable with enough sediment import where the accretion of tidal-flat can keep pace with SLR. But there are also some other systems approaching complete inundation (Wang et al., 2018). The tidal basin's evolution can be seen as a competition between the sediment supply and the sea level rise. Throughout the Holocene, the sediment supply along the Wadden sea was sufficient to maintain the intertidal morphology and the Wadden sea system exchanged little sediment with adjacent deeper the North Sea (van der Molen and van Dijck, 2000). Therefore, the Wadden sea can be treated as an individual system with respect to cross-shore sediment transport.

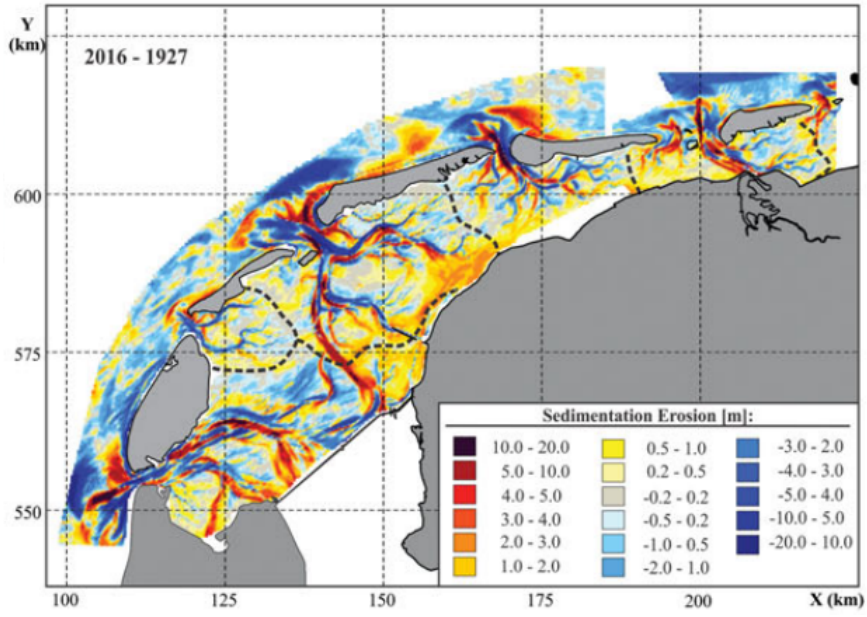

Figure 1.2: Sedimentation-erosion pattern over the interval 1927-2016 in the Dutch Wadden Sea (Wang et al., 2018)

Elias et al. (2012) proposed that over the period 1935-2005, an overall sedimentation trend can be found inside the Dutch Wadden Sea basin and on the contrary, ebb-tidal deltas are being eroded. Wang et al. (2018) also concluded that the amount of erosion along the North Sea coast is around the same order as the sedimentation inside the Wadden Sea basin. Especially for the Texel, Vlie, and Frisian Inlets, due to the closure of Zuiderzee and Lauwerszee, a smaller tidal prism is induced which leads to significant sedimentation inside basins. From Figure1.2, a more specific morphodynamic change pattern from 1927 to 2016 can be observed. An especially significant erosion happened at the ebb-tidal delta of Vile Inlet and Ameland Inlet which proves the erosion trend mentioned above. Besides, the main inlet channels of almost every basin of the Wadden Sea deepened during the period. In contrast, obvious sedimentation happened inside the basins especially the area near the onshore edge.

Even the intertidal area inside the Wadden Sea shows a sedimentation tendency over the past several decades, the future of morphodynamic change is still unknown when an accelerated SLR is faced. From 2015 to 2019, the global mean SLR rate was at around 5 mm/year (WHO, 2019) and the SLR rate in Dutch coast was slower at around 3 mm/year (Baart, 2019). Vermeersen et al. (2018) predicted the future SLR along the Dutch coast in different scenarios, corresponding to different situations of greenhouse gases emissions (Table 1.1) and all the scenarios have a higher SLR rate than now. Under the circumstance with accelerated SLR, the ebb-tidal deltas act as the source of sediment. But in the future, if the sediment can be eroded from ebb-tidal deltas become insufficient to cope with SLR, will the tidal basin be empty as well? A more reliable projection of the morphodynamic change is needed as the reference of the future action.

Table 1.1: Sea-level rise scenarios in different time periods (Vermeersen et al., 2018)

Time period	RCP2.6	RCP4.5	RCP8.5
2018–2030	0.06 ± 0.07 m	0.07 ± 0.06 m	0.08 ± 0.06 m
2018–2050	0.16 ± 0.12 m	0.19 ± 0.11 m	0.23 ± 0.12 m
2018–2100	0.41 ± 0.25 m	0.52 ± 0.27 m	0.76 ± 0.36 m

1.3. OBJECTIVE

This thesis aims to assess the future morphodynamic response of the Wadden Sea tidal basin under accelerating SLR. To be more specific, the Ameland inlet is chosen as the research area since it is the tidal Inlet inside the Wadden Sea with least human interventions and it acts relatively independent from the other Waddenzee basins. Therefore, it is more reasonable to assume the bathymetry in Ameland inlet is under equilibrium state. A new hybrid model combined with Delft3D and ASMITA is developed which is less aggregated than ASMITA and also has the fully computed hydrodynamics conditions. This model provides the possibility to connect the physical field data and the long-term morphodynamic trend.

The main objective of this thesis can be specified as:

Investigating the performance of the hybrid model in reproducing the real morphodynamic change in Ameland inlet with respect to SLR and subsidence.

The main objective can be divided into two sub-objectives:

1. Setting up the hybrid model and applying it to the Ameland inlet. Investigating the relationship between the model parameters and morphological response.

2. Predicting the morphological response of the Ameland inlet with SLR and subsidence.

1.4. RESEARCH QUESTIONS

To understand the research objective more easily, several questions are proposed regarding the research objectives mentioned above.

The main question is:

How will the hybrid model perform with different model settings and how well can the model's result reproduce the morphological change with SLR and subsidence?

Which contains several sub-questions:

1. Can the hybrid model predict the basic morphological trend in tidal inlet with SLR? What parameters do matter to the result of the simulation?

2. Compared with previous models, what's the difference?

3. How does the model perform with subsidence?

1.5. OUTLINE

In this Chapter an overview of the Wadden Sea and the potential influence of SLR is introduced. In Chapter 2, to get more familiar with the research area, the Ameland inlet, a general description of the Ameland inlet including its flow, sediment conditions and its long-term morphological evolution is analyzed. Chapter 3 describes the hybrid model which is going to be used in further simulations and its difference with the process-based models and the aggregated models. Also, some adjustments of models are going to be carried out to improve the reliability of the model and shorten the computation time. In Chapter 4, several long-term simulations will be executed with three SLR scenarios. The model's sensitivity analysis with five parameters will also be included in this Chapter. Chapter 5 is going to present the hybrid model's performance in simulating the morphological response to the subsidence induced by gas mining. At the end of this thesis, the discussion on the model and its performance can be found in Chapter 6 and the conclusion can be found in Chapter 7.

2

SYSTEM INFORMATION

2.1. AREA DESCRIPTION

Among all tidal inlets in the Wadden Sea, the Ameland inlet system is assumed as the most autonomous one since it has not been influenced significantly by the closure of the Zuiderzee (1932) or Lauwerszee (1969). And in the past century, the Ameland inlet has not been intervened by massive human activity, e.g., land reclamation and dredging inside the basin. Apart from that, it can be assumed as a relatively closed system that has a minimum connection with adjacent tidal inlets (Ridderinkhof, 1988). Therefore, the Ameland inlet is a preferable choice to study the morphological response to SLR.

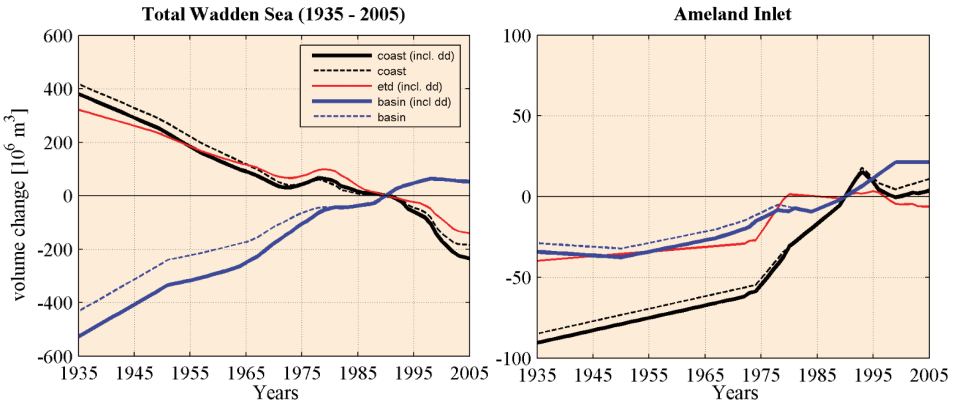

Figure 2.1: Sedimentation/erosion values of the entire Wadden Sea and the Ameland inlet over the period 1935-2005. The values are interpolated from the available datasets (Elias et al., 2012)

Figure. 2.2 depicts the bathymetry of the Ameland inlet archived in 2017. The Ameland inlet locates between the Terschelling island and the Ameland island, connecting the North Sea and the Wadden Sea. The Ameland inlet is composed of the ebb-tidal

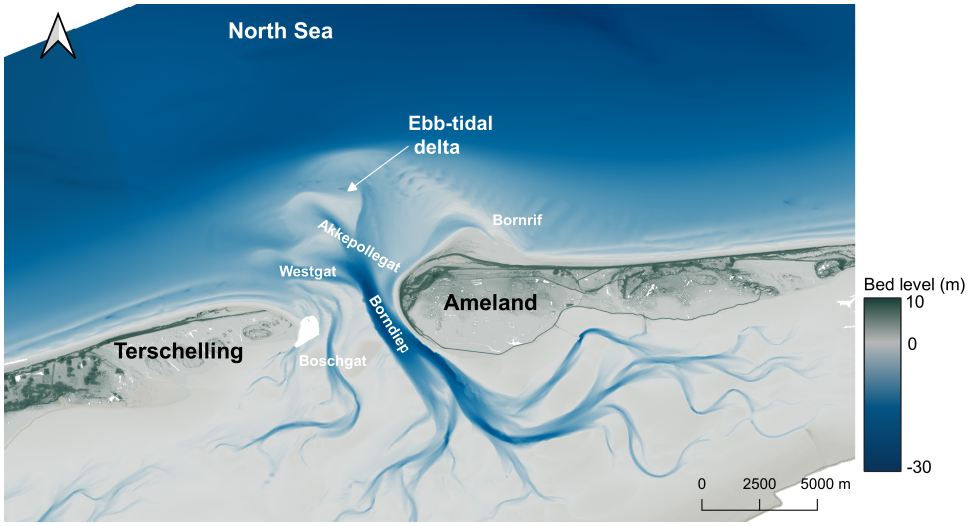

Figure 2.2: The Ameland inlet bathymetry in 2017 (Bathymetry data source: Rijkswaterstaat Vaklodingen. Barrier islands' elevation source: Actueel Hoogtebestand Nederland (AHN), Rijkswaterstaat)

delta, ebb channel, flood channel, intertidal flat and the sandy spit bar in the east of the ebb-tidal delta.

The channel Borndiep is the main flood channel of the Ameland inlet and its deepest part can be found in between two barrier islands close to the Ameland island. Another flood channel is in the east of Borndiep which is much shallower and not as stable as Borndiep. The semi-diurnal tide along the Dutch coast flows in and out the Ameland basin carrying sediment, which forms the ebb-tidal delta and the intertidal area. Meanwhile, the tide propagates in easterly and northerly directions along the coast bypassing the ebb-tidal delta. The sediment from the ebb-tidal delta and west Dutch coast accumulates near the Ameland coast forming the sand spit bar, as known as Bornrif.

Figure 2.1 shows that, for the entire Wadden Sea, the coasts and the ebb-tidal deltas have been eroded and the basins have been infilled over the whole period. But at the Ameland inlet, the ebb-tidal delta and the coasts were accumulating unlike the general trend of the entire Wadden Sea. And in the last a few years, the volume of elements at the Ameland inlet has remained at a stable level.

The Ameland inlet experiences a strong tidal driven current in the alongshore direction at around 0.3 m/s and through the inlet at around 1 m/s (Ehlers, 1988). The tide passing by the Ameland inlet propagates in the northerly and easterly directions at a celerity of about 15 m/s (Cheung et al., 2007). The tidal range near the Ameland is approximately 2.3 m (Pearson et al., 2019). The annual averaged significant wave height is 1.1 m and the dominant direction is northwest (Cheung et al., 2007). Based on the tide and wave conditions, the Ameland inlet is classified as meso-tidal and mixed-energy (Hayes, 1975, Davis Jr and Hayes, 1984). The northwest incident waves encounter the northeastern barrier coastline and generate an easterly alongshore sediment transport of about 0.7 Mm^3/y. Combining the residual tidal current, a total alongshore sediment

transport toward the northeast can reach 1.0 Mm^3/y (Steetzel, 1995).

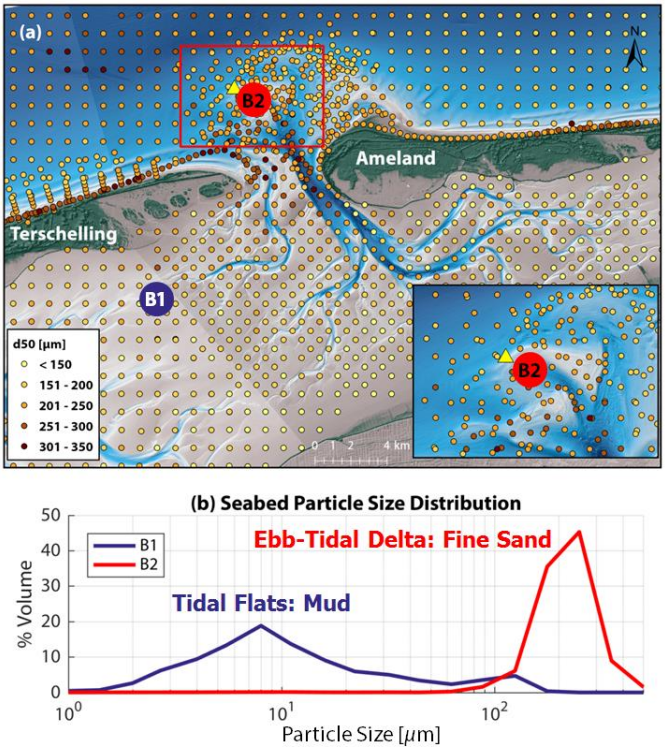

Figure 2.3: (a)Median bed sediment grain size. (b)Particle size distribution in the bed at location B1 and B2. (Pearson et al., 2019)

At the bed of the ebb-tidal delta, fine sands cover the largest part and the averaged median sediment diameter is 211 μm. When it comes to the channel, the sands become coarser and the median diameter increases to 289 μm (Pearson et al., 2019). From Figure 2.3, the sediment along the Terschelling coast is much coarser than that in the Ameland coast. Also, inside the basin, the median diameter of the sediment at the intertidal flat is smaller than that in the channel, and the mud proportion increases as well.

2.2. MORPHOLOGICAL EVOLUTION

One of the most important morphological features of the Ameland inlet is the migration of channels. The channel-shoal structure at the Ameland inlet is not fixed and the area experiences a cyclic evolution with a period of 50 to 60 years (Isreal, 1998).

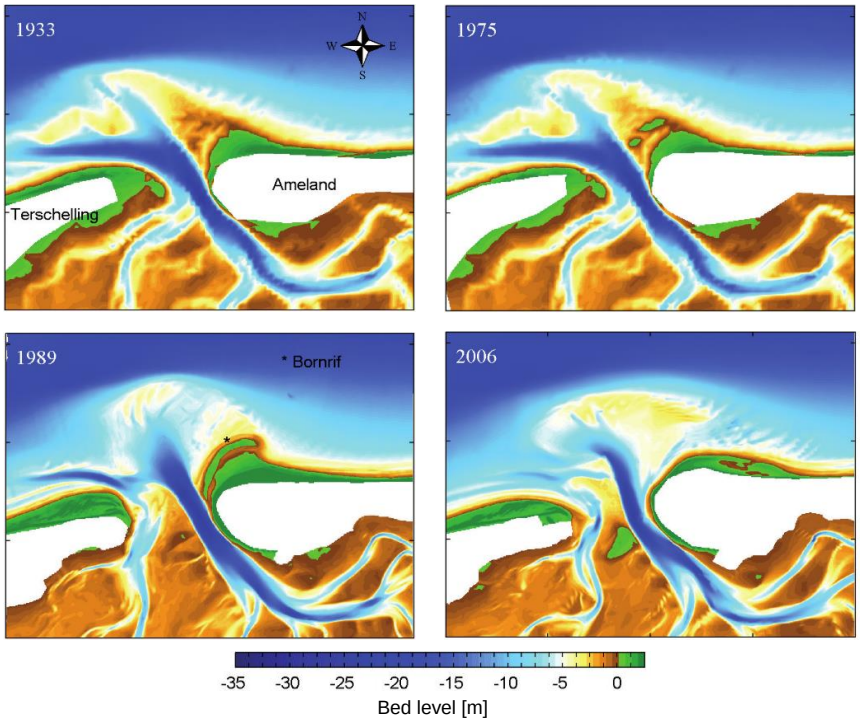

Figure 2.4: Cyclic evolution of the channel and ebb-tidal delta at the Ameland inlet (Elias et al., 2012)

Figure 2.4 shows that, the channel-shoal structure has been switching from the one-channel system to a two-channel system. Not only channels were evolving, but the ebb-tidal delta was also changing consequently. Cheung et al. (2007) gave a specific analysis of the cyclic behavior. In Figure 2.5 (a), a typical one-channel configuration is shown that two ebb channels, Westgat and Akkepollegat are directly connected to the main channel Borndiep. The ebb-dominant Westgat has a phase lag with the east-west lying Boschgat, which turns the direction of the Boschgat toward the north and forces it to have a more direct connection with the Westgat. Meanwhile, another ebb-dominant ebb channel, Akkepollegat, provides abundant sediment to the shoal, forming the bypassing sand bars, Bornrif. In Figure 2.5 (b), the Boschgat is partially connected with the Westgat and at the same time, the Borndiep flat expands to the north, which enhances the flow from the Borndiep to the Akkepollegat and weakens the flow to the Westgat. A stronger flow at the Akkepollegat carrying more sediment causes a migration of the Bornrif approaching the Ameland. With further development, in Figure 2.5 (c), the weak flow at the Westgat turns from ebb-dominant to flood-dominant and attracts lots of sediment. The in-

creased sediment demand induces the assembling of sediment near the Terschelling and eventually blocks the connection between the Westgat and the Boschgat. The Boschgat becomes an east-west running channel again. Meantime, the attached Bornrif becomes a progressive, attenuating sand wave along the Ameland with the current. To prevent severe erosion and maintain the Borndiep, a series of erosion control measures, such as building groynes along the coast and periodic nourishment at the Ameland, have been applied since 1947 (Elias et al., 2012).

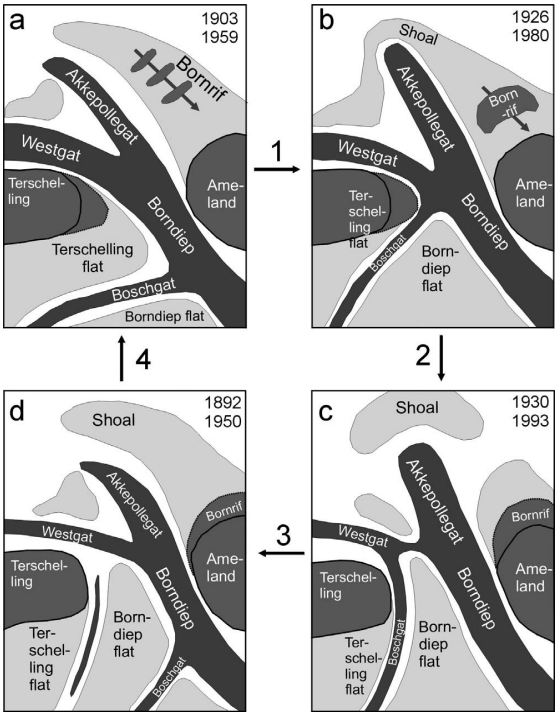

Figure 2.5: Cyclic evolution of the Ameland inlet between one-channel system and two-channel system

3

MODEL

3.1. PREVIOUS STUDY

Choosing a proper model is of great importance to the simulation result. Suspended sediment transport is the key to reproducing the bed level change. Sediment transport is based on the hydrodynamic conditions which are determined by model calculation. Generally, there are two types of model used regarding the morphodynamic change in the tidal basin which are **Process-based model** (e.g., Delft3D) and **Aggregated model** (e.g., ASMITA). The difference between the two types of model is the aggregation level which will be illustrated in the following sections.

3.1.1. PROCESS-BASED MODEL

The process-based model's calculation can be separated into the hydrodynamic and morphodynamic parts. By solving the continuity equations and momentum equations with shallow water assumptions, the hydrodynamic conditions are calculated from the model. Under the shallow water assumption, the vertical acceleration due to buoyancy or bottom topography change is negligible compared with the gravity acceleration. The vertical momentum equation is reduced to the hydrostatic pressure equation (Eq. 3.1) which simplifies the computation along the coast or inside the tidal basin.

$$\frac{\partial p}{\partial z} = \rho g z \tag{3.1}$$

Besides that, the advection-diffusion equation with the turbulence closure model solves the transport of physical quantities (e.g., salinity, temperature, and sediments) (Lesser et al., 2004). Based on the calculated flow conditions, the morphodynamic change can be calculated from the sediment transport. For a normal 3D process-based model, the sediment transport is simulated in both horizontal and vertical directions. For an aggregated 2DH model, the hydrodynamic part remains the same as the 3D model but the transport part is aggregated over depth.

The three-dimensional advection-diffusion equation (mass conservation, Eq. 3.2) described the sediment transport no matter what model is used. The process-based

model is the model with the lowest aggregation level, which means the model can reproduce the 3D sediment transport processes approaching reality.

$$\frac{\partial c}{\partial t}+\frac{\partial uc}{\partial x}+\frac{\partial vc}{\partial y}+\frac{\partial wc}{\partial z}-\frac{\partial}{\partial x}\left(\varepsilon_x\frac{\partial c}{\partial x}\right)-\frac{\partial}{\partial y}\left(\varepsilon_y\frac{\partial c}{\partial y}\right)=w_s\frac{\partial c}{\partial z}+\frac{\partial}{\partial z}\left(\varepsilon_z\frac{\partial c}{\partial z}\right) \tag{3.2}$$

Where:

c	= sediment concentration
t	= time
u, v, w	= flow velocity components
x, y, z	= coordinates
$\varepsilon_x, \varepsilon_y, \varepsilon_z$	= turbulent diffusion coefficients
w_s	= settling velocity of sediment particles

Delft3D is one of the most common process-based models used in the morphodynamic simulations. The low aggregation level of Delft3D can reproduce the hydrodynamic conditions more precisely and depicts the sediment transport processes approaching reality. The advection and diffusion terms are shown on the left side of the Eq. 3.2, and the right side is the sediment exchange in the vertical direction containing the settling and diffusion processes. The turbulent diffusion coefficients are normally unknown, which requires the user to choose a suitable model to close the equation. In Delft3D, the 2D turbulence can be specified by users beforehand or computed by an embedded Large eddy simulation (LES) model. The 3D turbulence is closed by the selected model, such as the $k-\epsilon$ model. The multiple modules supported by Delft3D provide the possibility to introduce wind, storm and other factors into the model. However, meanwhile more field data, for example, the bed composition, water level record, wind spectrum, is needed for the accuracy of more complex computations.

In a short-term simulation, Delft3D can be more suitable due to the higher accuracy, and more parameters can be explicitly determined in the calculation. But for a long-term simulation, Delft3D would become not that suitable compared to other models with higher aggregation levels due to the much longer computation time and the uncertainty in the equilibrium state. Dissanayake et al. (2012) used the Delft3D numerical model to predict the future morphological change at the Ameland inlet under different SLR situations. The model successfully reproduced the erosion at the ebb-tidal delta when SLR was applied and the flood dominance is enhanced which may lead to more sediment import. But the result still remained at a qualitative level and the computed critical SLR is far from the previous study due to too many uncertainties.

3.1.2. AGGREGATED MODEL

After a further aggregation in space and in time, the so-called aggregated model (or semi-empirical model) is established. Wang et al. (1998) and Stive (1998) firstly developed the ESTMORF and ASMITA, the two most usual models among aggregated models, in the morphological change at estuaries and tidal basins.

In the ESTMORF model, the computation area is schematized into a node's mesh connected by branches(channels). The sediment can be transported between the low

tidal flat, high tidal flats and channels. To obtain the change in channels, the 3D advection-diffusion equation (Eq. 3.2) is aggregated over-depth and width remaining the cross-section area in the formula. An example between channel and low tidal flat is shown below.

$$\frac{\partial A_{sc} c_c}{\partial t} + \frac{\partial A_{sc} u c_c}{\partial x} - \frac{\partial}{\partial x}\left(A_{sc} D_c \frac{\partial c_c}{\partial x}\right) = W_c w_s (c_{ce} - c_c) + F_{lc} \tag{3.3}$$

$$F_{lc} = D_1 \cdot \overline{\Delta h_l} \cdot \frac{c_l - c_c}{L_{lc}} \tag{3.4}$$

$$c_{ce} = C_E (\frac{A_{ec}}{A_{sc}})^n \tag{3.5}$$

Where:

A_{sc} = cross-sectional area of the channel
A_{ec} = equilibrium cross-sectional area of the channel
c_{ce} = equilibrium concentration in the channel
C_E = global equilibrium concentration
c_c = concentration in the channel
D_c = horizontal dispersion coefficient in the channel per unit width
F_{lc} = exchange rate of sediment between the channel and the low tidal flat per unit width
u = residual flow velocity
W_c = width of the channel
D_l = diffusion coefficient per unit width
$\overline{\Delta h_l}$ = effective water depth for low tidal flat
L_{lc} = distance between the center of the low tidal flat and the center of the channel

In the channel, the 3D hydrodynamic condition becomes 1D after integration, and the advection and diffusion terms are still valid here. But only the diffusion effect is taken into account when the transport happens between the flat and the channel (F_{lc}). In the ASMITA model, the whole domain is schematized into several elements and a further aggregation is applied for the whole area of each element. These elements including the ebb-tidal delta, main channels, the intertidal flat area can exchange sediment with adjacent elements directly.

$$\frac{dV_n}{dt} = \mu_n A_n w_s (c_{ne} - c_n) \tag{3.6}$$

$$\sum_m \delta_{mn} (c_n - c_m) = A_n w_s (c_{ne} - c_n) \tag{3.7}$$

$$c_{ne} = C_E (\frac{V_{ne}}{V_n})^n \tag{3.8}$$

Where:

V_n = volume of the element
V_{ne} = equilibrium volume of the element
μ_n = when referring to wet (channel) volume, it is equal to 1 and when referring to dry (intertidal area or delta) volume, it is equal to -1.
A_n = horizontal area of the element
δ_{mn} = horizontal exchange coefficient

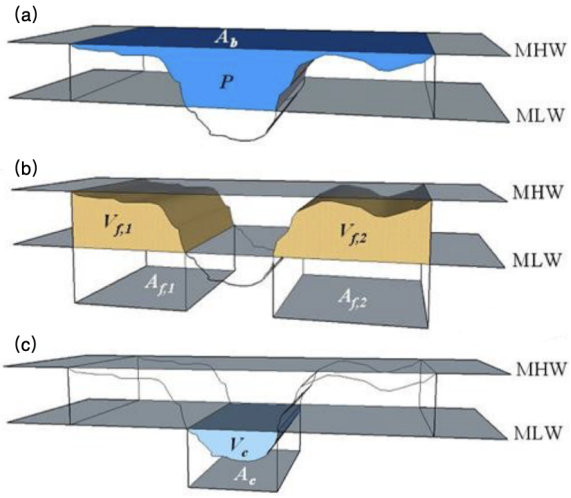

Figure 3.1: The volume of elements in the tidal basin: (a)Tidal prism and the area of the tidal basin, (b)Volume of the intertidal area, (c)Volume of the channel. (Wang, 2019)

Compared with ESTMORF, ASMITA ignore the advection transport exchange where the residual flow is assumed to be zero. Within one certain element, the sediment in the water column is conservative between the diffusion exchange with adjacent elements and the exchange with the bed. What is worth mentioning is the volume of each element can be separated into wet and dry volumes (Eq. 3.6). According to Figure 3.1, the volume of the channel is referring to the space between the MLW and the bed, which is wet volume. However, the volume of the intertidal area, the dry volume, is the sediment between the MHW and the MLW. When erosion happens, the wet volume will increase but the dry volume will decrease obviously.

Both ESTMORF and ASMITA model have a similar concept which is the equilibrium concentration (c_{ce} in Eq. 3.3 and c_{ne} in Eq. 3.6). Actually in Delft3D there is a similar concept in the open boundary which describes the sediment concentration which will not induce any erosion or sedimentation under the current flow conditions. The principle behind the equilibrium state in the aggregated model is analogous. In Eq. 3.8, the ratio between the current volume (V) of the element and the equilibrium volume (V_e) reflects the flow strength in the area. For instance, when the channel volume is bigger than its equilibrium volume and the tidal prism keeps the same, the flow velocity must decrease due to the wider cross-section.

The high aggregation level and the equilibrium state make the model be more robust

when faced with SLR. Even though it cannot reflect the bathymetry change in detail as Delft3D does due to the aggregation in space, it still can predict the trend in morphology precisely. Buijsman (1997) applied the ASMITA model at the Zoutkamperlaag inlet and the Pinkegat inlet to project the future morphological change with different SLR rates. The ASMITA model successfully reproduced the erosion in channels, regression at the coast and accumulation at the intertidal area. Later, Van Goor et al., 2003 also applied the ASMITA model in the Ameland inlet with coarser schematization (fewer elements). Except for predicting the morphological change with SLR, the critical SLR rate is proposed which is the maximum rate that the tidal basin can keep pace with and regain the equilibrium state. For a more reliable result, Wang and Van Der Spek (2015) calibrated the ASMITA model by taking finer sediment into account. Even though this didn't make the model be more reliable compared to the previous setting with only one fraction of sediment, but it did close the gap between the process-based model and the aggregated model in the calculation of critical SLR rate.

However, as mentioned above, the highly aggregated model is dependent on the empirical relationships and the underlying processes may be partially ignored. Wang et al. (2020) also pointed out that no matter what level the models are aggregated in, they are in the same degree of uncertainty. Besides that, those so-called micro-scale models like Delft3D, may find difficulties in reproducing the equilibrium status.

3.2. HYBRID MODEL

For the sake of a more robust performance in the projection of morphodynamic change, a hybrid model combining the process-based model and the aggregated model is developed. When faced with long-term simulation with natural bathymetry, the process-based model usually cannot reproduce the trend accurately and also it is normally time-consuming due to the complicated three-dimensional computation. A ten-year simulation usually takes days or even weeks depending on the area of domain and size of the grid. As for the aggregated model (e.g., ASMITA), it can reflect the morphodynamic trend of the tidal basin with respect to SLR. But it has the limitation in presenting the detail in bathymetry change. Also, due to the aggregation in space inside the basin, when faced with the regional ground subsidence, it is difficult to apply the subsidence only to a certain area.

Therefore, the two-dimensional hybrid model is going to be applied in simulating the morphodynamic change in the Ameland inlet with respect to SLR. The difference between the process-based model, the hybrid model, and the aggregated model is the aggregation level and whether the equilibrium concept intervenes the morphological change. The hybrid model is aggregated in the vertical direction but not in the horizontal direction, which makes its aggregation level is in between the three-dimensional process-based model and the aggregated model.

On the basis of the 3D advection-diffusion equation (Eq. 3.2), the sediment transport is integrated in vertical direction and the 2D advection-diffusion is shown as follow:

$$\frac{\partial h\bar{c}}{\partial t} + \frac{\partial \alpha_x \bar{u_x} h\bar{c}}{\partial x} + \frac{\partial \alpha_y \bar{u_y} h\bar{c}}{\partial y} - \frac{\partial}{\partial x}(D_x h \frac{\partial \bar{c}}{\partial x}) - \frac{\partial}{\partial y}(D_y h \frac{\partial \bar{c}}{\partial y}) = f_b \tag{3.9}$$

Where:

$\bar{c}$ = depth-averaged sediment concentration
$\bar{u_x}, \bar{u_y}$ = depth-averaged flow velocity components
h = water depth
α_x, α_y = coefficients counting for the effects of the shapes of the vertical distribution of flow velocity and sediment concentration
D_x, D_y = dispersion coefficients
f_b = sediment exchange flux between the bed and the water column

In the depth-integrated advection-diffusion equation, the advection (2^{nd} and 3^{th} on LHS) terms and the diffusion (4^{th} and 5^{th} on LHS) terms are in agreement with the normal 2D process-based model, for example, the depth-averaged model in Delft3D. What makes them different is the way to calculate sediment exchange flux on LHS. The sediment exchange flux contains the settling and stirring processes in different flow conditions. Normally, the sediment flux is expressed in the form as the Eq. 3.10. What is worth mentioning is the hybrid model only takes suspended sediment transport into account and the bed load is neglected.

$$f_b = \gamma w_s (c_e - c) \tag{3.10}$$

Where:

γ = transport coefficient
w = settling velocity
c_e = equilibrium sediment concentration
c = local sediment concentration

As discussed in Section 3.1.2, the flow condition can be connected with the suspended sediment formula. Normally, sediment transport can be expressed as: $S \propto u^n$ (Buijsman, 1997). After time-averaging, the suspended sediment transport $<S_s>$ is proportional to the odd moment$<u|u|^3>$ and the even moment $<|u|^5>$ (Bosboom and Stive, 2021). The power n in Eq. 3.11 is in agreement with that in the sediment transport formula. Back to the hybrid model, similarly, the flow strength can be reflected by the local depth (h) with equilibrium depth (h_e, Eq. 3.11).

$$c_e = C_E (\frac{h_e}{h})^n \tag{3.11}$$

The equilibrium water depth should be determined beforehand, which is downward positive and relative to the reference level specified in the model (0 m is the default value). When SLR is introduced into the model, the equilibrium water depth doesn't get influenced by the change of SLR. But the local water depth is increasing when SLR is positive since the reference level is lifted (Figure 3.2). So in this way, the corresponding water depth needs to decrease to adjust to the rising sea level, approaching equilibrium depth again. Within a short period that the morphodynamic change hasn't responded, there will be a deviation between the increased local water depth and the equilibrium water depth which are the same before SLR starts. The deviation in water depth will induce a change in local equilibrium concentration which leads to a further change in sediment exchange flux in the vertical direction. As shown in Figure 3.3, the negative

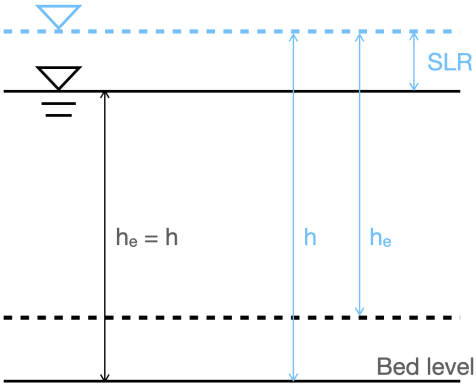

Figure 3.2: The definition of h and h_e (the solid lines indicate the water and bed level before SLR and the dash lines indicate the after)

feedback keeps the bed level sedimentation in pace with SLR when sediment supply is sufficient.

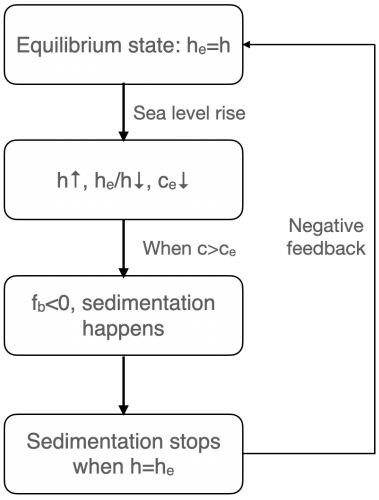

Figure 3.3: The negative feedback loop of the hybrid model

To conclude, the hybrid model is integrated in depth from the three-dimensional process-based model and the difference is the way to calculate sediment exchange flux between water column and bed. An equilibrium concept is inherited from ASMITA and ESTMORF model which decides the morphodynamic evolution's direction with respect to the sea level rise. The equilibrium concept always guides the bed level to move directly to the direction of the sea level change, which increases the robustness compared with the normal process-based model. In principle, there is no difference in the uncertainty level among the process-based model, the hybrid model, and the aggregated model. The

only difference is the level of aggregation.

3.3. MODEL FORMULATION

Before the simulation starts, the formulation of the model is a necessary step which is of great importance to the computation time and the accuracy of the model result.

3.3.1. GRID AND BATHYMETRY

The computation area is selected to cover all the tidal basin areas and a certain offshore area to simulate SLR and its influence. It expands about 44 km in the west-east direction and 36 km in the north-south direction. The computation domain and the grid is developed by De Fockert (2008) and later modified by Jiao (2014). The domain includes 324 grid points in east-west(x) direction and 348 grid points in north-south(y) direction. The Figure 3.4 shows the computation domain and the grid arrangement. For a clearer illustration, the grid has been derefined to half of the original number. The size of grids varies from the location, the grids near the throat of the Ameland basin are refined since the flow is more complicated here. Therefore, the size of grids changes from 300-350m at the boundaries to 30-40m at the inlet.

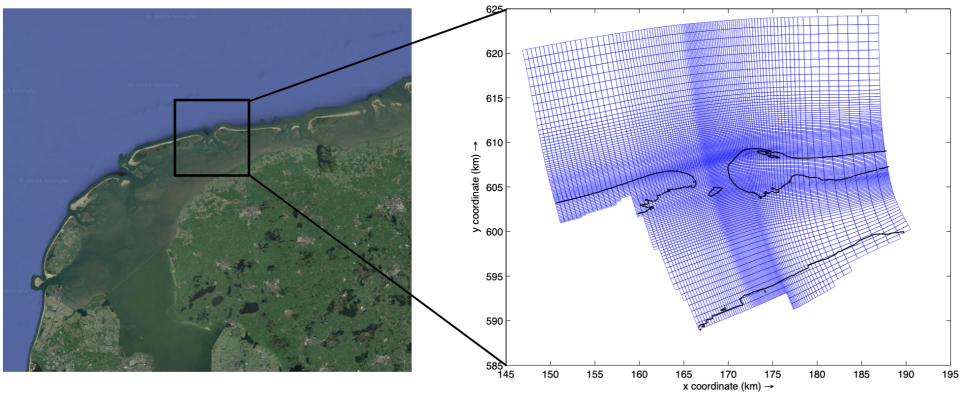

Figure 3.4: Computation domain and the grid (Left figure: Google Maps location of the Dutch Wadden Sea. From "Google Maps," by Google, n.d. (https://earth.google.com/web/@53.28453218,5.57895,-17.3108632a,123495.07922972d,35y,0h,0t,0r). Copyright by Google.)

The bathymetry in 2005 is chosen as the initial bathymetry in this model. From offshore to onshore, the water depth decreases from 27 m at the north boundary to 0 m at the barrier island beaches. The ebb-tidal delta is submerged and the water depth varies between 3 and 6 m. The deepest part inside the tidal basin is found at the main ebb channel, Borndiep, which is 26-meter deep at the throat and becomes shallower in onshore direction. The total areas of different elements of the Ameland inlet are shown in Tab. 3.1 and the definition of the area is described in Figure A.1. The area is calculated from the MSL at 0.05 m and the tidal range (H_m) at 2.4 m.

Table 3.1: The area of ebb channels and intertidal flat inside the Ameland inlet

Element category	Area [m^2]
Channel	1.147×10^8
Intertidal flat	1.985×10^8

3.3.2. PARAMETERS

The time step of the hydrodynamic calculation is chosen at 12 seconds according to the Courant number, which promises the numerical stability of the calculation. In practical cases, normally it's recommended to choose a proper time step to make Courant number smaller than 10 and the calculation of Courant number is specified in Appendix A.3. The water depth is used in the calculation of the Courant number will be introduced in the later section.

The default value of horizontal viscosity and diffusivity follow Jiao (2014), which are both 1 m^2/s. And the bed roughness is prescribed with the Chézy formula at 63 $m^{\frac{1}{2}}/s$ for the grids within the domain (Lenstra et al., 2019). One single non-cohesive sediment with the median diameter (d_{50}) of 250μm is applied and the sediment is assumed to separate homogeneously within the domain (De Fockert, 2008, Jiao, 2014).

The power n in Eq. 3.11 is chosen at 5 from the sediment transport formula (Bosboom and Stive, 2021). The global equilibrium concentration(C_{eq}) is firstly set at 0.045 kg/m^3 which to be discussed in sensitivity analysis.

3.3.3. BOUNDARY CONDITIONS

There are three open boundaries in the offshore area located in the north, west, and east. For the northern boundary, a harmonic water level boundary condition is applied and the boundary is separated into seven continuous boundaries to avoid incorrect interpolation along the boundary. The harmonic water level condition was derived by Jiao (2014). Jiao firstly computed the three water level boundaries of the Ameland inlet with the nesting tool under the simulation of the whole Wadden Sea.

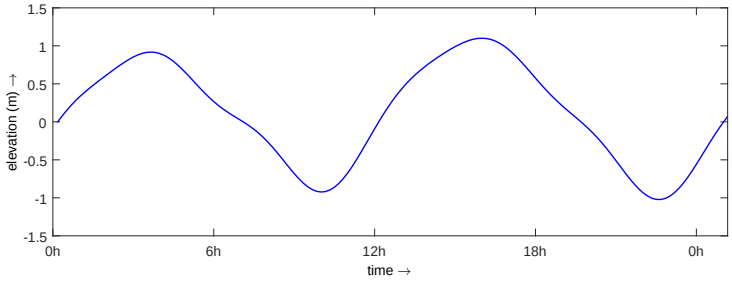

Figure 3.5: Water levels at the Northern boundary

To reproduce the residual transport of the complete spring-neap tide cycle in the long-term simulation and save the computation time, a morphological tide was chosen among the whole time-series water level records at the boundaries to represent the

residual transport as much as possible (Latteux, 1995). Due to the daily inequality at the Ameland system, a double tide cycle was chosen from two spring-neap cycles and the water level records were transformed into a harmonic boundary by using harmonic analysis. The tidal constituents are shown in Table A.1. Among the eight constituents, the O1, M2, M4, and M6 are the main components according to the amplitude.

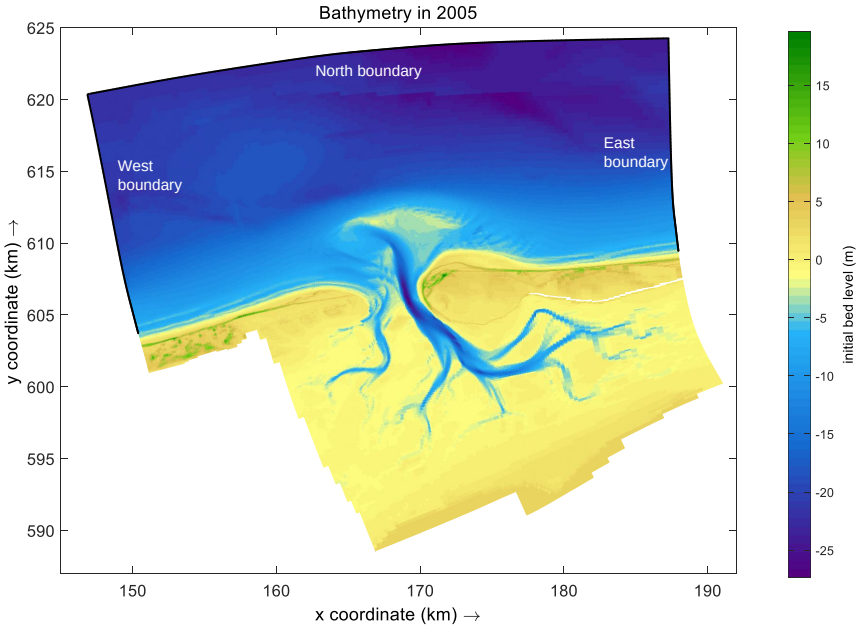

Figure 3.6: Bathymetry of the Ameland inlet in 2005 and three open offshore boundaries

In terms of the east and west boundaries, the Neumann conditions were applied. The Neumann boundary can prevent the happening of boundary disturbances and make it not necessary to determine the water level or velocity boundaries beforehand.

Inside the Ameland inlet, three closed boundaries are located in the North(landward), West and East. The Western and Eastern closed boundaries are at the watershed where the water and sediment would barely exchange with adjacent tidal basins (Bosboom and Stive, 2021). Therefore, the Ameland inlet can be assumed to be isolated with the Vile inlet in the west and the Pinkegat inlet in the east. The three closed boundaries together with the Terschelling island and the Ameland island form the Ameland tidal basin.

At the beginning of the simulation, the sediment concentration at the water column is set at 0, which is called cold start. In this case, the spin-up time is necessary otherwise the deviation between the local concentration and the local equilibrium concentration, and a local erosion will happen immediately. Within the spin-up time, no bed level change is allowed and the water carrying sediment will flow from the boundaries to the basin. A spin-up period at 2980 minutes, two tidal cycles, is applied, which promises the local concentration inside the basin is equal to the sediment supply at the boundaries.

3.3.4. REFERENCE LEVEL

The hybrid model is based on the Delft3D model, in which the reference level is set automatically at 0 m. The depth and water level are both referred to this reference level. After supplementing the hybrid model, another reference level can be specified by users which is related to the equilibrium depth. For a clearer statement, the reference level mentioned later is referred to the equilibrium reference level.

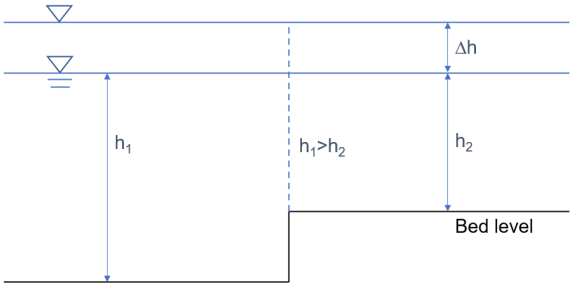

Figure 3.7: Two adjacent cells with different equilibrium water depth

As Figure 3.7 shown, with the unchanged reference level, the equilibrium depth is equal to the local depth when SLR hasn't been applied. And then an elevation is applied to the reference level and the Eq. 3.11 changes to the Eq. 3.12. Obviously, under the situation that Δh_2 keeps unchanged, when $\Delta h_1 > 0$, c_e becomes bigger, which means that the elevated reference level makes the vertical sediment exchange be less sensitive to SLR. Physically, when an elevation is applied at the reference level within the whole basin, the sensitivity of the shallower area, such as the intertidal flat, to SLR will decrease more dramatically than the deep area, which means a higher reference level will make the shallow area attract less sediment. As the default setting, the reference level is set at 0 m. The influence of the reference level is elaborated in Appendix A.4.

$$c_e = C_E\left(\frac{h_e + \Delta h_1}{h + \Delta h_1 + \Delta h_2}\right)^n \tag{3.12}$$

Where:

Δh_1 = reference elevation
Δh_2 = Sea-level rise

3.4. MODEL SETUP AND STANDARD RUN

Before the long-term simulations start, a standard run with the basic setting is necessary with parameters set as their "default value" described in the previous section. Those parameters are decided at the very beginning and only according to the known data. And the result of the standard run is worth being studied because it reflects the model's performance to SLR and from the result, we can investigate how does the model work.

With a MORFAC at 100, after 13.6 morphological years experiencing a total lift of MSL at 13.6 cm (1 cm/year), the channels inside the basin are eroded and there is a vast

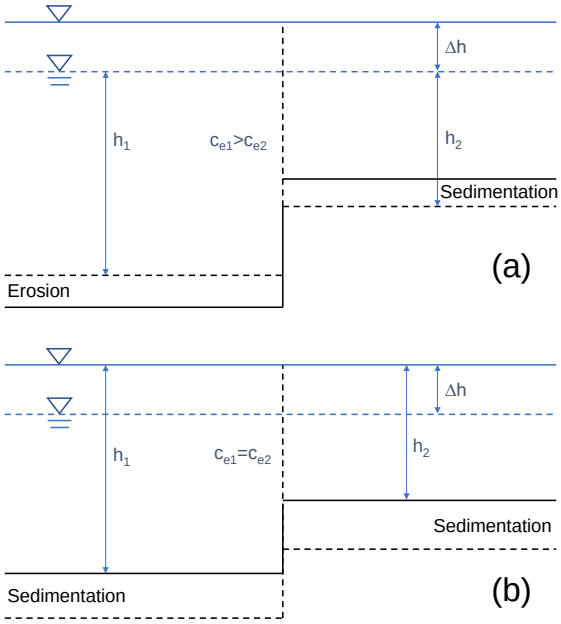

Figure 3.8: Morphological change in two adjacent cells with different equilibrium water depth in the hybrid model (a)stage 1: deeper cell starts to be eroded and shallow cell is accumulated, (b)stage 2-3: bed level for both cells lifts and water depth reaches the initial water depth

intertidal area where sediment accumulation happens. Also, the ebb-tidal delta shows a similar behavior with respect to SLR: some sediment is accumulated at the shallow part. This can be explained by the Eq. 3.11 that the shallow part (intertidal flat and ebb-tidal delta) has a smaller water depth and the channel has a much deeper bed. As shown in Figure 3.7 and the equation below, when applying the same SLR rate to the whole area, the smaller-depth area (h_2) is more sensitive to SLR and the equilibrium concentration at the smaller-depth area (c_{e2}) will decrease more than that of the larger-depth area (c_{e1}).

$$h_1 > h_2 \rightarrow \frac{h_1}{h_1 + \Delta h} > \frac{h_2}{h_2 + \Delta h} \rightarrow c_{e1} > c_{e2}$$

Therefore, sediment is more likely to accumulate in the area with a smaller equilibrium concentration. In the Figure 3.7, two adjacent cells with different depths are briefly shown which will be introduced as an example later. To reach a stable status, the equilibrium concentration of adjacent cells have an intention to decrease the difference, which means the area with a deeper depth (h_1) should be eroded to obtain a smaller equilibrium concentration (c_{e1}) close to c_{e2} at the early stage. Meanwhile, sedimentation is happening in the area with a smaller depth. The advection transport by cyclic flow inside the basin and the diffusion transport are the two main processes in the morphological change. So at stage one, the deeper cell will keep being eroded until the shallower cell reaches the same equilibrium concentration. The sediment accumulated

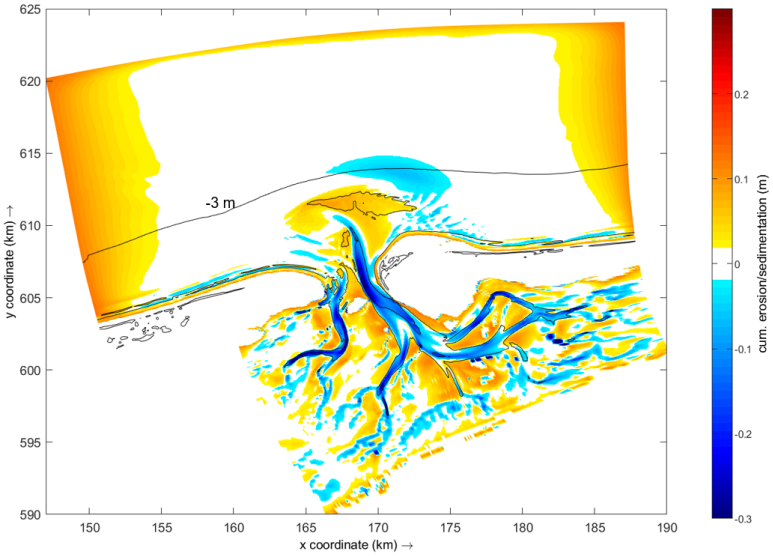

Figure 3.9: Cumulative sedimentation/erosion map after 13.6 years for the case with default setting (solid black line is the contour line of -3 m of initial bed level)

at the shallower cell is from the deeper cell and the boundary (Figure 3.8(a)).

At stage two, the deeper cell stops being eroded and the sedimentation will happen at both cells since the equilibrium concentration of both cells is smaller than the boundary concentration, which is equal to the global concentration. At stage three, two cells reach the equilibrium concentration as before and keep elevating with SLR (Figure 3.8(b)).

As the Figure 3.9 shown, inside the basin, a vast area with sedimentation can be found at the intertidal flat and the channel is deepened significantly. These behaviors are in agreement with the stage one introduced previously: the deeper parts are less sensitive to SLR so they will be eroded to balance the local equilibrium concentration with the adjacent area. In the ASMITA model, this behavior is shown in a similar way that the channel connects the intertidal area and the outside of the basin, and the channel is eroded to create a larger concentration gradient to attract more sediment into the basin (Van Goor et al., 2003). As for the area outside of the basin, the ebb-tidal delta accumulates as well since it behaves similar to the intertidal area. Therefore, a small nearby offshore area is eroded (the blue area next to the ebb-tidal delta) which can be assumed as the redistribution of the sediment. But this phenomenon is opposite to reality. When SLR is accelerated, the inlet is out of dynamic equilibrium and the sediment inside the basin is insufficient to keep pace with SLR. In this case, the ebb-tidal delta will act as the source of sediment and the delta will be eroded.

At three boundaries, the sediment concentration is set at 0.045 kg/m^3 which is equal to the global concentration (C_E). However, the reference level of all offshore grids is lifted at the same time and those grids need to keep pace with SLR as well. The tide-driven flow's direction is always parallel to the coast (Figure 3.10) which means the sediment exchange in cross-shore direction is not frequent. As Figure 3.9 shown, the sedimenta-

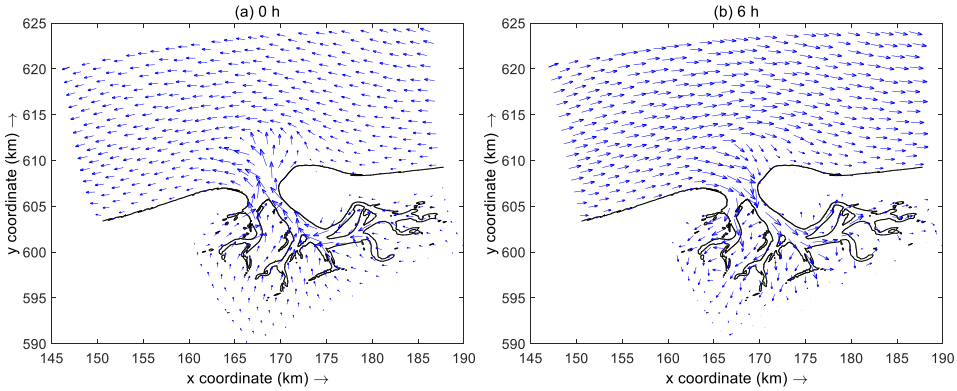

Figure 3.10: Velocity profile of the Ameland inlet during ebb (a) and flood (b)

tion only happens near the west and the east boundary, and the sediment redistribution similar to the basin doesn't happen in the offshore area. Even though the nearshore area has a shallower water depth which may help it attract more sands, the parallel flow limits the cross-shore sediment redistribution. The diffusion term may enhance the transport along the concentration gradient, but in this case, it is obvious that the default value of the diffusion term doesn't influence the transport significantly. From the Figure 3.11, as time goes, the gap between the local equilibrium concentration and global equilibrium concentration is getting bigger, which means the intertidal area cannot keep pace with SLR of 1 cm per year within this period.

Overall, the hybrid model with basic settings successfully reproduced the trend of the morphological change with respect to SLR, especially inside the basin. But there are also some details that should be discussed and some parameters are still to be determined. The offshore sea bed and the ebb-tidal delta tend to elevate with SLR which may attract too much sand that needs to be transported into the basin.

3.5. MODEL ADJUSTMENT

From the result of the standard run in Section 3.4, too much sediment settled near the boundaries and the ebb-tidal delta before entering the basin. This could result in a deficit of sediment supply and too much erosion at the channel. To cope with this problem, some methods are proposed.

3.5.1. LIMITED SEDIMENT AVAILABILITY

The local water depth (h) increases and exceeds the local equilibrium depth, leading to sediment accumulation. Therefore, the offshore accumulation can be limited by increasing the equilibrium water depth together with limiting the sediment availability that can be eroded. According to the Eq. 3.11, increasing the local equilibrium depth and making it exceed the local depth results in erosion but making the sediment availability at the offshore area at zero can counteract the erosion, which keeps the bed from being eroded.

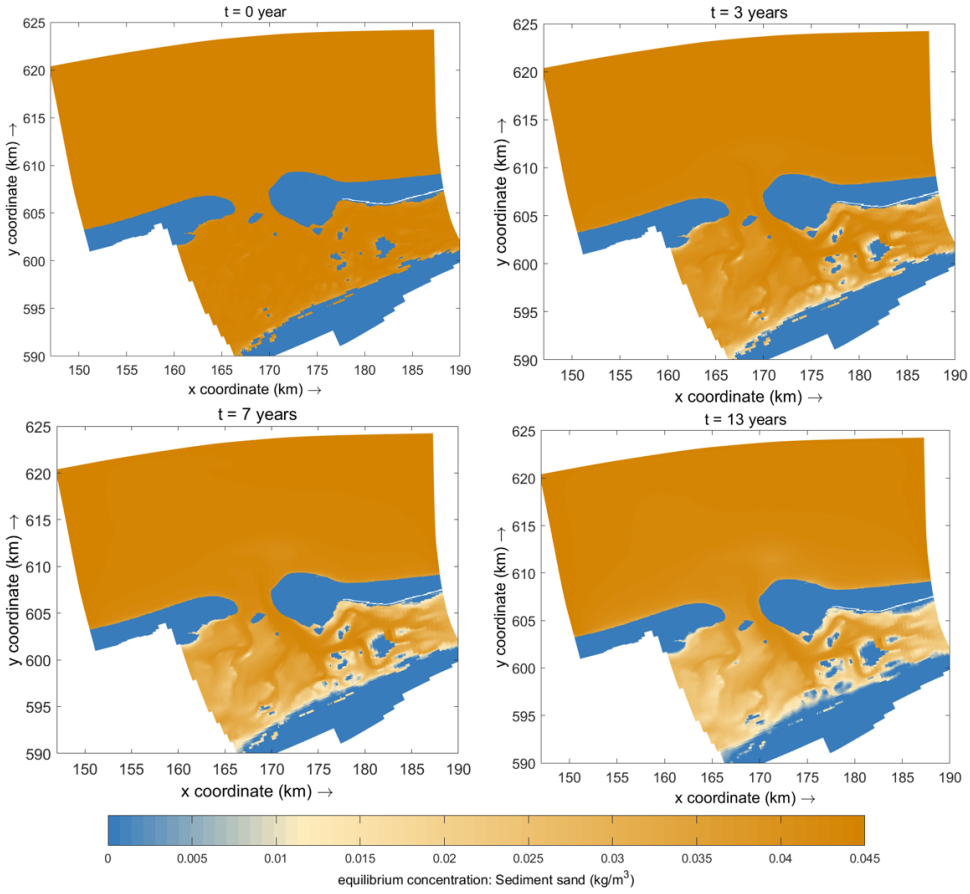

Figure 3.11: Equilibrium concentration evolution at the Ameland inlet with respect to the sea-level rise

The area outside the Ameland basin excluding the ebb-tidal delta is labeled (the blue area in Figure 3.12). For the labeled area, the equilibrium water depth is no longer equal to the initial depth but 10-meter deeper and the sediment availability is zero. That means when SLR is applied, the local depth increases but it is still smaller than the equilibrium depth. However, there is no sediment that can be eroded at the labeled area. The sediment at the water column will not settle earlier than approaching the ebb-tidal delta.

According to the bed difference at the end of the simulation shown in Figure 3.13, the case with no sediment availability outside the basin has no sedimentation outside the basin, and has slightly more sedimentation outside the ebb-tidal delta. But the bed level at the ebb-tidal delta and inside the basin are totally the same at the end of the simulation. This implies that the ebb-tidal delta traps the most of sediment which is supposed to be transported into the basin.

By applying this adjustment, the sediment from the boundaries will not accumulate just right after entering the domain. But the result also shows that the ebb-tidal delta is

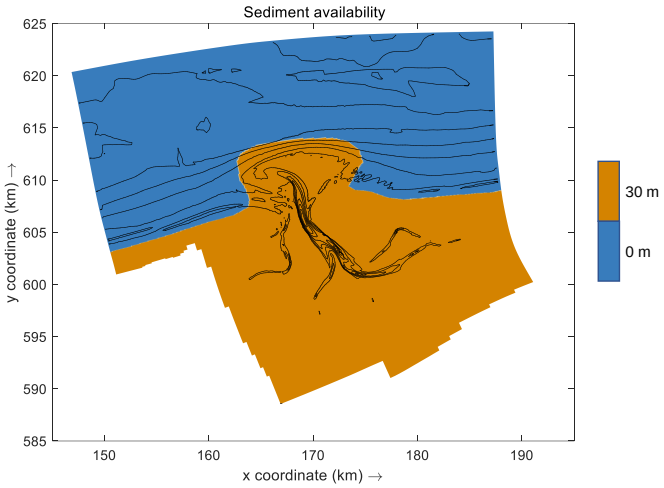

Figure 3.12: Sediment availability within the domain (solid line indicates the contour of the initial bed level)

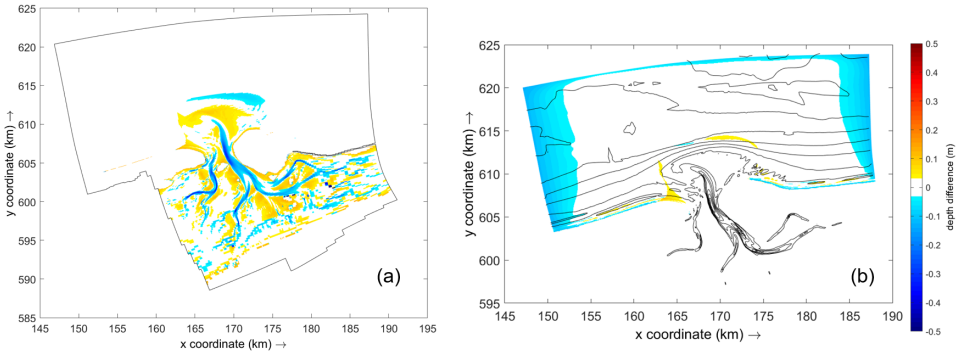

Figure 3.13: (a) Cumulative sedimentation/erosion of the case with no sediment availability at the offshore area. (b) Bed level difference between the case with sediment outside and without sediment outside ($\nabla_{\text{without sediment outside}} - \nabla_{\text{original}}$).

exactly the main trap of sediment. What's the role that the ebb-tidal delta really plays in reality is still ambiguous.

3.5.2. BED ELEVATION/SUBSIDENCE

To deal with the problem that sediment accumulates at the offshore area because the bed level cannot keep pace with SLR, an elevation is added to the offshore area manually at the same rate as SLR by applying the **subsidence** function in Delft3D to the model. The subsidence function provides the possibility to change the bed level regionally in time and the value of subsidence can be negative (elevation) or positive (subsidence). Therefore, if the bed level can elevate at the same rate as SLR, there will be no difference in the equilibrium depth and the local depth. Another way to achieve it is by giving a sub-

sidence rate inside the basin to simulate SLR. The difference between the two methods is shown below but the underlying principle is the same.

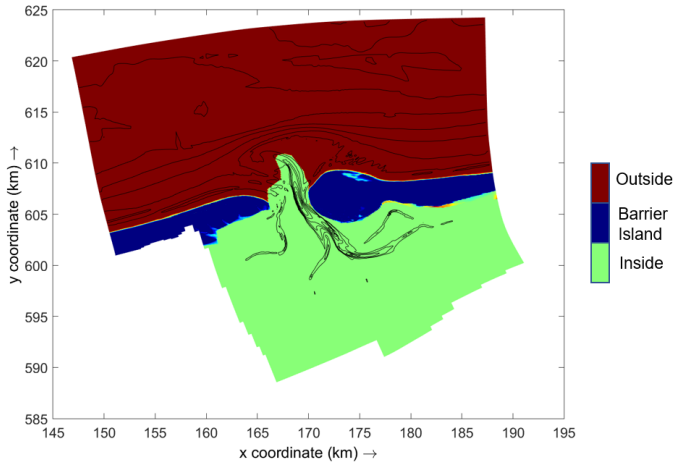

Figure 3.14: Three labeled areas within the domain: outside the basin (red), inside the basin (green) and barrier islands (blue)

- Method 1: Bed elevation outside the basin
  1. Applying SLR at the boundaries.
  2. Applying SLR in changing the reference level.
  3. Elevating the area outside the basin.
- Method 2: Bed subsidence inside the basin
  1. Applying subsidence at the area inside the basin.

The domain is separated into three parts which are the area outside the basin, the area inside the basin and the barrier islands which are not changing with SLR (Figure 3.14). The area outside the basin contains the ebb-tidal delta which differs from the labeled area in the last section.

METHOD 1

On the basis of the standard run, method 1 is applied: the outside area elevates at the same rate as SLR. The final bed level of the case with the bed elevation outside is compared with the standard run and there is more erosion of the ebb tidal delta, less erosion at the main channel but the bed level difference can be barely seen at the shallower and landward parts. Moreover, according to the accumulative sediment transport across the cross-section at the throat (Figure 3.15), an overall trend of sediment import can be found with the bed elevation, which is opposite for the standard run where the sediment is exported from the basin.

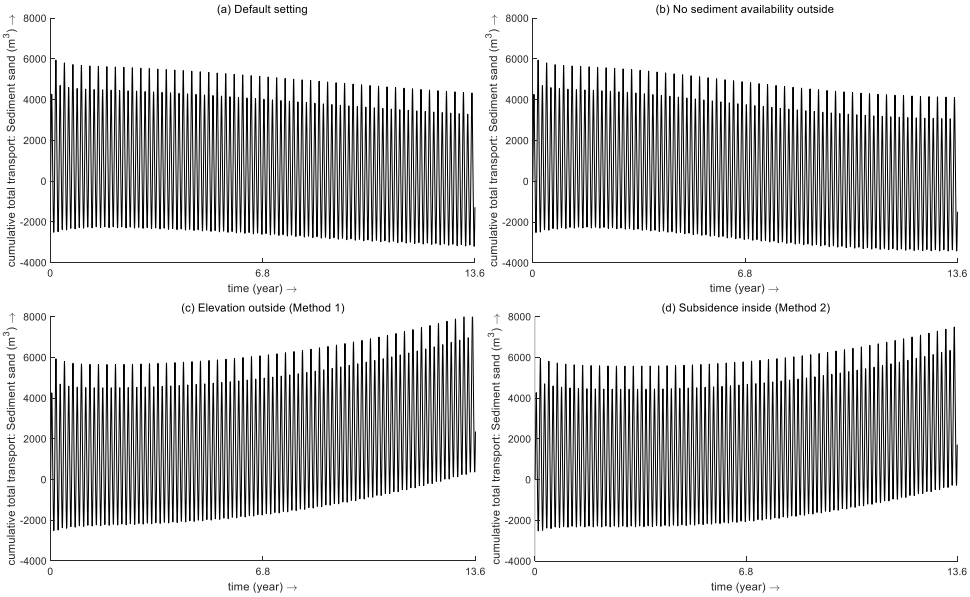

Figure 3.15: Total sediment transport across the throat of the Ameland basin for 4 cases.

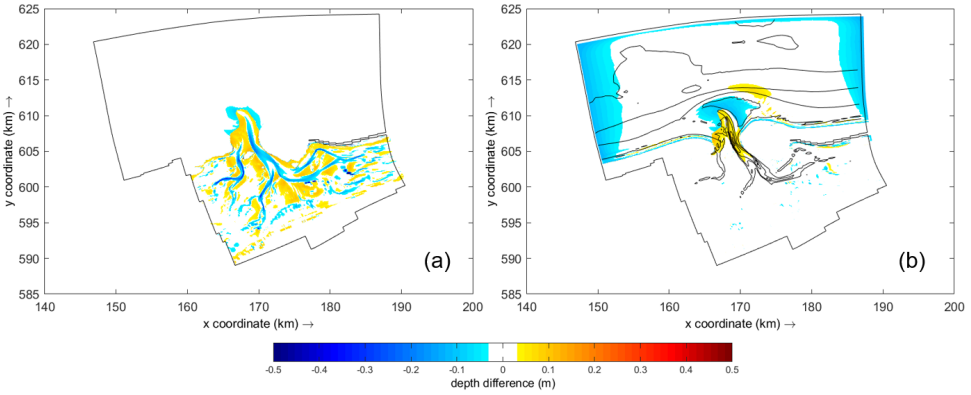

Figure 3.16: (a) Accumulative sedimentation/erosion map of method 1 and the elevation outside the basin is subtracted. (b) The depth comparison between the case with the elevation outside and the standard run.

From here, a conclusion can be drawn from the comparison between these two cases that the sediment that was blocked at the ebb-tidal delta, is now transported into the basin but cannot spread too widely into the more landward area, settling near the main channel. By applying an elevation at the outside area, the erosion at the main channel, whose sediment acted as the main source as the accumulation at the intertidal area, becomes less.

METHOD 2

By using method 2, subsidence is applied inside the basin at the green-ish area in Figure 3.14. The subsidence substitutes SLR which gives an increase to the local water depth at the same rate as SLR.

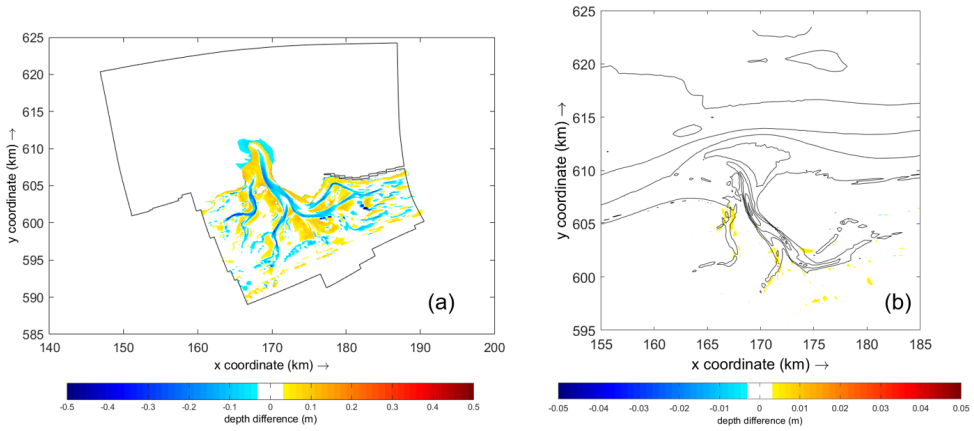

Figure 3.17: (a) Cumulative sedimentation/erosion map of method 2 and the subsidence inside the basin is added. (b) The depth comparison between method 1 and method 2

Method 1 and method 2 should show no difference in results since they are identical from the theory behind. To simulate SLR in the model, an increase in local water level should be added and then the gap between the local depth and equilibrium depth can force the model to evolve towards the equilibrium. In method 1, the water level at the boundaries, reference level and the bed elevation outside the basin should be applied at the same time. But for method 2, the subsidence alters those three steps at once.

The cumulative sedimentation and erosion map for both two methods are almost the same and there are still some slight differences in Figure 3.17(b) but their orders are around O(10^{-2}) to O(10^{-3}), which are relatively small compared with the bed level change. The reason why the two methods are not completely identical could be that in method 2, the water level increases at the same rate for all the places inside the basin but in method 1 and also in reality, the water elevation is specified at the boundaries and the elevation inside the basin is actually uneven. This may lead to different flow patterns and tidal prism for two cases and eventually influence the morphodynamic change.

CONCLUSION

After comparing the Figure 3.15(a) and Figure 3.15(b), the ebb-tidal delta was found as the main trap of sediment instead of the offshore area. There is no obvious difference in the results of method 1 and method 2 and their principles behind them are the same. For the sake of convenience, method 2 is applied for the following simulations because of its fewer procedures.

3.5.3. MORPHOLOGICAL SCALE FACTOR

The morphological scale factor (MORFAC) is a coefficient that can accelerate the morphological evolution which is supplemented in Delft3D. The MORFAC is simply multiplied by the sediment exchange flux between the bed and the water column for each time step. Especially in the case where the tidal condition is dominant and the flow can be assumed as cyclic flow (neglect the effect of the neap-spring cycle), the scale factor can effectively shorten the computation time. After introducing the MORFAC to the model, the time can be separated into morphological time and hydrological time and their relationship are as follow.

$$\Delta t_{morpho} = f_{MORFAC} \cdot \Delta t_{hydro} \tag{3.13}$$

However, the hydrological computation time and the scale factor cannot be selected randomly. As for hydrological computation time, it is better to not be too short which at least covers one whole tide cycle. Meanwhile, the MORFAC cannot be unlimited large when trying to shorten the computation time. The accelerated computation ignores the effect of bathymetry on the hydrodynamic flow which may lead to an unexpected error. How to choose a proper value for the morphological scale factor which can decrease the computation time as much as possible but at the same time won't result in an unacceptable numerical deviation becomes a problem.

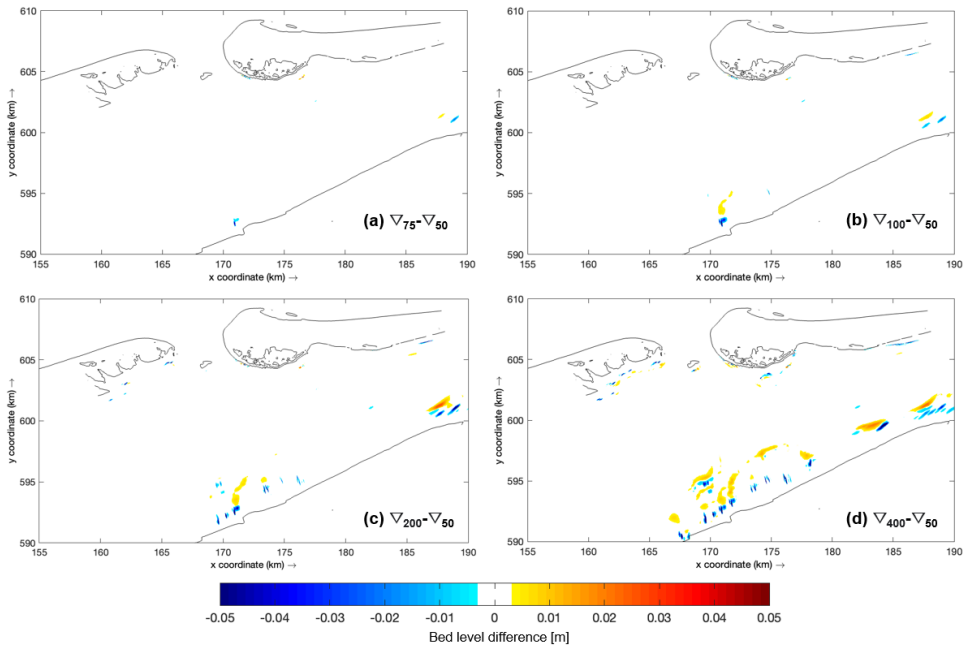

Figure 3.18: Bathymetry difference between five cases with different MORFAC (∇ indicates the bed level at the end of the simulation and the subscript indicates the value of MORFAC)

To investigate the influence of different MORFAC, a group of simulations without SLR

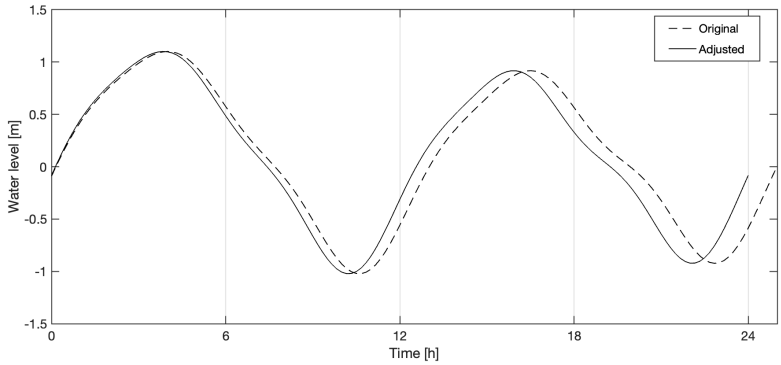

Figure 3.19: The water level at the North boundary before and after changing the tidal periods

are carried out. There are 5 cases with different MORFAC are compared, which are 50, 75, 100, 200, 400. Undoubtedly, the case with the smallest MORFAC at 50 provides the closest result with the case without acceleration. Hence, the smallest MORFAC case is set as the control group and the result will be compared with the other four cases. For each case, the only tidal condition is prescribed at the boundaries without SLR. Therefore, without change in MSL and reference level, there should be no erosion or sedimentation happening within the domain.

Table 3.2: Simulation time for different MORFAC

Morphological time [day]	MORFAC [-]	Hydrological time [day]
1200	50	24
	75	18
	100	12
	200	6
	400	3

Apart from that, the morphological computation time for all cases is the same, but due to the varied scale factor, the hydrodynamic time changes as well. The tidal boundary described in Section 3.3.3 mainly contains O1, M2, M4 constituents. For the convenience of finding a moment every case has the same water level, the frequencies of those tidal constituents are rounded to 15, 30,..., 120 degrees per hour. The water level at the north boundary is shown in Figure 3.19 and the period of the water level is 24 hours, which can promise the water level of each case will be the same at the end of the simulation if their simulation time can be counted as an integer in day. Therefore, a common morphological time of 1200 days can be applied to the simulation.

The bed level of each case is compared at the end of the simulation and the difference in bathymetry between them is shown in Figure 3.18. In principle, there is no change in bed level since no SLR is applied. However, from the figure there are still some unde-

sirable deviations that can be observed especially in the cases with high MORFAC. In Figure (a) and (b), the bed level deviation is small which is only at the order of 0.01. But when the MORFAC comes to 200 or even 400 (Figure (c) and (d)), there are some deviations appearing at the landward edge of the basin, and the magnitude of the deviation is reaching 0.05 m, which is relatively large compared with the bed level change when SLR happens. Hence, the MORFAC higher than 100 is not recommended to apply in this case. The deviation induced by the MORFAC at 100 is acceptable no matter in area or in magnitude. At the same time, the higher MORFAC can effectively save computation time. Under the consideration of the computation time and the accuracy, the MORFAC at 100 is preferable with the default settings.

Those undesirable deviations were found mostly at the place with extremely shallow water depth. Therefore, the numerical error may result in a significant difference in those shallow places where the equilibrium depth is small as well. To avoid the happening of numerical deviations and discover the possibility of using a higher MORFAC to save computation time, a higher reference level is proposed. The high sea level at the high tide inside the Ameland inlet is 1.2 m. Hence, as Section 3.3.4 described, an elevation at 1.2 m is added to the reference level which makes the area be less sensitive to SLR and the water level change.

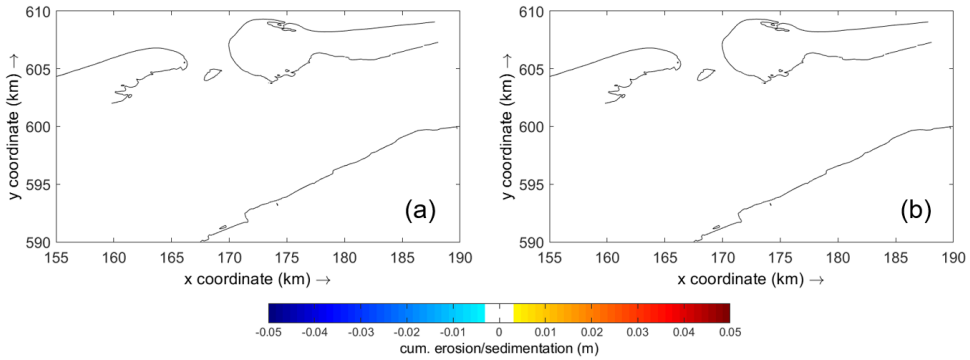

Figure 3.20: The cumulative sedimentation/erosion map (a) MORFAC=200 (b) MORFAC=400

With the elevation in the reference level, the landward area is not as sensitive as it did before changing the reference level. The numerical deviation was not amplified to morphological change from the Figure 3.20 and there is no abnormal bed level change as Figure 3.18. Which means that it is possible to adopt a higher MORFAC to shorten the computation time with a lifted reference level. What is worth mentioning is that MORFAC still cannot be unlimited large even there is no numerical deviation appearing anymore. The reason is no matter which method between subsidence inside and elevation outside is selected, there is a residual flow induced by SLR which can also lead to sedimentation or erosion inside the basin. Especially when SLR rate is large and under this circumstance, the water flows in during the flood period but at the ebb period, the MSL has changed, which induces a residual flow and also a morphological change. When applying the morphological scale factor to the model, the residual flow and its influence will be amplified as well. To avoid instability happening, MORFAC is not advised

to be too large. A MORFAC at 200 is applied for the following cases.

3.5.4. GRID COARSENING

For the sake of higher computation efficiency, except using a higher MORFAC, coarsening the computation grids is also a frequently used method. A coarser grid mesh shortens the computation time not only by providing fewer cells to be computed but also by permitting users to use a larger time step according to the Courant number. But coarsening is not suitable for all models and it may change the bathymetry and consequently influence the hydrodynamic conditions. To check the hybrid model's robustness, twice coarser and three times coarser grids are used and their results will be compared with

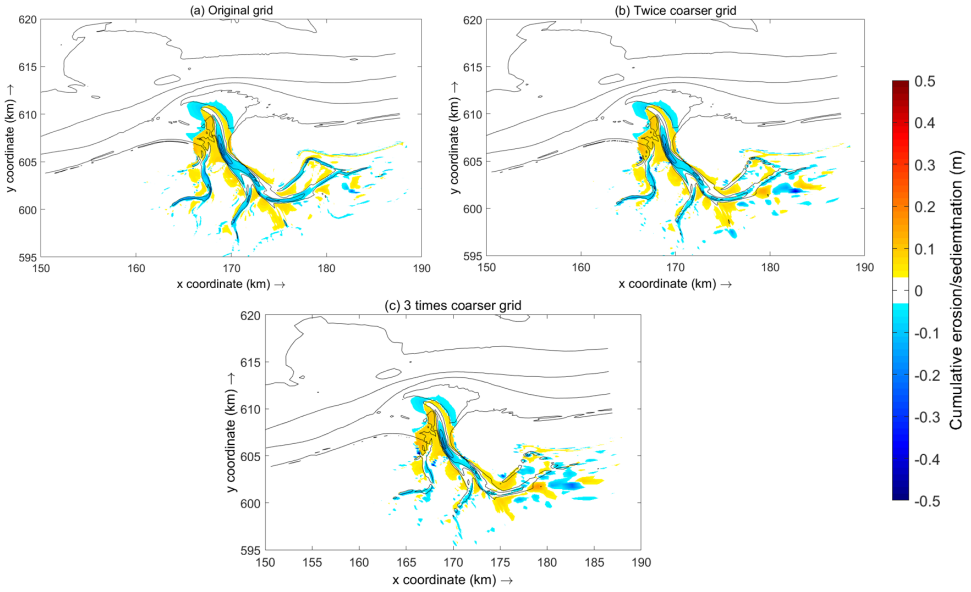

Figure 3.21: Cumulative erosion/sedimentation map for three grids

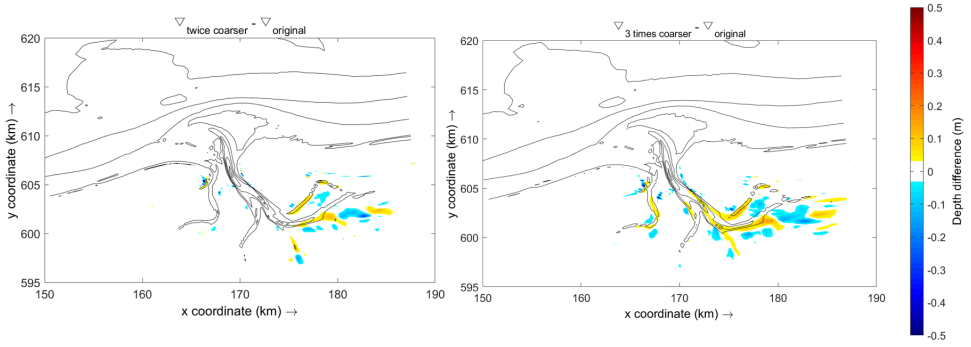

Figure 3.22: Bed level difference at the end of simulation between the original grids and two coarser grids

the original grids. Meanwhile, SLR is prescribed by method 2 and to avoid the appearance of instability, a 1.2 m elevation is added to the reference level. All other settings are identical with the standard run in Section 3.4 including SLR rate.

The twice coarser grid and the three times coarser grid present a quite similar morphological change pattern as the original one. From the Figure 3.21, some instabilities can still be observed at the landward area for two coarser grids, which might be induced by the further coarsening to the cells that are coarse enough at the landward area.

To investigate whether the coarsening changes the bathymetry, Figure 3.23(a)) and (b)) showing the hypsometric curve after and before the simulation compares the grids of three resolutions. At the end of the simulation, the twice coarser grid still presents a really close curve to the original one. But the 3 times coarser one has a smaller basin area which varies from the result of the original grid. The three curves overlap until the height comes to 0 m, and the coarsest one deviates from the other two curves getting steeper, which means the 3 times coarser grid has a smaller basin than the other two cases. The reason for it can be found from 3.23(b)): the initial hypsometric curve has been already changed after the coarsening and the 3 times coarser grid is too coarse to depict the original bathymetry. If a finer resolution than 2 times is used, the grid should be optimized to keep the bathymetry unchanged. Therefore, combining the bed level difference and the computation time, the twice coarser grid is the optimum choice. Meanwhile, a longer time step at 30 s could be applied according to the Courant number. The total computation time can be shortened to one-tenth of the previous computation time.

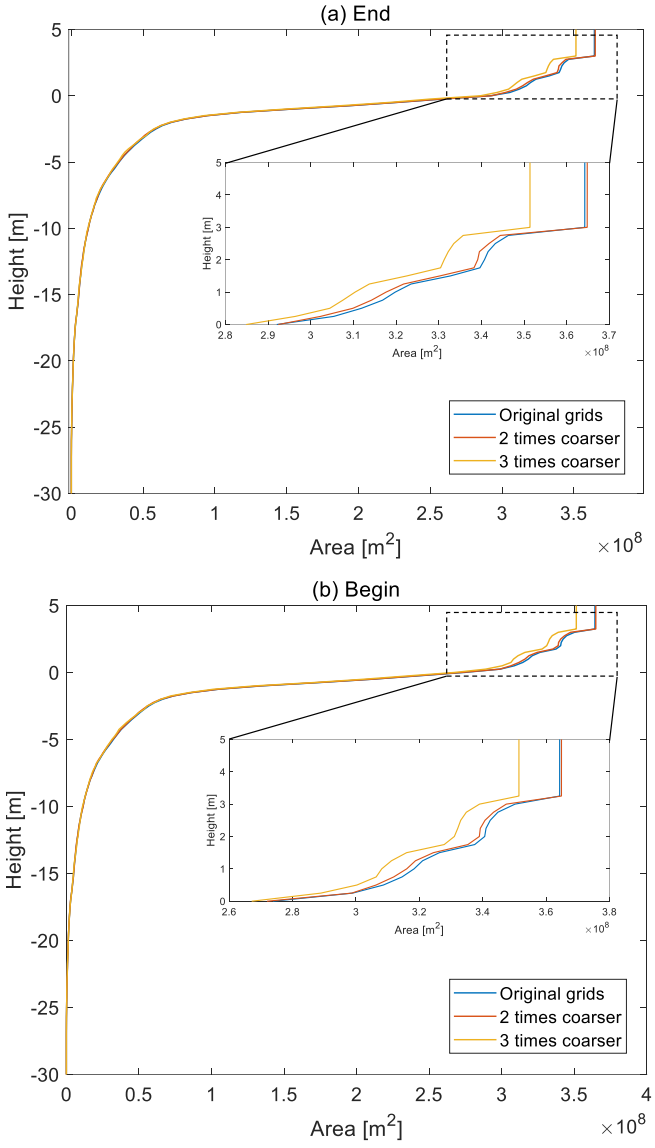

Figure 3.23: Hypsometric curve of the Ameland basin (a) End of the simulation (b) Begin of the simulation

4

LONG-TERM SIMULATION

The time scale of the morphological change induced by SLR is much larger than the time scale of local hydrodynamic conditions, like tides and waves. To investigate the influence of SLR, a 100-year or even longer period is necessary for the simulation duration. Besides that, the morphological change doesn't respond simultaneously to the water level change. A longer duration can show the time lag between the hydrological change and the morphological change more clearly. Moreover, SLR rate is relatively small compared with tidal water level fluctuation. The local bed level change induced by SLR may not that easily be seen due to its much smaller scale than the influence of other factors. In this section, the simulation time will be extended to 100 years and the model's performance in a long period will be studied.

4.1. SCENARIOS

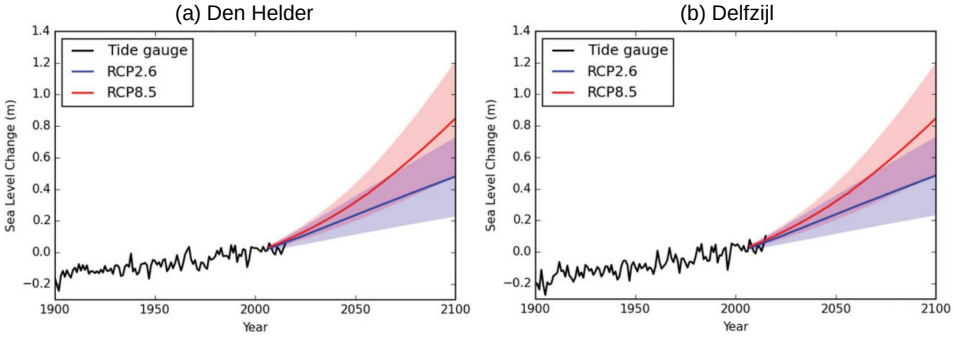

Figure 4.1: Tide-gauge observations (black and solid line) vs local relative sea-level projections for RCP2.6 (blue) and RCP8.5 (red) in Den Helder and Delfzijl (2005-2100, 95% confidence interval, Vermeersen et al., 2018)

Due to too many uncertainties, the prediction of SLR is not 100 percent precise, and

it is not a constant value for the whole period. Figure 4.1 shows the projection of SLR based on the IPCC AR5 results in Den Helder and Delfzijl, The Netherlands. The sea-level change in 2100 can vary from the up limit of RCP8.5 at 1.2 m to the down limit of RCP2.6 at 0.2 m. How the Ameland basin will respond to the uncertain SLR is still to be studied.

In this section, three independent long-term runs are carried out with SLR rate at 4 mm, 6mm, and 8 mm per year, respectively. The boundary conditions and the bathymetry remain unchanged as in Section 3.4 and a twice coarser grid is applied. Besides that, the SLR is achieved by method 2, i.e., subsidence inside the basin.

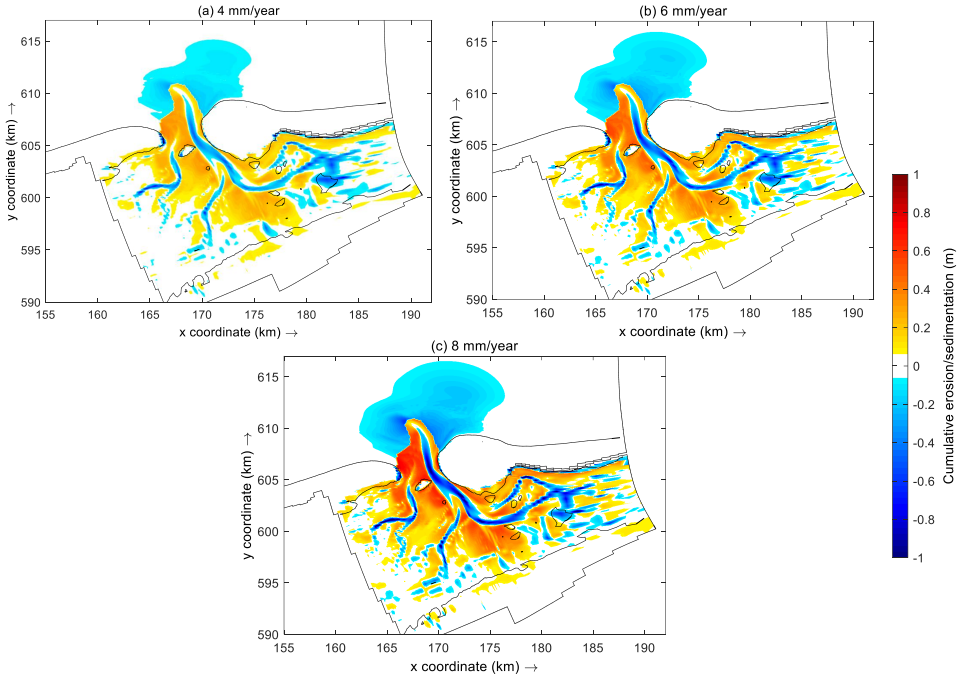

Figure 4.2: Cumulative erosion/sedimentation map for three SLR scenarios after 100 years

Figure 4.2 shows that a higher SLR rate leads to a faster and larger morphological change. Within the same period, three cases perform quite similarly: erosion happens at the ebb-tidal delta and its nearby area, which is the main source of sediment together with the alongshore sediment transport. At the east side of the throat, Borndiep which is the deepest part of the basin, the sediment is eroded and the erosion is still going on. At the west side of the throat near the Terschelling, here is much shallower than the Borndiep initially. Therefore, when sediment firstly enters the inlet, it will deposit here. The sufficient sediment supply ensures that the sedimentation at the west of the throat can always keep pace with SLR. Inside the basin, the main channel is still being eroded even with a much longer period at 100 years and the erosion degree is proportional to the SLR rate. The sedimentation of the intertidal flat located close to the main channel can also keep pace with SLR. When it goes further from the main channel, towards the

basin edge, the sedimentation at the intertidal flat gets less since the sediment exchange here is not as frequent as in the main channel. Hence, there are two necessary conditions for the area inside the basin to keep pace with SLR which are sufficient sediment supply and a relatively large gap between local equilibrium concentration and equilibrium concentration in the surrounding area. Although the main channel has the most sediment supply directly from outside, the sediment cannot be kept in the channel due to the equilibrium concentration gradient to its surrounding intertidal area.

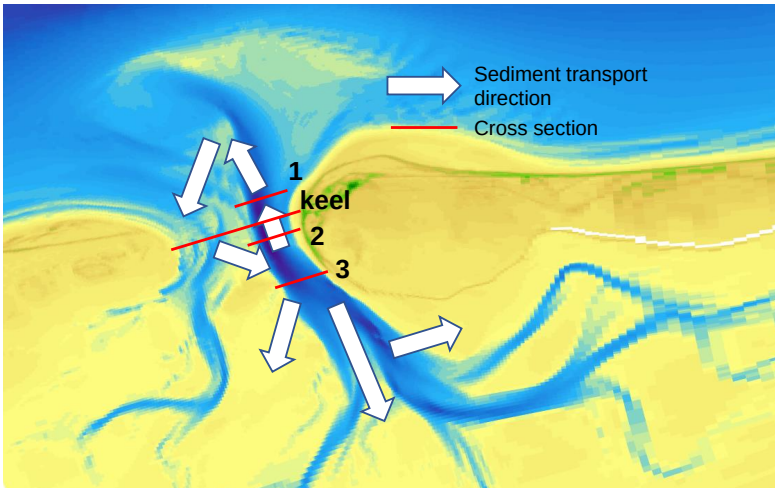

Figure 4.3: Four cross-sections at the Borndiep and sediment flux direction

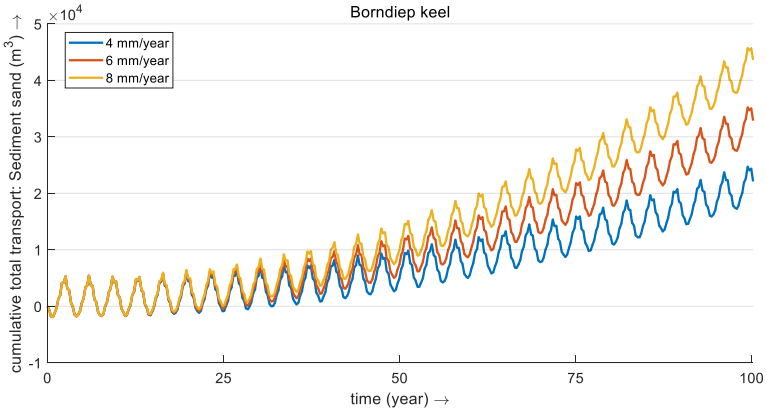

Figure 4.4: Cumulative sediment transport through the Ameland inlet (toward basin is positive, without multiplying MORFAC)

Four cross-sections are shown in the Figure 4.3 along the Borndiep from north to south, which are Borndiep 1, Borndiep keel, Borndiep 2 and Borndiep 3. Firstly, the

cumulative sediment transport through the Borndiep keel is recorded in Figure 4.4. For all three SLR rates, the sediment is being imported into the Ameland basin through the Borndiep keel for the whole period. In the first 25 years, the sediment imported into the basin doesn't change too much since the morphological change usually has a time lag after SLR starts. In the beginning, after the spin-up time, the sediment concentration in the water column inside the basin is equal to the global equilibrium concentration. When SLR starts, there is a gap between the local equilibrium concentration and local concentration. At this moment, the sediment in the water column will settle down firstly to compensate the gap. That's why in the first 20 years, there is barely any erosion at the channel and no much sediment from outside, but the intertidal flat can also elevate together with SLR. After this period, the sediment inside the basin, floating in the water column and eroded from the channel, is not sufficient for the shallow area to keep pace with SLR. Therefore, the sediment starts to be imported into the basin. The speed of the sediment import is proportional to the SLR: the higher rate of SLR leads to more sediment import.

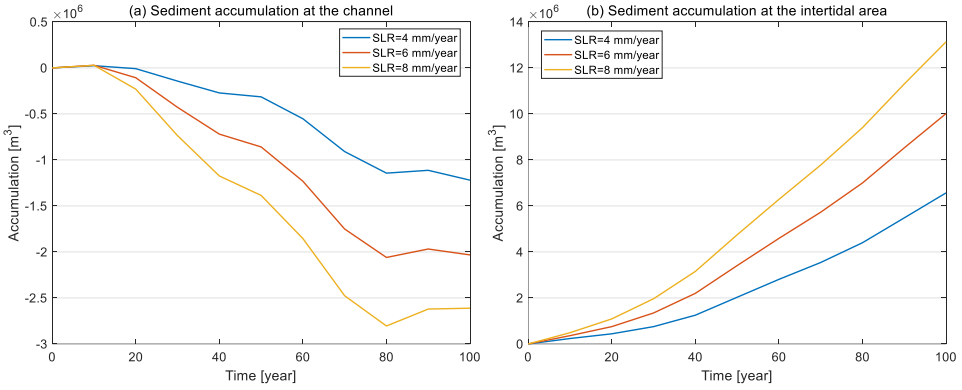

Figure 4.5: Sediment accumulation at the channel and the intertidal flat for three SLR rates

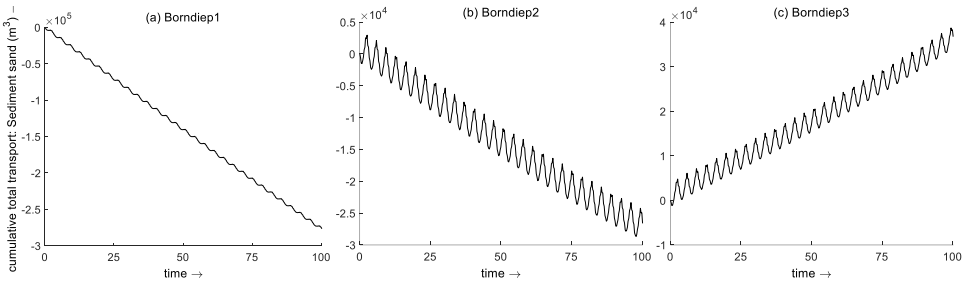

Figure 4.6: Cumulative sediment transport through cross-sections with SLR rate at 4 mm/year (a) Borndiep 1 (b) Borndiep 2 (c) Borndiep 3 (toward basin is positive, without multiplying MORFAC)

The cumulative sediment transport direction at the main channel also should be noticed. The Figure 4.6 shows the cumulative sediment transport with SLR at 4 mm per

year through three cross-sections at the main channels (without multiplying MORFAC). Borndiep 1 and 2 are both located between the Terschelling and the Ameland but the Borndiep 1 is closer to the ebb-tidal delta. Borndiep 3 is situated more landward compared with the other two cross-sections. At Borndiep 1 and 2, the sediment is being exported to the outside of the Ameland basin and at Borndiep 3, the sediment behaves in an opposite way, which is imported to the landward and shallower area. The reason for it is that the area between Borndiep 1 and 3 is the deepest part of the main channel which is always being eroded to supply the sediment needs at its surrounding shallow area. And the area at the north side of Borndiep 1 is shallower than the channel at the south side of Borndiep 2. Therefore, even with the sediment supply from outside the basin, the sediment will keep being transported from the channel to the north entrance until the equilibrium state of both two places is the same, i.e., their equilibrium concentrations are equal. That's why in Section 3.5.2, when method 1 is applied, the erosion at the main channel decreases compared with the case without sediment supply from outside. The sediment supply from outside truly alleviates the erosion at the main channel since it acts as another source of the shallow area at the entrance where the main channel is the only source before. The sediment transport direction at Borndiep 3 can be also explained by this.

The sediment eroded from the main channel is separated into two directions. One is being transported to the landward intertidal area and another one is to the outside the basin. In the latter case, the sediment settles at the shallow area and later it is stirred up and transported to the side channel near the Terschelling. In Figure 4.4, the sediment is always being transported into the basin through the inlet but at the Borndiep, sediment is exported. That's because there is lots of sediment coming inside the basin through the side channel which is even more than export at the main channel. From Figure 3.10, during flood a large proportion of water which enters into Boschgat passes over the shoal between Boschgat and Borndiep with sufficient sediment, returning Borndiep and forming a transport cycle. The sediment exchange between two channels is of great importance in the morphological change with SLR in the Ameland inlet. The sediment transport direction is marked in Figure 4.3 by those white arrows.

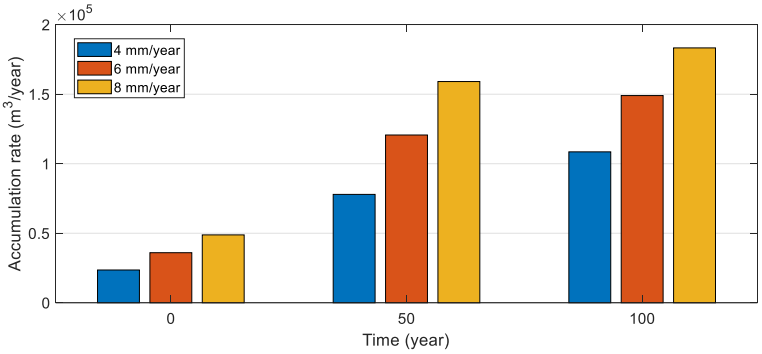

Figure 4.7: Accumulation rate at the intertidal area in year 0, 50, 100 with three SLR rates

The basin's behavior with varied SLR rates is also worth being investigated. In both

Figure 4.3 and 4.5, when SLR rates increase, the accumulation rate at the intertidal area and the erosion rate at the channel speed up at the same time. The accelerated SLR creates a larger gap between the local water depth and equilibrium depth within the same period, which drives more sediment to be transported to the shallow area. As Figure 4.5 shown, in the first 50 years, the accumulation rate at the intertidal area increases dramatically, but in the following 50 years, the increasing rate slows down. The reason is in the first 50 years, the local concentration difference, $c_e - c$, is also increasing which leads to an increase in accumulation rate simultaneously. When the difference is large enough and can attract enough sediment, the intertidal area is approaching the dynamic equilibrium state, which is described in the ASMITA model as well. Under the equilibrium state, the local concentration difference is no longer increasing and the sediment is imported at a nearly constant speed to hold the difference. And obviously, a faster SLR rate needs a greater difference in concentration which consequently leads to a higher accumulation speed. For three cases, at the end of the simulation, the channel is still being eroded and the sediment keeps being imported at the throat, and the sediment eventually settles down at the intertidal area.

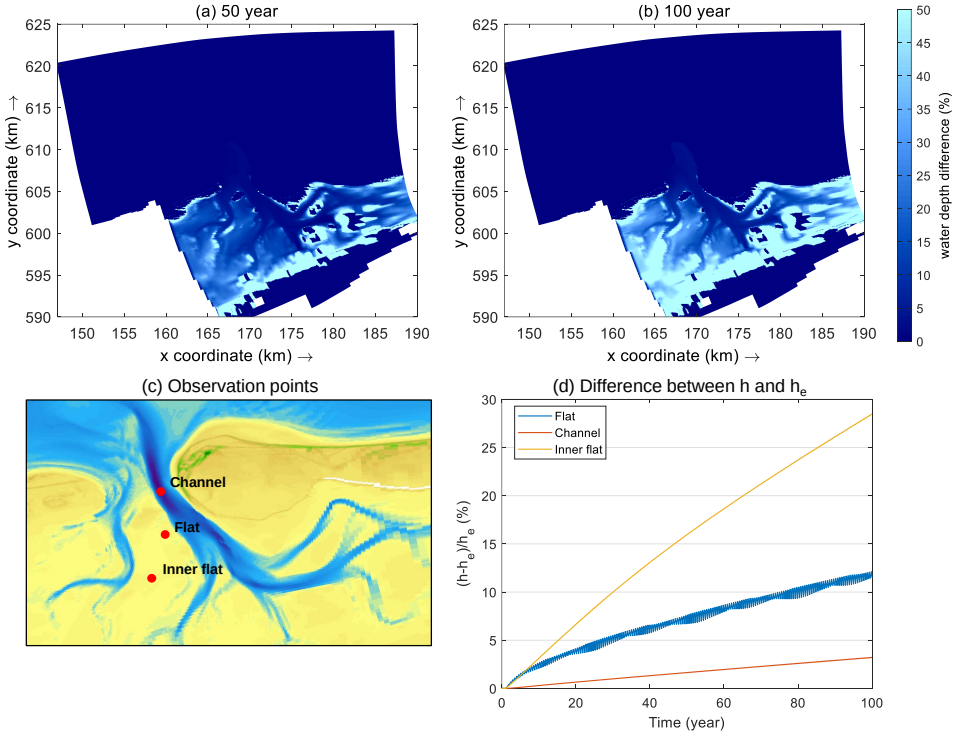

Figure 4.8: The evolution of the local water depth compared with the equilibrium depth $(h - h_e)/h_e$

The difference between the local water depth and the equilibrium depth reflects the how far the area is left from the equilibrium state. Figure 4.8(a) and 4.8(b) show the difference between the local water depth and the equilibrium water depth. The lighter

color, the further the area away from equilibrium. In subfigure (c) and (d), three points represent the channel, the area at the intertidal flat close to the channel and the area at the intertidal flat far from the channel, respectively. All three points are evolving away from the equilibrium within 100 years and none of them reaches the dynamic equilibrium state, i.e., the gap between h and h_e doesn't change anymore. In subfigure (a) and (b), the inner flat area used to be dark blue in year 50 changes to light blue in year 100 quickly and the increase of the gap between h and h_e is ongoing after 100 years. The depth gap at the flat near the main channel increases for the whole period but the speed is slightly decreasing which means the area is approaching its dynamic equilibrium. If the simulation is extended, the flat near the main channel is the area that most likely reaches its equilibrium compared with other areas.

4.2. SENSITIVITY ANALYSIS

To set up the hybrid model and apply it to the morphological change prediction, there is a group of parameters that needs to be determined beforehand because their influence is still unknown. In this section, the sensitivity analysis will be carried out for each coefficient used in the hybrid model and two main questions will be discussed:

1. How do these parameters change the erosion and sedimentation pattern?
2. How to explain these corresponding phenomenons?

This analysis is trying to figure out the principle behind the model, find out the sensitivity of all parameters, and finally give some suggestions to future users in the scale of the parameters and how significantly the results will be influenced.

The initial conditions for the sensitivity analysis are the same as the long-term run described in the previous section. The SLR rate is selected with a lower value at 4 mm per year. As introduced previously, the higher SLR rate can induce a more dramatic bed level change. However, until now, the numerical limit of the hybrid model is still unknown. For the sake of numerical stability, the most conservative value of SLR is applied to avoid the extreme case that sedimentation happens too fast to keep the original hydrodynamic conditions. In terms of simulation time, the same morphological time at 100 years is applied. When the SLR starts, from the sedimentation and erosion pattern, the horizontal sediment flux through the cross-sections, and other outputs, the influence of each parameter can be compared. And in each group, only one parameter will be changed. The list of parameters which are going to be modified is as follow:

- Sediment diameter (settling velocity)
- Diffusivity
- Equilibrium concentration
- Power n
- Multiple sediment fractions

4.2.1. DIAMETER

The diameter of the sediment decides the settling velocity which consequently influences the spreading of the sediment. In the hybrid model, the settling velocity is calculated by the embedded Van Rijn et al. (1993) formula, which is inherited from Delft3D. Therefore, only the diameter of the sediment needs to be specified by users. The relationship between the non-cohesive sediment median diameter (D_{50}) and its settling velocity is described below.

$$w_{s,0}^{(\ell)} = \begin{cases} \frac{(s^{(\ell)}-1)gD_s^{(\ell)2}}{18\nu}, & 65\mu\text{m} < D_s \leq 100\mu\text{m} \\ \frac{10\nu}{D_s}\left(\sqrt{1+\frac{0.01(s^{(\ell)}-1)gD_s^{(\ell)3}}{\nu^2}}-1\right), & 100\mu\text{m} < D_s \leq 1000\mu\text{m} \\ 1.1\sqrt{(s^{(\ell)}-1)\,gD_s^{(\ell)}}, & 1000\mu\text{m} < D_s \end{cases} \tag{4.1}$$

Where:

$s^{(\ell)}$ = relative density $\rho_s^{(\ell)}/\rho_w$ of sediment fraction(ℓ)
$D_s^{(\ell)}$ = representative diameter of sediment fraction(ℓ), which is equal to the median diameter multiplied by the FACDSS (parameter defining the relationship between the diameter of sediment on the bed and in the water column (Deltares, 2011))
ν = kinematic viscosity coefficient of water

Table 4.1: 5 runs with varied diameters and the corresponding settling velocity

D_{50} [μm]	75	125	250	375	500
w [m/s]	0.005	0.014	0.056	0.126	0.225

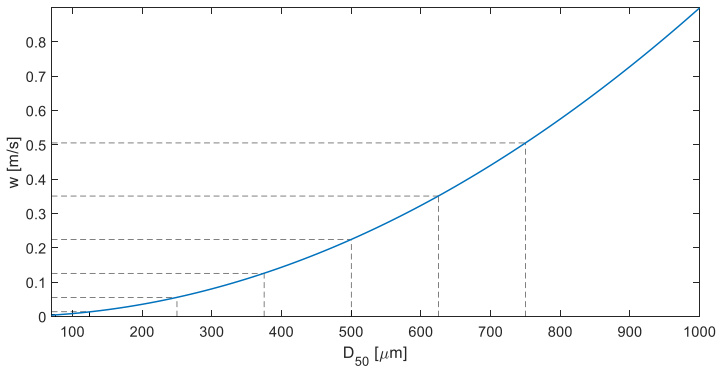

Figure 4.9: The relationship between the median diameter (D_{50}) and the settling velocity (Van Rijn et al., 1993)

In the hybrid model, the diameter of the suspended sediment and that of sediment on the bed are assumed the same. Therefore, the FACDSS is set at 1 and D_s is equal to the user-specified median diameter. Besides that, only one non-cohesive fraction is applied in the model. Five simulations with different sediment diameters are carried out and

SLR is prescribed within the domain at the rate of 4 mm per morphological year. And the sediment sizes of 5 runs are shown in Table. 4.1 and Figure 4.9.

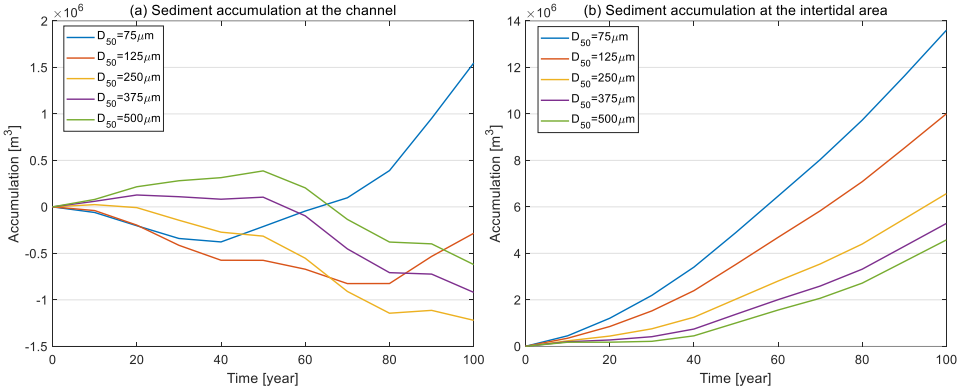

Figure 4.10: Sediment accumulation inside the Ameland basin for five diameters

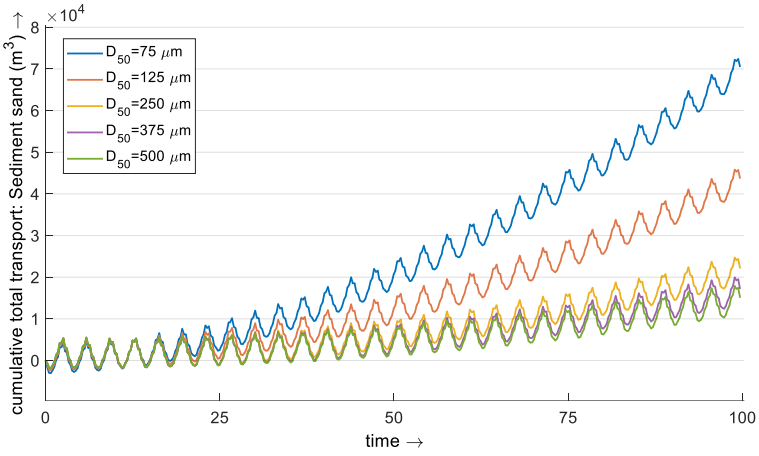

Figure 4.11: Cumulative sediment import through the inlet for five diameters (toward basin is positive, without multiplying MORFAC)

Firstly, the cumulative sedimentation and erosion map, the difference between the bed level at the end of the simulation and the initial bed level of all cases are compared graphically (Figure 4.13). Overall, the sedimentation happens at the intertidal flat and the erosion happens at the channel and outside area where the water depth is shallow. The smaller sediment has the widest area under sedimentation at the intertidal area and also the most significant erosion at the main channel. Besides that, there is a large area under erosion outside the basin which plays as a main sediment source of the intertidal flat. When the sediment gets coarser, the erosion at the nearby area outside the basin and the main channel become less and at the same time, the sedimentation at the flat

gets less. Another thing needs to be noticed is that at the west edge of the intertidal flat, there is an area being eroded abnormally. Similarly, at the south end of the channel, an extreme rise of the bed level could be found. This could be induced by the coarsening of grids. In Figure 3.22, the differences also appear at those areas where the grids are too coarse. Those abnormal differences might get alleviated by optimizing the grids in the future but they don't influence the general trend of the morphological change significantly. So they are not going to be discussed in this section.

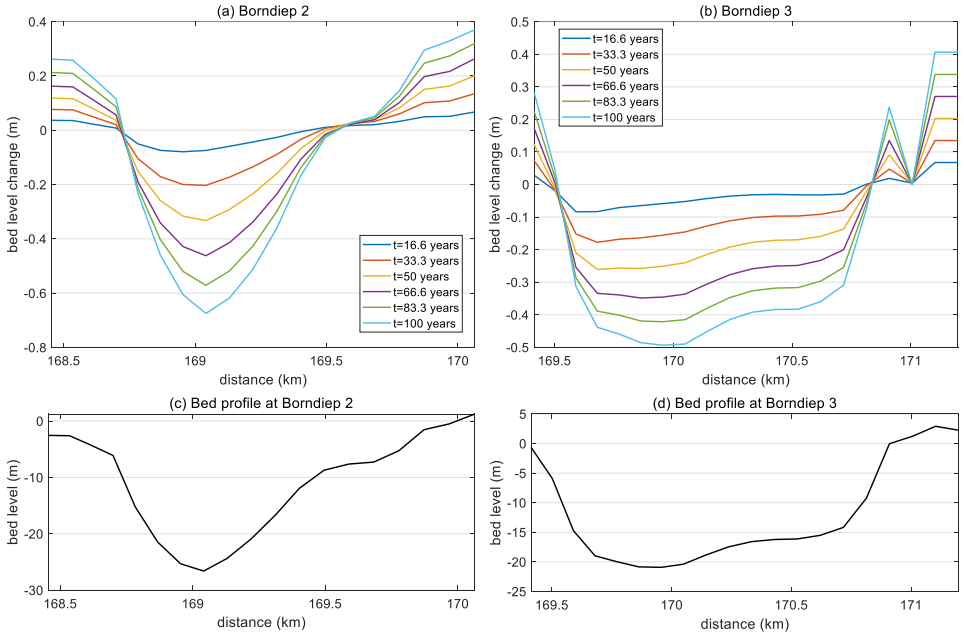

Figure 4.12: Bed level change of cross-section Borndiep 2 and 3 in 100 years (a, b) and the original bed level profile (c, d) with a diameter at 75 μm

Figure 4.10 shows the accumulation trend at the channel and the intertidal area. No matter which diameter is chosen, the overall trend of morphological change at the intertidal area doesn't change too much, which is that the sediment has a smaller diameter causes more sedimentation at the shallow area and vice versa. The reason for this is intuitive. Finer sediment has a smaller settling velocity which makes the suspended sediment roam longer and further to the more landward area. At the channel, the situation is more complicated. Compared with the 250 μm, the finer sediment and coarser sediment show a significantly different erosion trend. For the coarser sediment, in the first 50 years, there is more sediment accumulating at the channel than being eroded. And later the sediment volume at the channel gets less since the sediment is transported to the intertidal area. On the contrary, the finer sediment doesn't show the beginning accumulation but the erosion. And after years, the erosion stops and the total volume of sediment at the channel turns to increase, which is not seen for the coarser sediment within 100 years. The coarser sediment has a higher settling velocity which makes it

cannot spread widely. When the sediment enters the basin, it will firstly settle at the main channel, that's why an accumulation is observed at first. And after a period, there is no sufficient sediment supply at the intertidal flat, the gap between local equilibrium concentration and the local concentration becomes larger and larger until the concentration gradient is great enough to attract sediment from the channel. As for the finer sediment, it can be carried further into the shallow area with water flow, which promises an adequate sediment supply. With a much faster accumulation rate at the intertidal flat, there is no need to erode that much sediment from the channel to compensate for the sediment deficit at the flat. That's why after a while a tipping point shows and the channel starts to accumulate. At this moment, the channel can be assumed that it is approaching the dynamic equilibrium, and in the future, it can be predicted that the accumulation rate at the channel and intertidal flat will become constant and eventually reach the dynamic equilibrium.

In the case with the diameter at 75 μm, after 40 years the channel turns to accumulate. To study how the does channel behaves under the overall accumulating trend, the bed level changes at Borndiep 2 and 3 are depicted in Figure 4.12. Even the sediment volume at the channel is increasing, but meanwhile, not all the area is rising together with SLR. At the deep part of Borndiep 2 and 3, the area is still being eroded and the bed level is lowering. But at the area which is located below the MLW and above -10 m (from the graph), it is elevating because it has a shallower depth which entitles the area to attract more sediment than the area deeper than it. The overall increasing trend after 40 years in Figure 4.10 only indicates the accumulation volume is more than erosion volume but cannot prove all the area is under accumulation. Hence, another conclusion can be drawn that the time scale for each area with different water depth in turning from erosion to sedimentation is different which depends on the order of obtaining sediment. Normally, the deepest area has the longest time scale because it has the least sediment settlement. Apart from that, the sediment size has a significant influence on the morphological time scale since the settling velocity directly influences the horizontal sediment exchange.

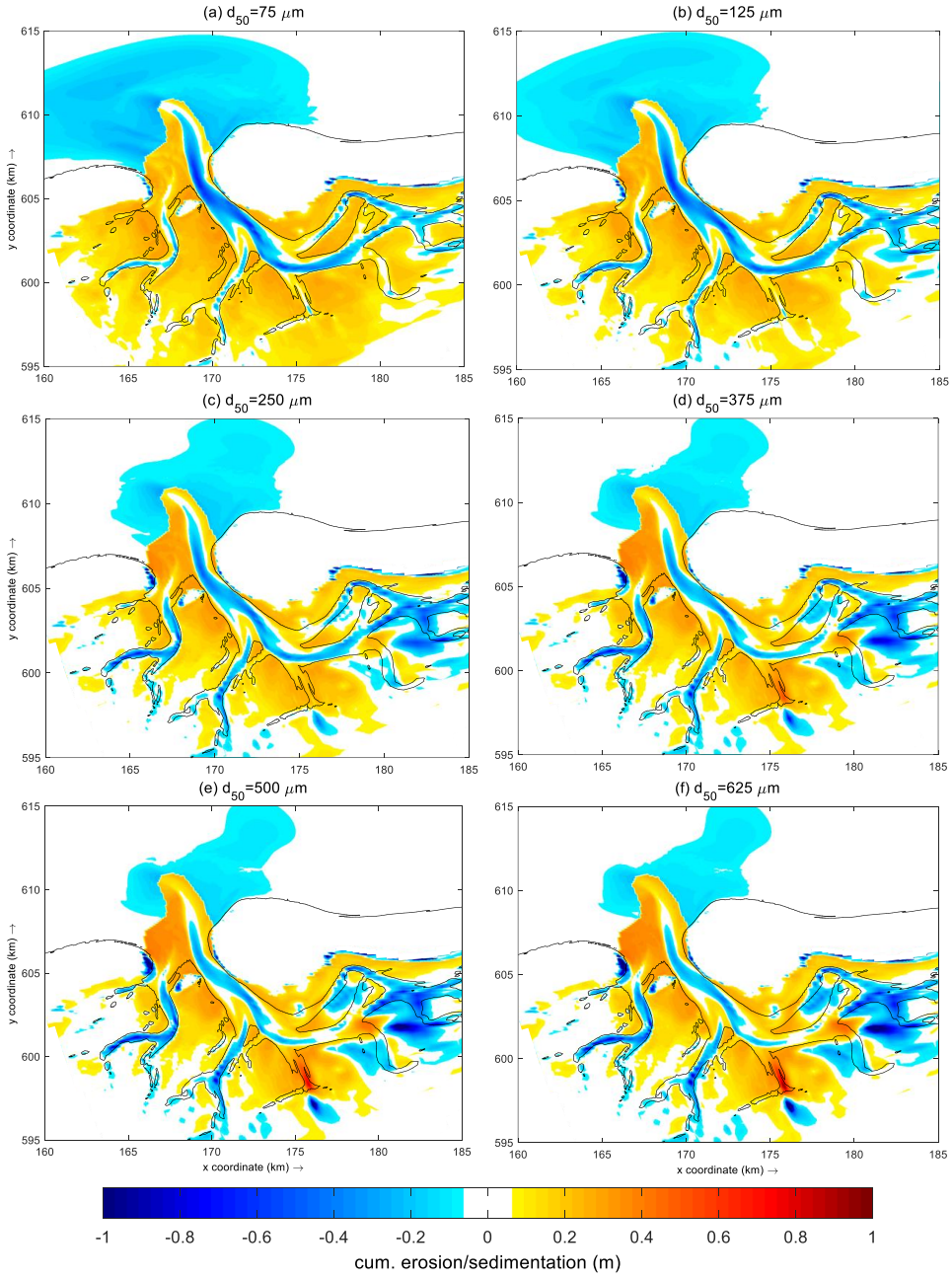

Figure 4.13: Cumulative erosion/sedimentation map for 6 median sediment diameters at the end of the simulation (a)75μm (b)125μm (c)250μm (d)375μm (e)500μm (f)625μm

4.2.2. DIFFUSIVITY

Diffusivity controls the diffusion term in the advection-diffusion equation (Eq. 3.9). A higher diffusivity coefficient can enhance the sediment transport along the sediment concentration gradient. As introduced previously, there is a huge gap between the concentration at the channel and that at the intertidal flat. With a higher or lower value of diffusivity, a more or less active horizontal sediment exchange could be observed theoretically. Therefore, five cases with varied diffusivity of 0.01, 0.1, 1, 10, and 100 m^2/s are carried out.

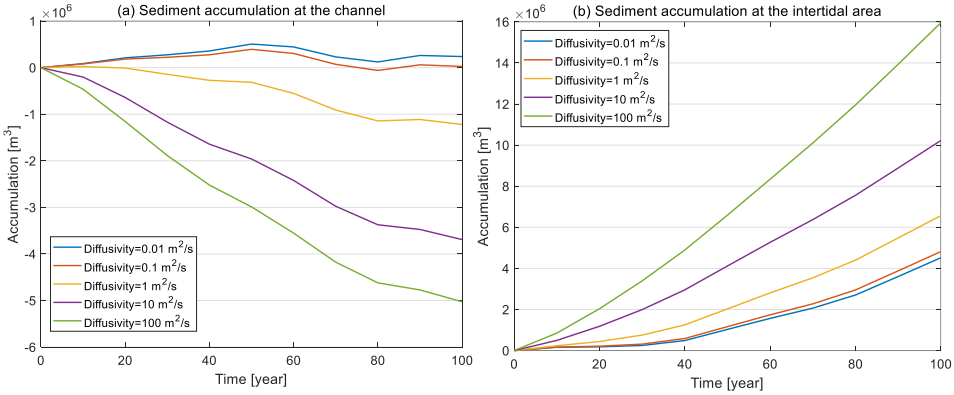

Figure 4.14: Sediment accumulation inside the Ameland basin for five diffusivity coefficients

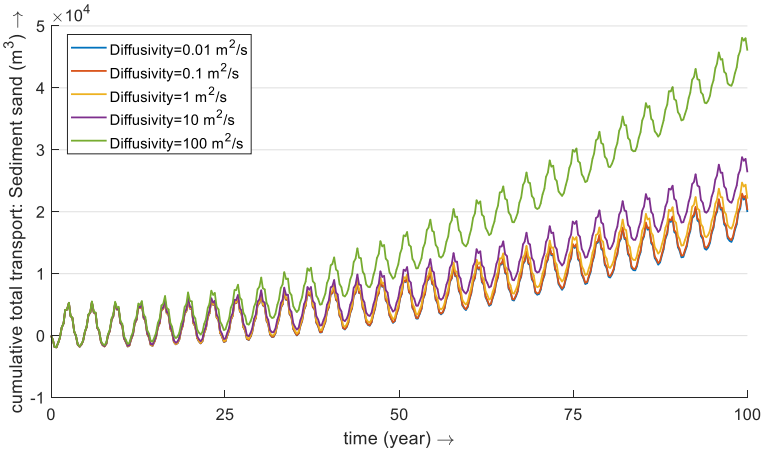

Figure 4.15: Cumulative sediment import through the inlet for five Diffusivity coefficients ((toward basin is positive, without multiplying MORFAC)

Figure 4.14 shows the sediment accumulation at the channel and the intertidal flat for five diffusivity coefficients. Compared with the default value (D=1 m^2/s), two smaller

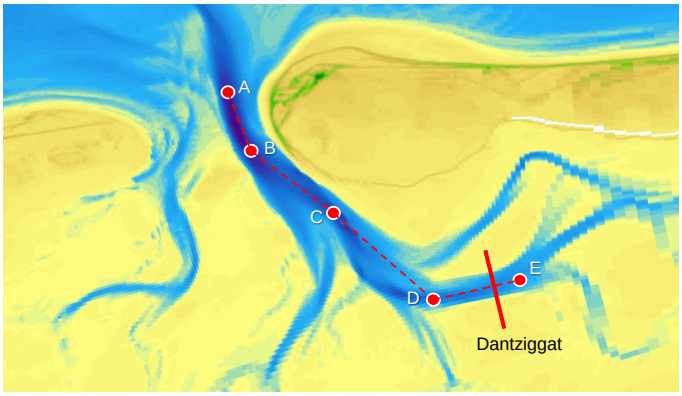

Figure 4.16: Five observation points along the main flood channel and the cross-section Dantziggat

diffusivities at 0.1 and 0.01 are selected and their accumulations at the intertidal flat decrease slightly, but the difference between those cases is quite small. Also, at the main channel, the difference can be barely seen between two lower diffusivity cases. In this circumstance, the diffusion term is no longer dominant in the sediment transport processes and the advection is way more important than the diffusion. When increasing the diffusivity, the erosion at the channel and the accumulation at the flat both increase. Between the flat and the channel, there is a large difference in suspended concentration as well as in equilibrium concentration. The difference creates a concentration gradient that diffusivity plays an important role on. A higher diffusivity intends to close the gap between them which enhances the sediment exchange between the low concentration area with high concentration area and sediment will be transported to the low concentration area, i.e., shallow area, more frequently.

Even though both decreasing sediment diameter and increasing the diffusivity can speed up the accumulation rate at the intertidal flat, they achieve it in a different way. For the case with diameter at 125 μm and with diffusivity at 10 m^2/s, the accumulations at the flat after 100 years are both around 10×10^6 m^3 but their erosion at the channel is 0.25×10^6 m^3 and 3.7×10^6 m^3, respectively. Apparently, higher diffusivity induces much more erosion than finer sediment when the accumulations at the flat are around the same order. The higher diffusivity drives more sediment to be eroded at the deeper area and transported to the shallow area. From Figure 4.11 and 4.15, the cumulative sediment transport into the basin of d=125 μm in 100 years is about 8×10^6 m^3, which is 3×10^6 m^3 more than that of D=10 m^2/s. Therefore, the main sediment sources for the two cases are different: one is the eroded sediment from the channel and another one is mainly from outside the basin. And also one thing that should be mentioned is that the diffusivity increases from 0.01 to 10 m^2/s, the sediment imported into the basin doesn't change dramatically which means the diffusivity only rules the horizontal exchange inside the basin but between the basin and the outside, it doesn't influence that much.

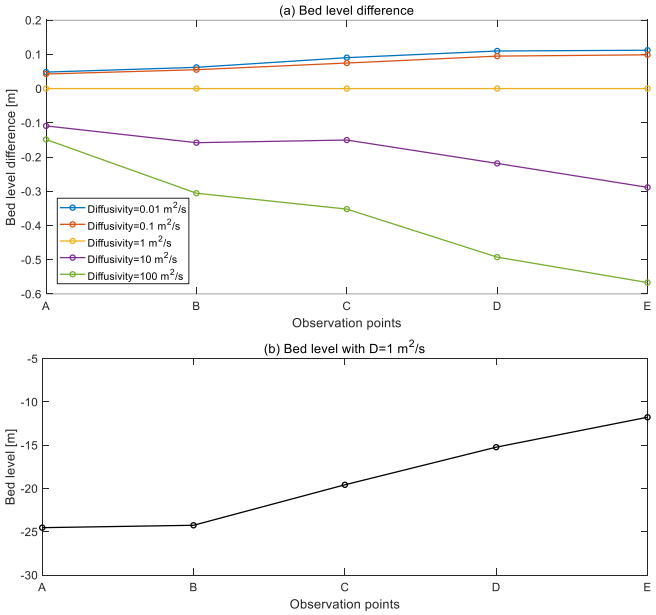

Figure 4.17: (a)Bed level difference at five observation points in 100 years compared with D=1 m^2/s. (b)Bed level in 100 years of D=1 m^2/s.

To investigate the influence of the diffusivity in morphological change, five observation points are labeled in Figure 4.16 and their bed level differences compared with the default case (D=1 m^2/s) are shown in Figure 4.17(a). For a clearer reference, 4.17(b) shows the bed level in 100 years and from A to E, the water depth decreases. Increasing the diffusivity makes the erosion at the deepest point, A, become more but at E whose water depth is the shallowest, the erosion is even more severe compared to point A. The higher diffusivity makes the slope of the channel milder instead of steeper. According to Eq. 3.11, the shallower area has a smaller c_e which is supposed to be eroded less than the deeper area. But here the situation is the opposite. That's because the channel is not a closed system and the sediment finally is transported to the flat. Compared with point E's adjacent flat, point E is still a relatively deep area and a sediment source of the flat. What's different between A and E is that at A, there is sufficient sediment supply from outside but at E there is not. Hence, the erosion at E is even more than that at A.

Figure 4.18 compares the bed level difference in 100 years at the cross-section Dantziggat which is labeled in Figure 4.16 for different diffusivity coefficients and diameters. The higher diffusivity induces a severe erosion at the channel which reaches 0.6 m for the case with D=100 m^2/s at the deepest point but the smaller diameter promises a sufficient supply, so there is no significant erosion at the channel, even though the accumulations at the shallow area are about in the same order.

Overall, a strong diffusion term has an intention to flatten the sediment concentration gradient which can attract more sediment to the shallow area and also normally lead to more severe erosion at the channel.

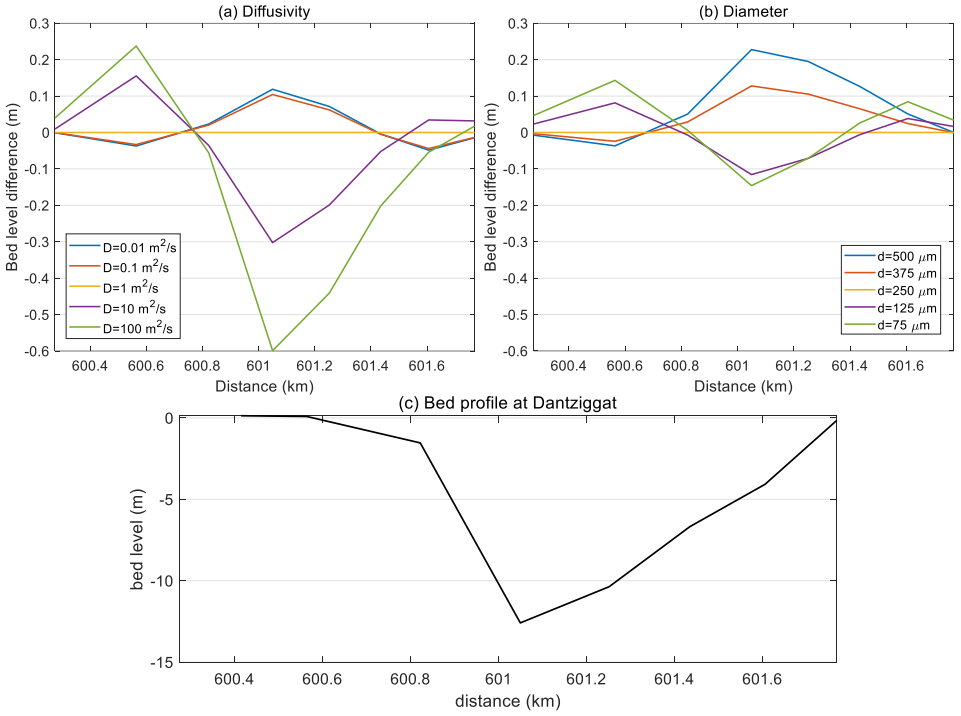

Figure 4.18: (a, b)Bed level difference at Dantziggat compared with D=1 m^2/s and d=250 μm in 100 years. (c)Bed level profile of cross-section Dantziggat.

4.2.3. EQUILIBRIUM CONCENTRATION

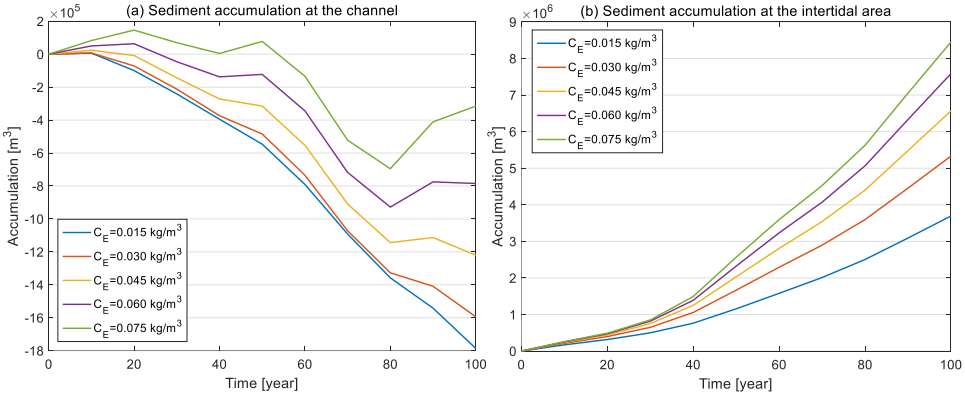

Figure 4.19: Sediment accumulation inside the Ameland basin for five global equilibrium concentrations

In Eq. 3.11, there are two equilibrium concentrations controlling the sediment ex-

change processes and the local equilibrium concentration is proportional to the global one depending on the water depth difference. Therefore, the one is going to be discussed is the global equilibrium concentration (C_E) which is also prescribed at the boundaries. In physical meaning, the C_E reflects the sediment availability in the water column and also the sediment supply from the boundaries. In the aggregated models, C_E influences the time scale of the model. The larger C_E the shorter the time scale of all elements (Buijsman, 1997). Also, Wang et al. (2007) stated that the C_E is the parameter indicating the level of morphological activity. Therefore, investigating the C_E can help people understand the relationship between the morphological time scale and the physical processes.

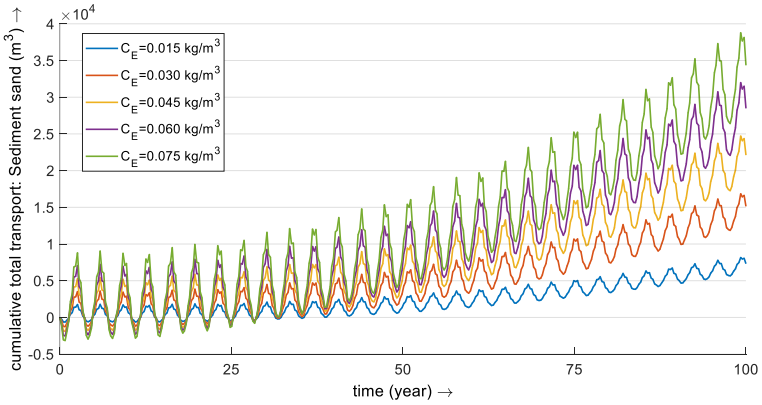

Figure 4.20: Cumulative sediment import through the inlet for five Diffusivity coefficients ((toward basin is positive, without multiplying MORFAC)

A higher C_E results in more sedimentation at the flat and also less erosion at the channel from Figure 4.19. With regard to the accumulation after 100 years at the flat, when the C_E increases from 0.015 to 0.03 kg/m^3, the accumulation increases from 3.7 × 10^6 m^3 to 5.2 × 10^6 m^3, but when the C_E increases in the same interval, the increase in accumulation gets less and less. But in terms of the erosion at the channel, it behaves in an opposite way. When C_E is small, the increase in C_E doesn't influence the erosion at the channel as much as it does at flat. But when the C_E gets higher, a higher C_E does decrease the erosion at the channel and even changes the shape of the accumulation curve. Therefore, it can be deduced that when the C_E is at a low level and the sediment availability in the water column is not abundant, the increased C_E provides more sediment at the boundaries which is transported to the flat preferentially. When the C_E reaches a certain level where the sediment in the water column is relatively sufficient for the flat, part of the sediment will also be transported to the deeper area, i.e., the channel. With more sediment settled at the channel, the tipping point appears earlier than other cases after 80 years for C_E=0.075 kg/m^3.

The cumulative sediment import through the inlet at the end of the simulation in Figure 4.20 is linearly proportional to the C_E. And the amplitude of the cumulative sediment curve, which indicates the sediment volume is imported into the basin in a tidal cycle, increases when C_E increases. In a word, the results prove the point of view of Wang

et al. (2007) that the C_E controls the sediment availability which eventually influences the morphological activity within the domain and the time scale of each element.

4.2.4. POWER N

The power n is applied in Eq. 3.11 which is inherited from the sediment transport formula. From the previous study in the aggregated models, the time scale is inversely proportional to the power n which means a larger n can shorten the time in reaching the equilibrium state (Buijsman, 1997). According to Eq. 3.11, the n influences the vertical sediment exchange by amplifying or narrowing the difference between local water depth and equilibrium water depth which consequently changes the local equilibrium state.

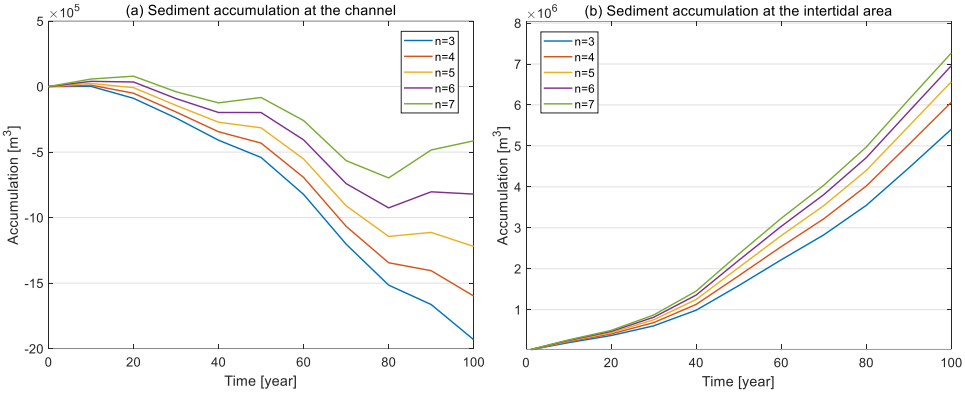

Figure 4.21: Sediment accumulation inside the Ameland basin for five values for power n

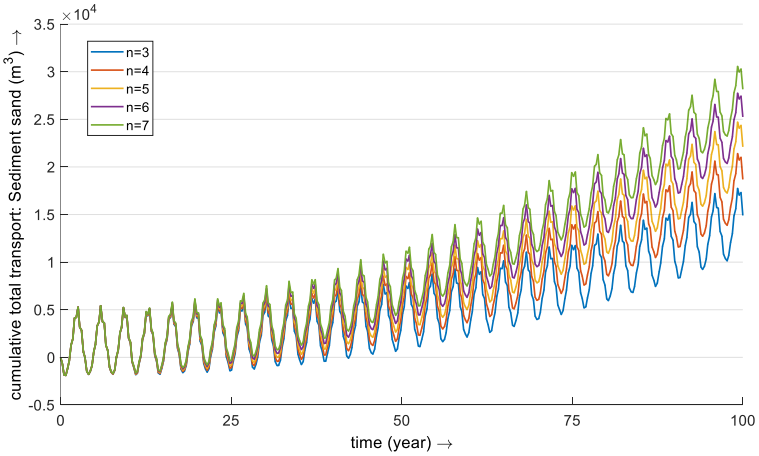

Figure 4.22: Cumulative sediment import through the inlet for five values of power n (toward basin is positive, without multiplying MORFAC)

The effect of changing the power n is similar to changing the reference level de-

scribed in Section 3.3.4. By increasing or decreasing the power n, areas become more or less sensitive to SLR, especially at the shallow area. From Figure 4.21, the accumulation at the flat doesn't change too much with varied n but a slight increase in the accumulation volume can be observed when n increases. Unlike the volume change at the flat, the accumulation at the channel changes quite dramatically with changed n, not only in the volume, but also in the time scale. A higher n makes the channel reach the equilibrium state earlier since the moment when the erosion stops appears earlier than other cases with lower n. The influence of n and C_E are quite similar observed from the accumulation patterns which is in agreement with their effects in the aggregated models (Buijsman, 1997).

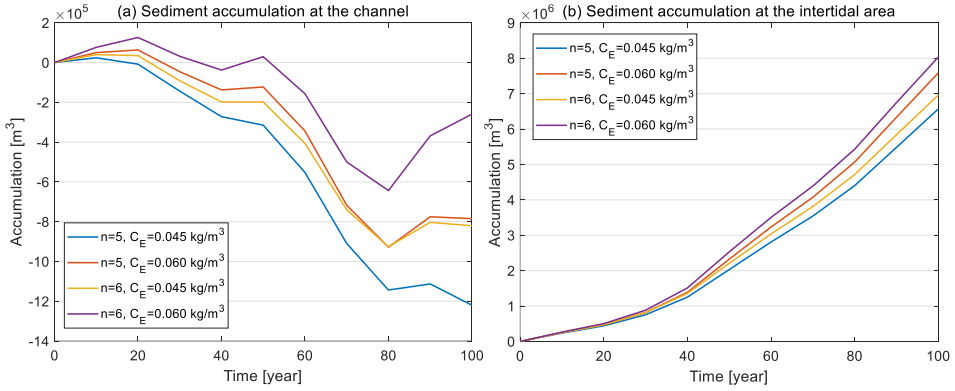

Figure 4.23: Sediment accumulation at the channel and the intertidal flat for four combinations of C_E and n

With the theoretical analysis in the aggregated models, n is not independent with C_E and the morphological time scale is decided by the product $n * C_E$. Therefore, four combinations of n and C_E are shown in Figure 4.23. Based on the default setting with n=5 and C_E=0.045 kg/m^3 (case 1), two independent cases (case 2 and 3) with a higher n at 6 and with a higher C_E at 0.06 kg/m^3 are carried out. They perform really similarly on channel erosion and the time scales for the two cases are approximately identical. But the case with a higher C_E obtains slightly more sediment at the flat. When both two parameters increase at the same time (case 4), even the accumulation at the flat only increases modestly, the erosion behavior at the channel change dramatically and the time scale obviously gets shortened. The results prove that the study in the aggregated models that n and C_E have a quite similar effect on the morphological activity is also valid in the hybrid model.

Two different combinations (case 2 and 3) still result in similar behavior and two parameters have a comparable effect on the sediment accumulation, no matter they are changed jointly or severally. Thus, during calibrating the model in the application, one parameter can be fixed beforehand and calibrating the model by modifying another parameter.

4.2.5. MULTIPLE SEDIMENT FRACTIONS

Wang and Van Der Spek (2015) claimed the necessity of applying more than one single fraction of sediment to both the process-based model and the aggregated model since each fraction plays its role in infilling the basin. Therefore, another sediment fraction is supplemented to the simulation to check the influence of each sediment fraction. Three cases with two sediment fractions are carried out. For all three cases, the median sediment diameter is the same at 250 μm and the sediment compositions are shown in Table 4.2. The global equilibrium concentration and the sediment concentration at three boundaries keep the same at 0.045 kg/m^3. The equilibrium concentration of each fraction is related to its ratio in the bed which is equal to its ratio times the global concentration (fC_E). In this case, there are two sediment fractions and their volume in the bed is the same. Meanwhile, at the boundaries, the suspended concentration for each fraction is 0.0225 kg/m^3.

Table 4.2: Sediment composition of four cases

Case #	D_{50} [μm]	percentage (f_1)	D_{50} [μm]	percentage (f_2)
1	100	50%	400	50%
2	150	50%	350	50%
3	200	50%	300	50%
Single	250	100%		

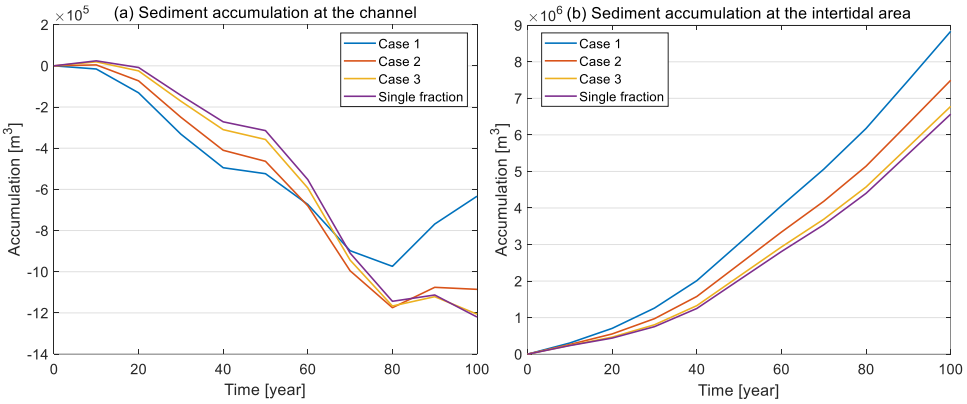

Figure 4.24: Sediment accumulation inside the Ameland basin for three cases with two sediment fraction and one case with a single sediment fraction

Figure 4.24 shows the accumulation and erosion at the channel and the intertidal flat. Even though four cases have a same median sediment diameter, they perform quite differently. Case 1 has the finest and the coarsest sediment fraction among all cases. Due to the appearance of the much finer sediment fraction, the flat accumulates faster than other cases and also the time scale of the channel is shortened.

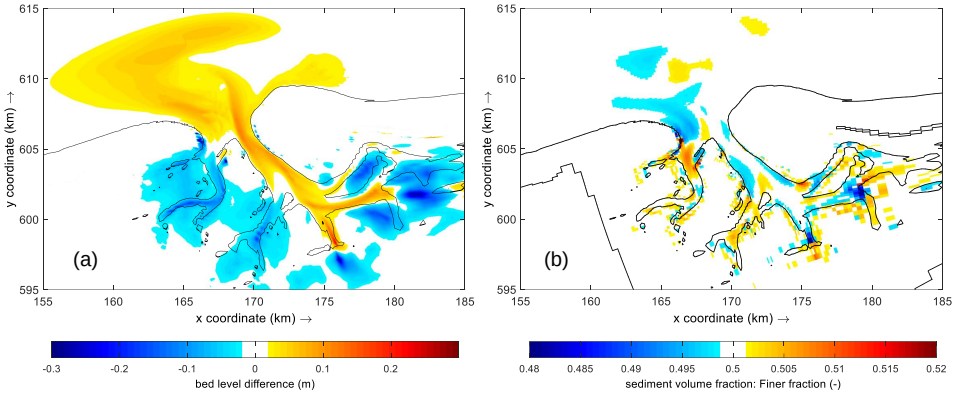

Figure 4.25: (a) bed level different between the case with single fraction and case 1 at the end of the simulation, the yellow area indicates single fraction is higher than case 1. (b) ratio between the volume of the finer fraction and total sediment volume.

The difference between the case 1 and the single fraction case is shown in Figure 4.25. In subfigure (a), the case with two fractions has a lower bed level at the channel but a higher level at the flat. This is because the finer sediment has a longer adaptation length (Wang and Van Der Spek, 2015) and can be easier transported to the flat. That also means there is less sediment settling at the channel which induces a lower bed level at the channel. Subfigure (b) indicates how sediment is spreading in the basin. In the model settings, to promise there is enough sediment to be eroded, the total thickness of sediment is set at 30 meter and two fractions contribute a half, respectively. The sediment in the bed and the water column is assumed as well-mixed. So the ratio between the volume of the finer sediment and the total sediment volume can reflect the erosion or sedimentation of different fractions. The blue area indicates that at the area the finer fraction is less than the coarser fraction and the yellow area indicates the opposite. At the inlet and some parts of the main channel, the coarser sediment is dominant since the coarser sediment has a higher settling velocity and it is easier to settle down just after entering the basin. Meanwhile, the finer sediment is more than coarser sediment at the landward end of the channel and some parts of the intertidal flat. This is in agreement with the observation that at the flat the sediment is much finer containing lots of mud fraction and at the channel, the sediment is coarser (Pearson et al., 2019).

Besides that, the percentage of every fraction will evolve approaching the ratio of the suspended sediment at the boundary. For instance there are two fractions 1 and 2. When two fractions' ratios are both 50% at the boundary but in the bed, fraction 1 is more than fraction 2 which means f_1 is higher than f_2 and $f_1 C_E$ is higher than $0.5 C_E$. For fraction 1, the local concentration is higher than the equilibrium concentration. At this moment, even though the water depth is at the equilibrium state, the fraction 1 is still eroding and fraction 2 is accumulating. And the ratio in the well-mixed bed will evolve towards the ratio at the boundary.

For the stratified bed the evolution is quite similar. Although both fractions have the same volume in the bed ($f_1 = f_2$), the upper layer only contains fraction 1 and fraction

2 is in the lower layer. For example, the bed at the channel is stratified and SLR is applied. The channel is eroded according to the morphological change pattern and only fraction 1 can be eroded. Therefore, the volume of fraction 1 decreased and $f_1 < f_2$ at this moment. There will be more fraction 2 accumulating at the channel which makes the bed become well-mixed again. In reality, coarser sediment covers fine sediment at the main channel and it is stratified. But in this case, if the upper layer at the channel only contains coarser sediment, the channel will become another trap of fine sediment which influences the accumulation at the intertidal flat. Hence, only well-mixed bed is considered in this section.

5

SUBSIDENCE

The hybrid model provides us with an effective and more robust tool to simulate the morphological change of tidal basins with respect to the water level change. The sea-level rise and the ground subsidence both increase the water level externally. Therefore, the hybrid model should be capable of morphological simulation with respect to the ground subsidence. In this chapter, the performance of the model in reproducing the bed level change with subsidence is going to be discussed.

5.1. MODEL SETUP

The basic parameters' setting keeps unchanged as used in Section 4.1 but without SLR applied. A circle area with a geographically uneven subsidence is applied inside the basin as Figure 5.1 shown.

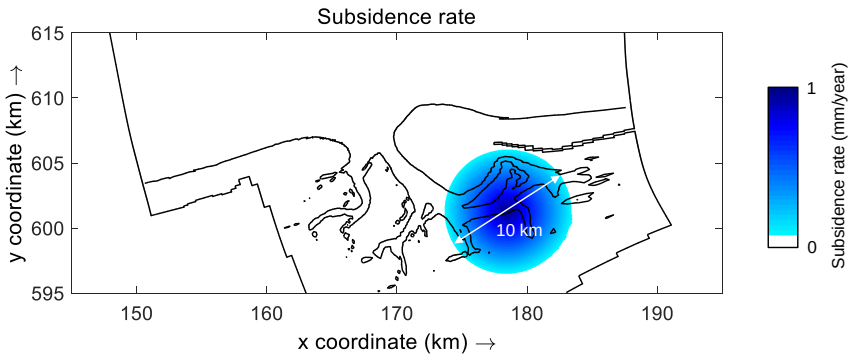

Figure 5.1: Subsidence area and the rate inside the Ameland basin

The center of the subsidence circle is situated southeast of the throat inside the basin and near the end of the channel. The diameter of the subsidence circle is 10 km and at

the center the subsidence speed is 1 mm/year which linearly decreases to 0 at the edge of the circle. The subsidence lasts for the beginning 40 years and in the following 60 years, the subsidence stops.

5.2. RESULTS

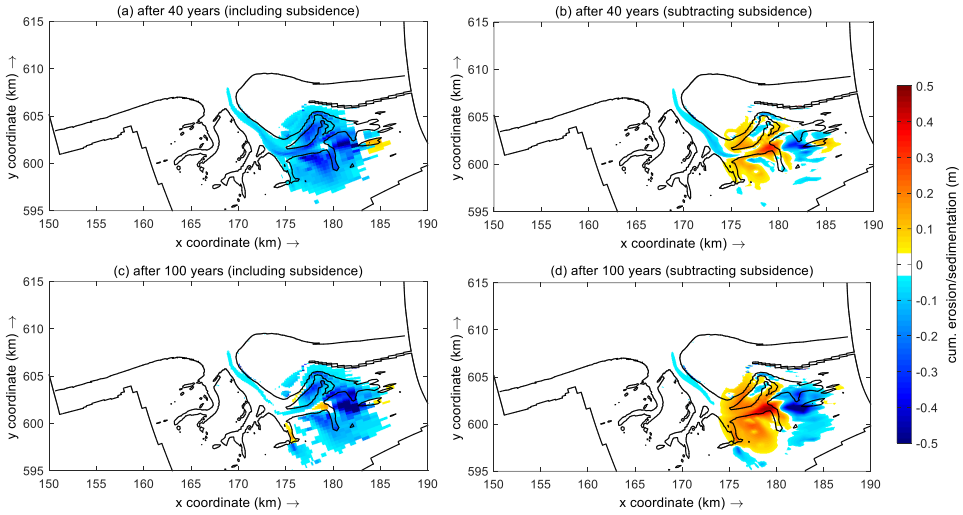

Figure 5.2: Cumulative erosion/sedimentation map in 40 years and 100 years at the Ameland inlet. (a) and (c) show the bed level change including the subsidence in year 40 and 100, (b) and (d) show the bed level change after subtracting the subsidence in year 40 and 100.

The subsidence results in a local water depth increase which eventually leads to a morphological change similar to the response to SLR. Figure 5.2 shows the cumulative erosion and sedimentation pattern at the Ameland inlet after 40 years and after 100 years. In the first 40 years, the bed level within the circle area subsides at a constant speed and when the subsidence stops, the bed level change can be not only observed within the circle area, but also at the main channel. The subsidence area is out of equilibrium and has an intention to recover to the original water depth, which needs more sediment import. In this circumstance, the main channel acts as the primary source of sediment which is in agreement with the ASMITA model. The main channel connects the flat and the outside area and the erosion at the channel induces a larger concentration gradient with the outside which helps the basin attract more sediment. And in the following 60 years, the basin tends to recover to the original bed level since the equilibrium water depth doesn't change. 60 years after the subsidence has stopped, the erosion at the channel is alleviated and the erosion degree at the flat becomes lower which can be observed from the smaller erosion area and the lighter color in Figure 5.2(c).

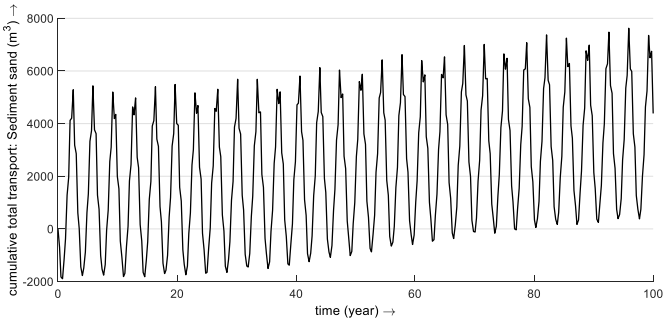

Figure 5.3: Cumulative sediment import through the inlet (toward basin is positive, without multiplying MORFAC)

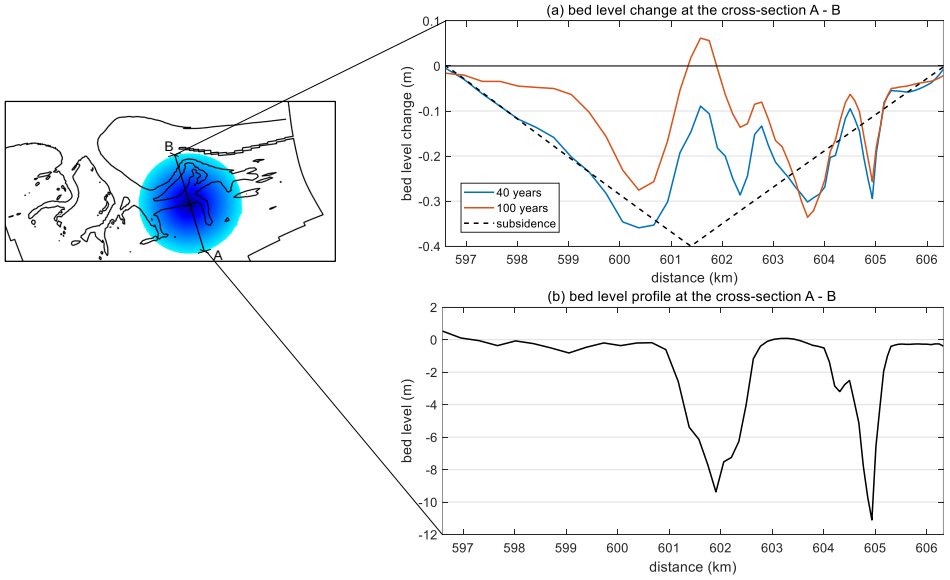

Figure 5.4: (a)subsidence after 40 years and bed level change after 40 years and 100 years at the cross-section A-B. (b)initial bed level at the cross-section A-B.

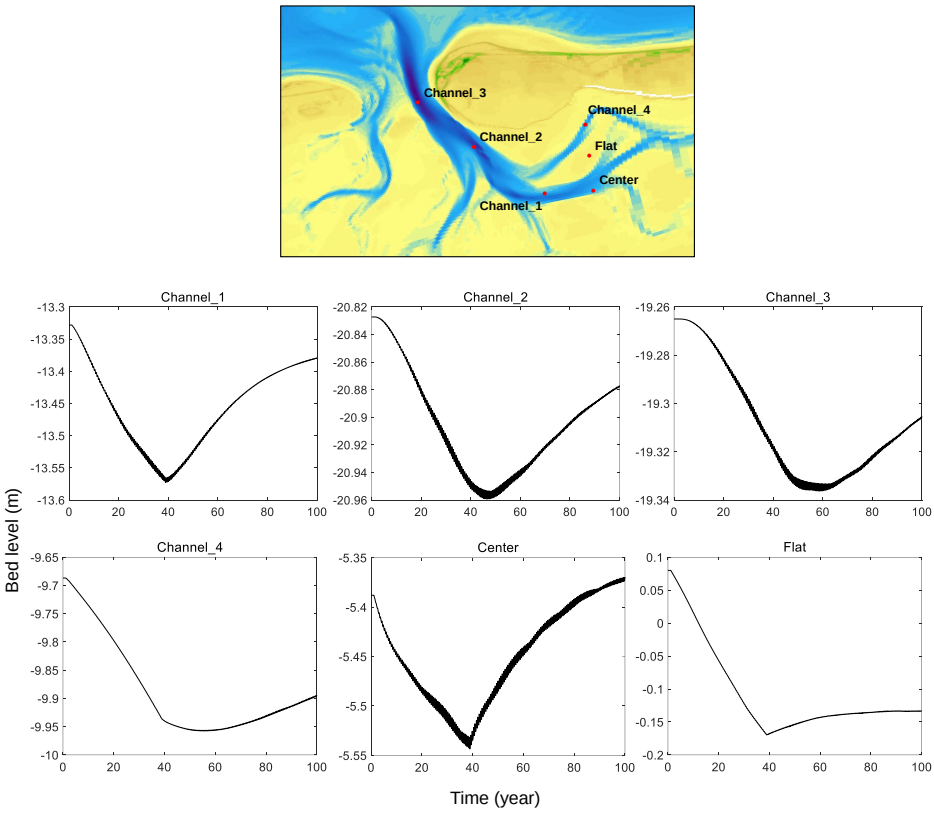

Figure 5.5: Bed level change in 100 years at six observation points inside the basin

The sediment import through the inlet doesn't respond immediately when the circle area starts to subside (Figure 5.3). Between year 40 and year 80, the sediment shows an obvious import into the basin which is transported to the sunk area and this increase slows down after year 80. There is a time lag between the subsidence and the sediment import.

A cross-section A-B is drawn in Figure 5.4 which crosses two channels and the intertidal flat in between. The center of the cross-section is also the center of the subsidence circle which is near the deepest part of the side channel. In this first 40 years, the bed level change at the southern flat is basically equal to the subsidence and no additional morphological change happens. But the deep area of the southern channel is only 0.1 m lower than the original bed level which is much smaller than the subsidence. Referred to the subsidence, the southern channel accumulates but the middle flat and the northern channel are further eroded to -0.3 m. In year 100, the bed level at the southern channel and the southern flat are elevating and especially the bed level at the main channel is 0.05 m higher than the original level before subsidence. The profile of the northern channel keeps the almost same shape as that in year 40. Overall, the southern channel

and the southern flat can recover from subsidence quickly but the northern channel is under a sediment shortage for the whole period.

In Figure 5.2, those areas close to the main channel (west part of circle area) have abundant sediment supply which helps them quickly recover from the subsidence approaching the original depth. When it comes to the east, the flow is not as strong as that at the main channel (Figure 3.10) and the exchange between the flat and the channel is much less frequent. Therefore, the landward area at the east of the subsidence circle can hardly restore from subsidence. The weaker horizontal sediment exchange can also explain why the main channel can restore faster than the flat.

In Figure 5.5, along the main channel from the throat to landward three observation points, Channel 3, 2, 1, are set. Channel 1 has an immediate response in bed level change since it is located within the circle, and channel 3 has a 5-year delay between its response and the subsidence. Although the channel 2 and 3 are not situated inside the circle, they both experienced an erosion of 0.13 and 0.07 m, respectively. This follows the principle behind that if there is a point inside the basin under a sediment shortage, the nearby deeper area will be the first source of sediment. It is worth mentioning that according to the curve, after the stop of subsidence can distinguish the state of the area. When the subsidence stops, if the bed level curve shows a convex curve, that means the sediment at this area is accumulating and the area is attracting sediment. But if the curve is concave, the area is being eroded previously and acts as a source of sediment. Therefore, it can be deduced that point channel 1, center, and flat are attracting sediment and channel 2, 3, 4 are being eroded.

6

DISCUSSION

The hybrid model has been adjusted and applied at the Ameland inlet to simulate the morphological response with SLR and subsidence. The adjustment to the model and the result of the long-term simulation are going to be discussed in this chapter.

6.1. SEDIMENT SOURCE

In Chapter 3, the phenomenon behind is elaborated and a further modification is conducted to re-arrange the sediment morphological activity outside the basin, which also adjusts the sediment source of the basin. Whether the ebb-tidal delta is labeled (see Section 3.5) is of great importance to the sediment supply inside the basin. According to the model formulation, all the shallow areas including the ebb-tidal delta and the intertidal flat behave quite similarly as they are more sensitive to SLR and attract most of the surrounding suspended sediment. If it is labeled as the outside area, the sedimentation can happen at the delta which can block almost all the sediment from the boundaries. If it is not labeled, the sedimentation is not allowed at the ebb-tidal delta which will not attract the sediment passing by. This promises a more abundant sediment supply than the latter case.

However, the role that the ebb-tidal delta plays when SLR is applied is ambiguous. The Ameland inlet's behavior with SLR is simulated by the process-based model and also the aggregated model, and the ebb-tidal delta is being eroded with an accelerated SLR (Dissanayake et al., 2012, Stive and Wang, 2003). It is commonly accepted that the most of basin infilling is supplied by the ebb-tidal deltas (Elias et al., 2019). In this model, to promise a sufficient sediment supply through the inlet, the ebb-tidal delta is excluded from the area where the sedimentation can happen. Even though sediment cannot accumulate at the delta, the delta can be still eroded. From the long-term simulation's result in Chapter 4, the ebb-tidal delta is always being eroded with different SLR speed which is in line with the result of Dissanayake et al. (2012). But the difference between them is that in the process-based model the behavior is decided by the hydrodynamic and morphodynamic conditions, but in the hybrid model it is decided by the equilibrium state beforehand.

In the present circumstance, the ebb-tidal delta in the simulation is acting as the source of sediment to keep the sediment supply inside the basin approaching to reality. But when the relationship between the SLR speed and the morphological activity of the ebb-tidal delta is clearer, it's possible to adjust its role in the whole system by modifying the equilibrium depth of the ebb-tidal delta.

To reproduce the real sediment transport processes, the alongshore transport cannot be ignored, which is the main source of the basin and the deltas. From the Bruun (1954) Rule, a higher mean sea-level results in a retreat of barrier islands' shoreline. The eroded sediment will be carried by the alongshore flow, settling at the ebb-tidal delta, bypassing the inlet, or being transported into the basin. Due to the concept of equilibrium state, the Bruun Rule can hardly be applied in the model. Even a relatively larger equilibrium depth can be prescribed at the littoral area to achieve the shoreline retreat, the quantity of the erosion and the erosion rate are out of control. If do so, the shoreline retreat can only be compared qualitatively. Thus, in this model the shoreline is fixed and the alongshore transport only contains the sediment from the east and west boundaries. The hybrid model's performance in reproducing the behavior outside the basin is to be developed and more adjustments should be applied to the model to make the whole sediment transport process more realistic.

6.2. SEDIMENTATION/EROSION PATTERN

In Chapter 4, the model simulates the morphological response of the Ameland inlet to three SLR speed of 4, 6, 8 mm/year in 100 years. For all three cases, the degrees of sedimentation and erosion are different but the general trends are identical. The main channel Borndiep and the side channel Boschgat are being eroded for the whole period and the ebb-tidal delta is eroded as well. Meanwhile, the intertidal flat experiences a significant sedimentation especially in the area near the channel. Those characteristics are pronounced when the SLR speed increases. These results are in line with previous studies using the ASMITA and Delft3D (Stive and Wang, 2003, Dissanayake et al., 2012). But a slight difference among them is that when the sediment imported into the basin is insufficient to infill the space induced by SLR, the erosion at the channel would happen in the process-based model. But for both the hybrid model and the aggregated model, the deep area of the channel is always being eroded within the period no matter how much sediment is imported. Similarly, in the ASMITA model, the channel is eroded from the start and the erosion lasts for the whole simulation.

The equilibrium depth decides the morphological change's direction of each element. In this project, the Ameland inlet is assumed as under the equilibrium state and the equilibrium depth is determined at the depth in 2005. But when dealing with the case that the tidal inlet is not under the equilibrium state, the determination of equilibrium depth would become a problem. But for the aggregated model, the empirical formula indicates the relationship between the equilibrium volume of each element and tidal range, tidal prism, and the area of the basin, which decides the evolution's direction. The difference in the way to determine the equilibrium state of each point or each element leads to the difference in the morphological trend.

Another remarkable morphological feature at the Ameland inlet is the migration of the channels, which is introduced in Chapter 2. But due to the local equilibrium depth,

the channel-shoal structure is fixed. Therefore, it's difficult to reproduce the channel's horizontal development by using the hybrid model.

The sedimentation and erosion pattern is also affected by the hydrodynamic conditions. Even all simulations in this thesis only contain tidal conditions, the hybrid model provides a possibility to add other processes into it, i.e., wind and wave, based on its fully calculated 2-D hydrodynamic computation. Dissanayake et al. (2012) adds waves to the process-based model and proves waves enhance an easterly net transport in combination with tides. Wind can also play an important role in the sediment transport inside the basin. Wind has a significant influence in re-directing the flow which may enhance the sediment spreading at the shallow area and the transport between the channel and the flat. So far, the simulations' results already reflect the morphological trend with SLR successfully, but when enough data is collected, the calibration can be carried out and other processes can be supplemented to the model.

6.3. PARAMETER ANALYSIS

Those five parameters are selected in Section 4.2 and it is proved that they do influence the morphological activity in different degrees from the comparison. Firstly, the sediment diameter (settling velocity) is of the greatest importance to the morphological activity among those five parameters. Especially, the accumulation time scale at the channel is affected significantly by changing the diameter. Furthermore, it decides the order of the sediment volume accumulated at the flat. Secondly, the diffusivity mainly influences the horizontal sediment exchange particularly between the flat and the deep area of the channel. This value decides how much sediment is going to be eroded at the channel and transported to the flat and only has a modest effect on the sediment import through the inlet. Thirdly, the global equilibrium concentration and the power n basically have a quite similar influence on the accumulation pattern. The sediment import of both two parameters is linearly proportional to these two parameters. And they have a significant effect on the morphological time scale of the channel.

Although changing the sediment from one fraction to two fractions with the median diameter unchanged has a quite similar influence as changing the median diameter directly, it provides another way to modify the morphological behavior of the flat and the channel separately. The finer sediment plays an important role in infilling the additional space induced by SLR at the flat and the coarser sediment is important in maintaining the channel. Hence, when two or more sediment fractions are introduced in to the model, it is possible to calibrate them separately and no need to keep the median diameter at the same value. And it's no doubt that the simulation with two fractions produces a more realistic sediment distribution approaching to the observation data.

According to the previous study in the aggregated model, Wang et al. (2007) proposed that the calibration of the parameters follows the order that firstly the power n and settling velocity (diameter), then the diffusivity, finally the C_E. Here in the hybrid model a similar order is recommended based on the result of sensitivity analysis:

1. Choosing a power n based on the sediment transport formula.
2. Choosing a proper sediment diameter (D_{50}) according to the order of sediment imported into the basin and overall erosion pattern of the channel. The multiple

sediment fractions can be introduced in this step to achieve a more realistic morphological activity.

3. Choosing a diffusivity to adjust the sediment arrangement between the flat and the channel, i.e., balance the priority of two elements in attracting sediment.

4. Changing the C_E to decide the specific time scale of the channel.

6.4. SUBSIDENCE

In Chapter 5, a subsidence circle area with a diameter of 10 km is applied inside the Ameland basin behind the Terschelling island to simulate the real ground subsidence induced by gas mining. Subsidence and SLR both result in a gap between the local water depth and the equilibrium water depth which induces a further morphological change. Due to their similar principle, the hybrid model predicts the bed level change of the whole basin during the subsidence and after the subsidence stops. Although the center of the subsidence circle has the fastest subsidence rate at 1 cm/year, it doesn't have the biggest bed level change at the end of subsidence compared with other areas where subsidence is slower. Instead, the bed only sinks for 0.1 m where the subsidence is 0.4 m, which indicates that the sediment is being attracted to the center from the subsidence starts. The main channel is eroded even at the area excluded from the subsidence circle, showing that the main channel is always the first source of sediment when there is a demand inside the basin. And the priority to gain the sediment is inversely proportional to the equilibrium depth. Similarly, the priority to give away the sediment when needed is proportional to the equilibrium depth.

The results prove the principle behind the sediment transport that sediment always follows the gradient of sediment demand. Also, if the gas mining center is at the channel, the bed level of it can quickly recover from the subsidence. From the result in Section 4.2, the diffusivity is dominant in sediment distribution between the channel and the flat, especially at the channel located more landward. When the data in the field is collected, calibration can be carried out by modifying the diffusivity to balance the erosion or accumulation rate of the flat and the channel. Besides that, the sediment transport between the area gaining sediment at the west and the area losing sediment at the east can be calibrated by adjusting the diffusivity. The erosion at the main channel and the time scale of the accumulation and erosion inside the subsidence circle can be calibrated by changing the sediment size.

7

CONCLUSIONS

The content of this thesis will be concluded in this Chapter by answering the research questions proposed in Chapter 1.

7.1. CONCLUSION

Can the hybrid model predict the basic morphological trend in tidal inlet with SLR? What parameters do matter to the result of the simulation?

The hybrid model has fully computed 2-D hydrodynamic conditions in the horizontal direction and in the vertical direction, a new sediment exchange equation containing the equilibrium state substitute the original equation in the Delft3D. The equilibrium state is inherited from the aggregated model which is defined by the local equilibrium water depth and the present water depth. Simply speaking, when SLR is applied, all the areas are chasing for their equilibrium but different areas with different water depths have different sensitivity to SLR. The varied sensitivities influence the equilibrium concentration and eventually affect the sediment transport.

Before applying the adjustments, the ebb-tidal delta blocks almost all the sediment from outside the inlet. So when SLR is applied, the sediment accumulating at the intertidal flat is mostly eroded from the channel and only little from outside. To reproduce a more realistic sediment import, the ebb-tidal delta turns from accumulating to being eroded by applying the adjustments. And due to the robustness of the hybrid model, a coarser grid and higher morphological scale factor can be used to shorten the computation time.

Three different scenarios of the SLR speed at 4, 6, 8 mm/year are applied at the Ameland inlet and the simulation time is 100 years. For the whole period, the channel is being eroded. On the contrary, the intertidal flat is accumulating and the sediment settling at the flat is from both outside and the channel. The erosion/sedimentation is pronounced with a higher SLR speed. Besides that, Faster SLR speed also increases the sediment import through the inlet since the demand for sediment is expanding. Because of the fully calculated hydrodynamic conditions, the sediment transport trace could be

tracked. The sediment at the Borndiep partially is imported to the flat to compensate for the additional space induced by SLR. And another part of sediment at the Borndiep is exported to the outside during ebb, and settles at the nearby area, e.g., the ebb-tidal delta, and in the next flood is transported into the basin through the Boschgat. One part of sediment will be carried more landward to the west of the basin and settle at the flat near the Boschgat. Another part of sediment passes over the shoal between the Borndiep and the Boschgat and returns the Borndiep at the end.

To investigate the influence of different parameters, a sensitivity analysis is carried out. The sediment diameter which decides the settling velocity of particles is of great importance to the sediment import. The finer sediment can spread further inducing the most sedimentation at the flat. And the tipping point of the channel turning from being eroded to accumulating appears earlier with a smaller diameter, which is corresponding to the time scale of the channel. The diffusivity plays an important role in the sediment balance between the shoal and the channel. A higher diffusivity enhances the transport induced by diffusion and results in more erosion at the channel and more sedimentation at the flat. The global equilibrium concentration and the power n from the sediment transport equation have a similar effect on the whole process. The time scale is inversely proportional to these two parameters. Especially, the channel is sensitive to these two parameters which have a significant influence on its time scale. The model performance with two sediment fractions is studied as well. Introducing more than one fraction can present a more realistic sediment distribution and it is easier to calibrate the morphological activity at different elements.

Compared with previous models, what's the difference?

The process-based model and the aggregated model are the most frequently used in the morphological response of tidal basins to SLR. The aggregation level of the hybrid model is in between those two types of models since the computation is integrated in depth. Compared with the aggregated model, the hybrid model has the fully calculated horizontal hydrodynamic computation which provides the possibility to track the sediment transport. This is not feasible when using the aggregated model.

The equilibrium concept inherited from the aggregated model makes the hybrid model more robust. In the process-based model, a small deviation might mislead the whole simulation to another direction since there is no such an equilibrium concept. The equilibrium state of all the areas controls not only the evolution's direction but also the sediment distribution and the priority of attracting sediment. The higher robustness allows users to use a coarser grid and a higher morphological scale factor which shorten the computation time dramatically. However, also because of the equilibrium state, the shoal-channel structure is fixed, which means the channels and the shoals cannot migrate and the number of channels cannot change, either. But in the process-based model, it is proved that the evolution of channels is able to be simulated.

With regard to the model results, three types of model are in agreement: the channel and the ebb-tidal delta are being eroded and the flat is accumulating. The only difference is on the erosion at the channel that in the process-based model, the channel will only be eroded when the SLR speed is fast enough and the sediment import from outside is not enough. But in both the hybrid model and the aggregated model, the channel is eroded from the beginning no matter how fast the SLR speed is. This is induced by the

concentration gradient between the flat and the channel which consequently influences the diffusion term. The sensitivity analysis of the hybrid model also gives a quite similar recommendation in calibrating the parameters as the aggregated model since they share a common equilibrium concept.

How does the model perform with subsidence?

The principle behind the process of subsidence is similar to imposing SLR as the morphological response shown. An uneven subsidence circle simulating the subsidence induced by gas mining is applied inside the basin behind the Ameland. The area near the center where the subsidence speed is the fastest doesn't subside as fast as the subsidence rate since the sediment is being attracted to this area. However, the area at the main channel where is not located in the circle is eroded, which means that the equilibrium state is not a local concept but a global concept. If one part of the area inside the basin is out of equilibrium, the sediment will firstly be redistributed from the deeper area which is the primary source of sediment to the shallow area or the area influenced by depth change the most. The hybrid gives a very reasonable deduction about the morphological change induced by subsidence but the result needs to be further calibrated with the observed data.

7.2. RECOMMENDATIONS

No model is perfect. There are still some imperfect points in this model which may be improved in the future.

1. The retreat of coastline at the barrier islands is a important feature in the morphological change in the Wadden Sea. But in this model, the equilibrium concept restricts the shift of the coastlines. The beach erosion also contributes to the alongshore transport. So the sediment import into the basin is limited due to the lack of one of the main sources. So the sediment source outside the channel could be a key point to improve the model.

2. The fully calculated hydrodynamic conditions provide the possibility for researchers to apply wind and wave into the model which is missed in this project. The wind plays an important role in the sediment redistribution inside the basin and this may enhance the sediment exchange between the shoal and the channel.

3. The up limit of the robustness of the hybrid model is not fully checked. The new vertical exchange formulation makes it possible to use a much coarser grid and higher MORFAC without affecting the morphological activity. Therefore, a limit check could be carried out and if possible, the calculation time could be shortened significantly.

4. For now when the sediment contains multiple fractions, the equilibrium concentration of each fraction is directly related to the proportion of each fraction in the bed. In the future research the way to calculate the equilibrium concentration in the case with multiple fractions could be developed to make the stratification in the bed be more realistic.

5. When the data is enough, a calibration can be carried out to compare the result of the hybrid model with the other two types of model.

BIBLIOGRAPHY

Baart, F. (2019). *De stand van zaken rond de zeespiegelstijging langs de Nederlandse kust* (tech. rep.). Deltares. Utrecht. https://www.deltares.nl/app/uploads/2019/03/Zeespiegelmonitor-2018-final.pdf

Bahlke, C. (2017). *Harbours and shipping. In: Wadden Sea Quality Status Report 2017* (tech. rep.). Common Wadden Sea Secretariat (CWSS). Wilhelmshaven, Germany.

Blew, J., Günther, K., Hälterlein, B., Kleefstra, R., Laursen, K., Ludwig, J., & Scheiffarth, G. (2017). *Migratory birds. In: Wadden Sea Quality Status Report 2017* (tech. rep.). Common Wadden Sea Secretariat (CWSS). Wilhelmshaven, Germany.

Bosboom, J., & Stive, M. J. F. (2021). *Coastal Dynamics* [ISBN: 9789463663717]. Retrieved July 23, 2021, from https://textbooks.open.tudelft.nl/textbooks/catalog/view/37/92/233-1

Bruun, P. (1954). *Coast erosion and the development of beach profiles* (Vol. 44). US Beach Erosion Board.

Buijsman, M. C. (1997). The impact of gas extraction and sea level rise on the morphology of the Wadden Sea: Extension and application of the model ASMITA. Retrieved August 22, 2021, from https://repository.tudelft.nl/islandora/object/uuid%3Afb69f73a-7314-496c-84a8-46c5a48a1f84

Cheung, K. F., Gerritsen, F., & Cleveringa, J. (2007). Morphodynamics and Sand Bypassing at Ameland Inlet, The Netherlands [Publisher: Coastal Education and Research Foundation]. *Journal of Coastal Research, 2007*(231), 106–118. https://doi.org/10.2112/04-0403.1

Davis Jr, R. A., & Hayes, M. O. (1984). What is a wave-dominated coast? *Developments in Sedimentology* (pp. 313–329). Elsevier.

De Fockert, A. (2008). Impact of relative sea level rise on the Amelander inlet morphology [Publisher: TU Delft, Civil Engineering and Geosciences, Hydraulic Engineering]. Retrieved August 10, 2021, from https://repository.tudelft.nl/islandora/object/uuid%3A5fd29cd3-8673-4319-89b1-a758703a8d36

Deltares. (2011). *Delft3D-FLOW, Simulation of multi-dimensional hydrodynamic flows and transport phenomena, including sediments, User Manual* (tech. rep.). Deltares.

Dissanayake, D. M. P. K., Ranasinghe, R., & Roelvink, J. A. (2012). The morphological response of large tidal inlet/basin systems to relative sea level rise. *Climatic Change, 113*(2), 253–276. https://doi.org/10.1007/s10584-012-0402-z

Ehlers, J. (1988). *The morphodynamics of the Wadden Sea*. Balkema.

Elias, E., Spek, A. J. F. v. d., Wang, Z. B., & Ronde, J. d. (2012). Morphodynamic development and sediment budget of the Dutch Wadden Sea over the last century [Publisher: Cambridge University Press]. *Netherlands Journal of Geosciences, 91*(3), 293–310. https://doi.org/10.1017/S0016774600000457

Elias, E., Van der Spek, A. J., Pearson, S. G., & Cleveringa, J. (2019). Understanding sediment bypassing processes through analysis of high-frequency observations of

Ameland Inlet, the Netherlands. *Marine Geology, 415*, 105956. https://doi.org/10.1016/j.margeo.2019.06.001

ESPO. (2019). *European Sea Ports Organisation Annual Report 2018-2019* (tech. rep.). European Sea Ports Organisation (ESPO), Brussels, Belgium.

Hayes, M. O. (1975). Morphology of sand accumulation in estuaries: An introduction to the symposium. *Geology and Engineering* (pp. 3–22). Elsevier.

Isreal, C. (1998). *Morfologische ontwikkeling Amelander zeegat.* (tech. rep.). RIKZ. Utrecht, The Netherlands.

Jiao, J. (2014). Morphodynamics of Ameland Inlet: Medium-term Delft3D Modelling. Retrieved August 11, 2021, from https://repository.tudelft.nl/islandora/object/uuid%3Ae3d05254-1291-4334-b044-033e367b81fe

Koffijberg, K., Frikke, J., Hälterlein, B., Laursen, K., Reichert, G., & Soldaat, L. (2017). *Breeding birds. In: Wadden Sea Quality Status Report 2017* (tech. rep.). Common Wadden Sea Secretariat (CWSS). Wilhelmshaven, Germany.

Latteux, B. (1995). Techniques for long-term morphological simulation under tidal action. *Marine Geology, 126*(1-4), 129–141. https://doi.org/10.1016/0025-3227(95)00069-B

Lenstra, K. J. H., Pluis, S. R. P. M., Ridderinkhof, W., Ruessink, G., & van der Vegt, M. (2019). Cyclic channel-shoal dynamics at the Ameland inlet: The impact on waves, tides, and sediment transport. *Ocean Dynamics, 69*(4), 409–425. https://doi.org/10.1007/s10236-019-01249-3

Lesser, G. R., Roelvink, J. A., van Kester, J. A. T. M., & Stelling, G. S. (2004). Development and validation of a three-dimensional morphological model. *Coastal Engineering, 51*(8), 883–915. https://doi.org/10.1016/j.coastaleng.2004.07.014

Oost, A. P., Winter, C., Vos, P., Bungenstock, F., Schrijvershof, R., Röbke, B., Bartholdy, J., Wurpts, A., & Wehrmann, A. (2017). *Geomorphology. In: Wadden Sea Quality Status Report 2017* (tech. rep.). Common Wadden Sea Secretariat (CWSS). Wilhelmshaven, Germany. waddensea-worldheritage.org/reports/geomorphology

Pearson, S., Van Prooijen, B., De Wit, F., Meijer-Holzhauer, H., De Looff, A., & Wang, Z. (2019). OBSERVATIONS OF SUSPENDED PARTICLE SIZE DISTRIBUTION ON AN ENERGETIC EBB-TIDAL DELTA. *Coastal Sediments 2019*, 1991–2003. https://doi.org/10.1142/9789811204487_0172

Ridderinkhof, H. (1988). Tidal and residual flows in the western Dutch Wadden Sea I: Numerical model results [Publisher: Elsevier]. *Netherlands Journal of Sea Research, 22*(1), 1–21.

Steetzel, H. J. (1995). Voorspelling ontwikkeling kustlijn en buitendelta's Waddenkust over de periode 1990-2040 [Publisher: Deltares (WL)]. *H1887*. Retrieved October 21, 2021, from https://repository.tudelft.nl/islandora/object/uuid%3A544509b3-692e-43ce-8576-20d631e503f2

Stive, M. J., & Wang, Z. (2003). Chapter 13 Morphodynamic modeling of tidal basins and coastal inlets. *Elsevier Oceanography Series* (pp. 367–392). Elsevier. https://doi.org/10.1016/S0422-9894(03)80130-7

Stive, M. (1998). Morphodynamics of a tidal lagoon and adjacent coast. *8th International Biennial Conference on Physics of Estuaries and coastal Seas, The Hague, The Netherlands, 1998*.

Tulp, I., Bolle, L. J., Dänhardt, A., de Vries, P., Haslob, H., Jepsen, N., & Scholle, J. (2017). *Fish. In: Wadden Sea Quality Status Report 2017* (tech. rep.). Common Wadden Sea Secretariat (CWSS). Wilhelmshaven, Germany.

van der Molen, J., & van Dijck, B. (2000). The evolution of the Dutch and Belgian coasts and the role of sand supply from the North Sea. *Global and Planetary Change, 27*(1), 223–244. https://doi.org/10.1016/S0921-8181(01)00068-6

Van Goor, M. A., Zitman, T. J., Wang, Z. B., & Stive, M. J. F. (2003). Impact of sea-level rise on the morphological equilibrium state of tidal inlets. *Marine Geology, 202*(3), 211–227. https://doi.org/10.1016/S0025-3227(03)00262-7

Van Rijn, L. C. et al. (1993). *Principles of sediment transport in rivers, estuaries and coastal seas* (Vol. 1006). Aqua publications Amsterdam.

Vermeersen, B. L. A., Slangen, A. B. A., Gerkema, T., Baart, F., Cohen, K. M., Dangendorf, S., Duran-Matute, M., Frederikse, T., Grinsted, A., Hijma, M. P., Jevrejeva, S., Kiden, P., Kleinherenbrink, M., Meijles, E. W., Palmer, M. D., Rietbroek, R., Riva, R. E. M., Schulz, E., Slobbe, D. C., … Wegen, M. v. d. (2018). Sea-level change in the Dutch Wadden Sea [Publisher: Cambridge University Press]. *Netherlands Journal of Geosciences, 97*(3), 79–127. https://doi.org/10.1017/njg.2018.7

Wang, Z. B. (2019). *Sediment exchange between the Wadden Sea and North Sea Coast* (tech. rep. 1220339-008-ZKS-0006). Rijkswaterstaat Water, Verkeer en Leefomgeving. Utrecht.

Wang, Z. B., de Vriend, H., Stive, M., & Townend, I. (2007). On the parameter setting of semi-empirical long-term morphological models for estuaries and tidal lagoons. *Proceedings of 5th IAHR Symposium on River, Coastal and Estuarine Morphodynamics*. IAHR. Retrieved March 30, 2021, from http://www.iahr.net/

Wang, Z. B., Elias, E. P. L., Spek, A. J. F. v. d., & Lodder, Q. J. (2018). Sediment budget and morphological development of the Dutch Wadden Sea: Impact of accelerated sea-level rise and subsidence until 2100 [Publisher: Cambridge University Press]. *Netherlands Journal of Geosciences, 97*(3), 183–214. https://doi.org/10.1017/njg.2018.8

Wang, Z. B., Karssen, B., Fokkink, R., & Langerak, A. (1998). A dynamic-empirical model for estuarine morphology [Publisher: Balkema, Rotterdam]. *Physics of estuaries and coastal seas*, 279–286.

Wang, Z. B., Townend, I., & Stive, M. (2020). Aggregated morphodynamic modelling of tidal inlets and estuaries. *Water Science and Engineering, 13*(1), 1–13. https://doi.org/10.1016/j.wse.2020.03.004

Wang, Z. B., & Van Der Spek, A. (2015). IMPORTANCE OF MUD FOR MORPHOLOGICAL RESPONSE OF TIDAL BASINS TO SEA-LEVEL RISE. *The Proceedings of the Coastal Sediments 2015*. https://doi.org/10.1142/9789814689977_0208

WHO. (2019). *The Global Climate in 2015–2019* (tech. rep.). World Meteorological Organization. Geneva, Switzerland. https://library.wmo.int/doc_num.php?explnum_id=9936

A

MODEL SETTING

A.1. TIDAL BASIN ELEMENTS

A tidal basin can be separated into the ebb channels and the intertidal flat. The MLW separates those two elements according to the water depth. And the area of the ebb channels and the intertidal flat mentioned in this thesis are both referred to $A_{ch,MLW}$ and $A_{f,MLW}$ in Figure. A.1.

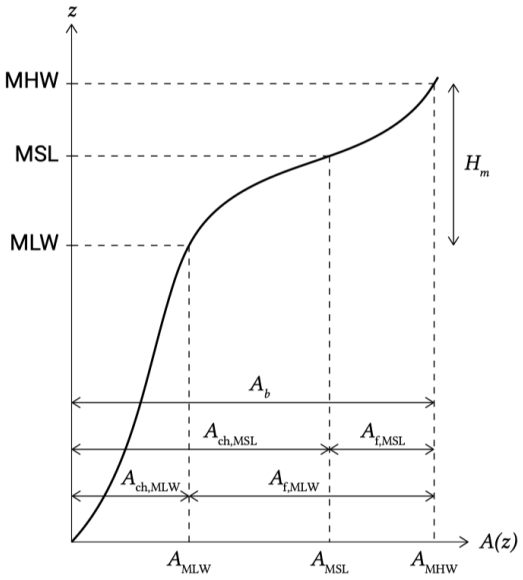

Figure A.1: Definition of the basin area, channel area and flats area relative to the tidal levels (Bosboom and Stive, 2021)

A.2. BOUNDARY CONDITIONS

A.2.1. HARMONIC BOUNDARY

The harmonic water level boundary conditions at the Northern boundary are shown in the following table.

Table A.1: Harmonic boundary at the northern boundary

Frequency [degree/h]	Period	Amplitute at A [m]	Phase at A [degree]	Amplitute at B [m]	Phase at B [degree]
0		0.1163	0	0.1163	0
14.497	24h 50m	0.122	183.45	0.127	192.32
28.993	12h 25m	0.897	54.33	1.002	77.8
43.49	8h 17m	0.01	100.44	0.011	139.89
57.987	6h 13m	0.113	333.14	0.121	181.11
72.483	4h 58m	0.008	79.19	0.01	121.8
86.98	4h 8m	0.095	203.64	0.064	274.73
101.477	3h 33m	0.007	224.6	0.003	155.97
115.973	3h 6m	0.003	357.93	0.004	49.18

A.2.2. NEUMANN BOUNDARY

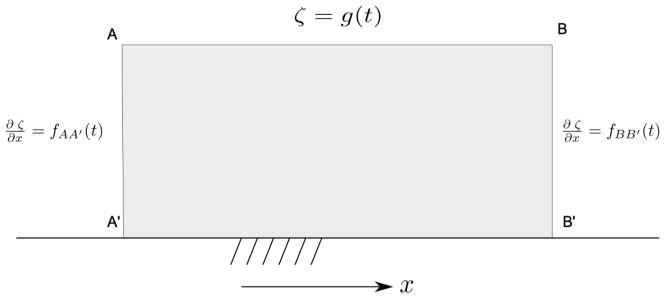

Figure A.2: Neumann boundaries at the cross section A-A' and B-B'(Deltares, 2011)

The cross section A-A' and B-B' in Figure. A.2 are corresponding to the west and the east offshore boundaries of this model. The water level gradient in alongshore direction is prescribed at each boundaries.

$$\frac{\partial \zeta}{\partial x} = \sum_{j=1}^{N} k_j \hat{\zeta}_j \sin\left(\omega_j t - k_j x\right) = \sum_{j=1}^{N} k_j \hat{\zeta}_j \cos\left(\omega_j t - \left(\varphi_j + \frac{\pi}{2}\right)\right) \tag{A.1}$$

A.3. COURANT NUMBER

Normally, the time step will be selected for the sake of accuracy and also computation time. The courant number is introduced to the numerical model to decide the numerical stability from the grids size and time step. Once the local courant number exceeds the up limit, the instability will probably appear which is not favourable for the result itself. In the Hybrid model, the courant number is calculated as follow(Deltares, 2011):

$$Courant = 2\Delta T c\sqrt{1/\Delta x^2 + 1/\Delta y^2} \tag{A.2}$$

In most of cases, it is not recommended to have courant number exceeding 10. But when the variants don't vary too much in space and in time too much, a higher up limit for courant number can be applied.

A.3.1. ORIGINAL GRID

The courant number map with time step at 12 seconds is shown below.

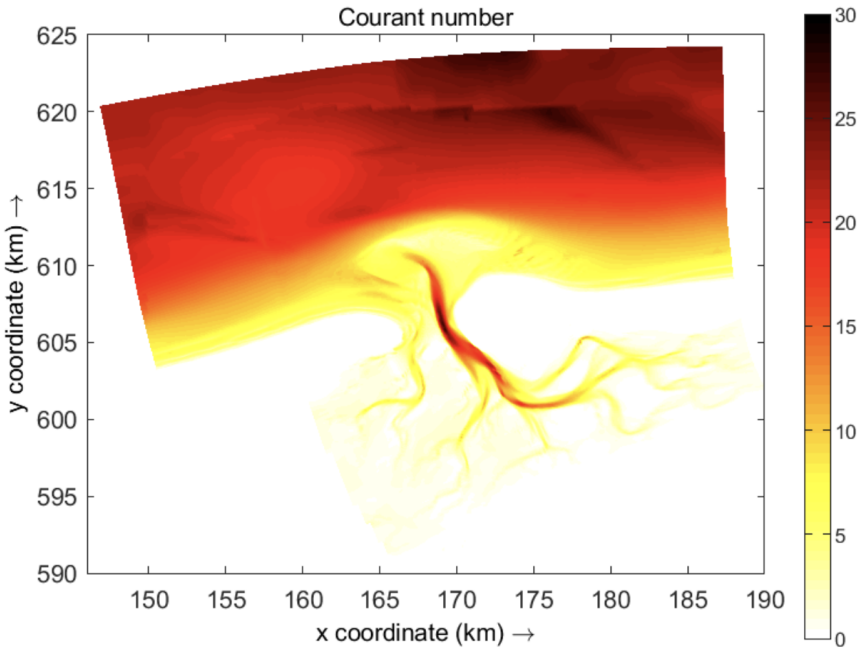

Figure A.3: Courant number map with the time step at 12 seconds

From the map, at the intertidal area and the ebb-tidal delta, the courant number is smaller than 10. When it comes to the offshore area and the main channel, where the water depth is deep, the courant number exceeds the limit. But in this computation case, only tidal flow is applied to the model which varies slowly. Therefore, the time step at 12 seconds is acceptable in this case.

A.3.2. COARSER GRID

For the twice coarser grid, according to the Courant number, the time step could be larger simultaneously. Therefore, the Courant number map is drawn for the coarser grid.

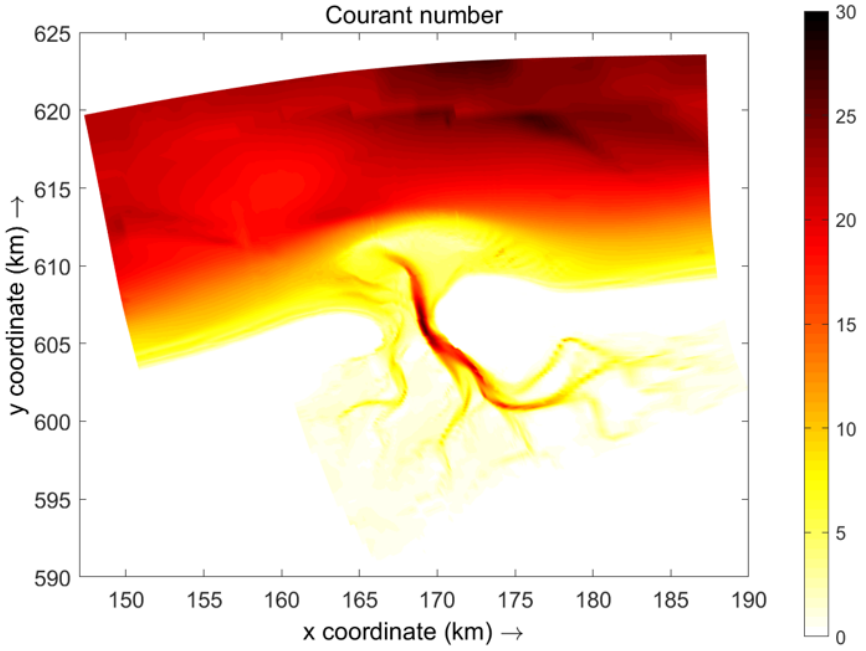

Figure A.4: Courant number for with a coarser grid and the time step at 30s

A.4. REFERENCE LEVEL

Reference level is related to the equilibrium state which further influences the bed level change. As the default setting, the reference level is set at 0 m as high as the global reference level, which means that the the initial water depth is equal to the equilibrium water depth. To investigate the influence of the reference level, three additional simulations are carried out.

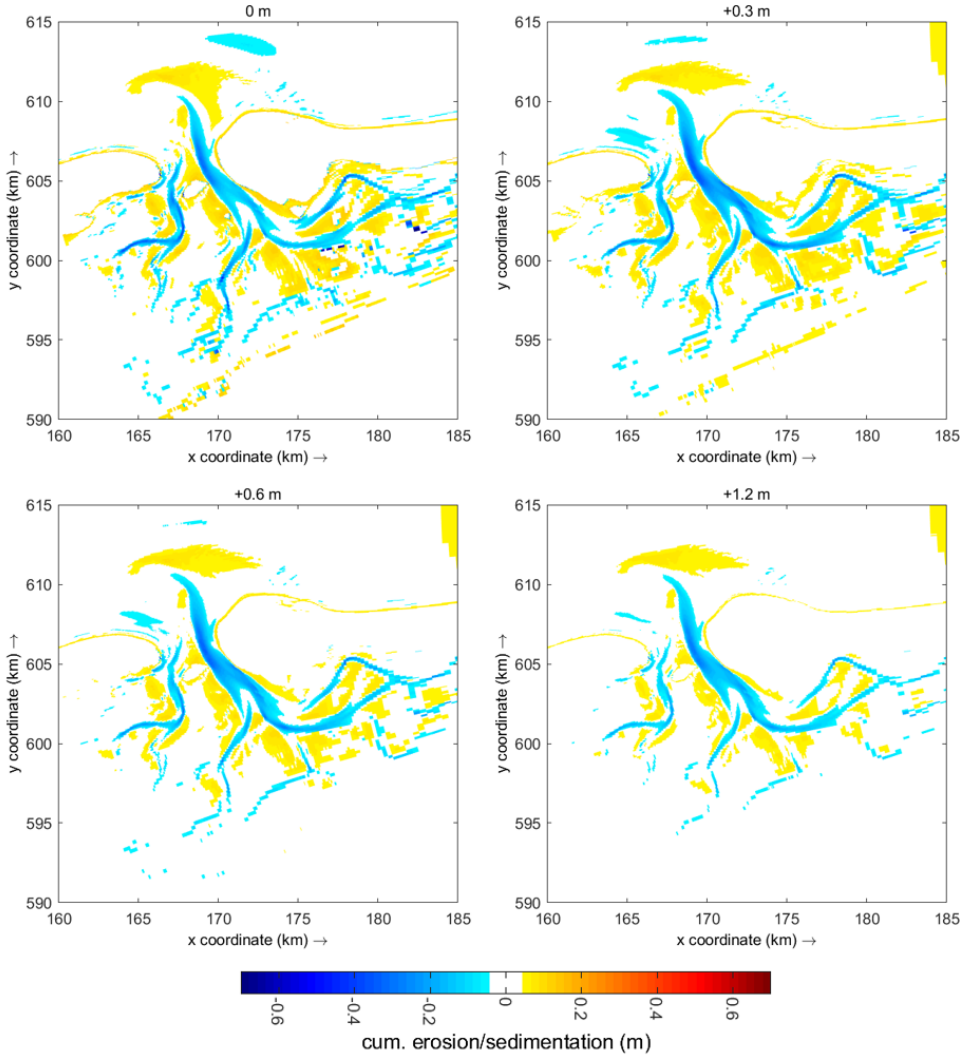

Figure A.5: Cumulative erosion/sedimentation map of four reference levels

Lifting the reference level can make the basin less sensitive to the SLR, and vice versa. But decreasing the reference level is not proposed to do because the drop will make the

equilibrium depth of some shallow points decrease below zero. The abnormal bed level change may happen at the point whose equilibrium depth is at a negative value, since these points are treated as 'emerged' points referred to the reference level but they are actually submerged during high tide. Therefore, only the lift at reference level is carried out.

As the reference level goes up, there are less erosion at the channels and less sedimentation at the ebb-tidal delta and the intertidal area. For the case with no change (upper right figure), at the intertidal area approaching to the edge of basin, where the water depth is shallow, there are some instabilities could be found (the dark blue points). When the reference level reaches to 1.2 m, which is the high water level inside the basin, no instability appears within the domain. The elevation of reference level promises that all the areas below the high water level have a positive depth related to reference level. Therefore, having a higher reference level can increase the stability of the model.